Characterization of Interleukin 10 gene variations and serum levels as predictive factors for the clinical outcome of Non-Hodgkin Lymphoma patients and Analysis of molecular mechanisms of Interleukin 10 gene regulation in B cells

Doctoral Thesis

In partial fulfillment of the requirements for the degree

“Doctor rerum naturalium (Dr. rer. nat.)”

in the Molecular Medicine Study Program

at the Georg-August University Göttingen

submitted by Christina Heemann

born in Lüneburg

Göttingen, 2012

Members of Thesis Committee

apl. Prof Dr. Dieter Kube (Supervisor)

E-Mail	dkube@med.uni-goettingen.de
Postal Address	Universitätsmedizin Göttingen Zentrum Innere Medizin Abteilung Hämatologie und Onkologie Robert-Koch-Straße 40 37075 Göttingen

Jun. Prof. Dr. Steven Johnsen

E-Mail	Steven.Johnsen@zentr.uni-goettingen.de
Postal Address	Universitätsmedizin Göttingen Göttinger Zentrum für Molekulare Biowissenschaften (GZMB) Abteilung Molekulare Onkologie Ernst-Caspari-Haus Justus-von-Liebig-Weg 11 37077 Göttingen

Prof. Dr. Heike Bickeböller

E-Mail	hbickeb@gwdg.de
Postal Address	Universitätsmedizin Göttingen Abteilung Genetische Epidemiologie Humboldtallee 32 37073 Göttingen

Date of Disputation: 27. April 2012

Affidavit

By this I declare that I independently authored the presented thesis:

“Characterization of Interleukin 10 gene variations and serum levels as predictive factors for the clinical outcome of Non-Hodgkin Lymphoma patients and Analysis of molecular mechanisms of Interleukin 10 gene regulation in B cells”

and that I did not use other auxiliary means than indicated. Paragraphs that are taken from other publications, by wording or by sense, are marked in every case with a specification of the literary source.

Furthermore I declare that I carried out the scientific experiments following the principles of Good Scientific Practice according to the valid “Richtlinien der Georg-August-Universität Göttingen zur Sicherung guter wissenschaftlicher Praxis”.

Christina Heemann

Göttingen, March 2012

Table of Content

Abstract

Aggressive Non-Hodgkin lymphoma (aNHL) comprises a heterogeneous group of lymphatic malignancies. Although current treatment regiments can achieve high response rates, many patients do not achieve complete remission. Reliable and clinically applicable prognostic markers are needed to improve treatment strategies. Previous studies suggested a role for the cytokine interleukin 10 (IL10) for the initiation and progression of lymphomas. Conflicting data about associations of *IL10* gene variations or elevated IL10 serum levels with the clinical outcome of aNHL exists. Therefore, this study aimed at elucidating whether these two factors could be of prognostic relevance for aNHL outcome in independent larger clinical cohorts and to investigate molecular mechanisms contributing to this.

Overall 1724 aNHL patients from three different clinical trials (NHL-B, RICOVER-60 and MInT) have been included into this study. 604 patients were from RICOVER-60 trial, of which sera were available from 523 patients. Survival analyses revealed that patients with low IL10 serum levels had a better treatment outcome compared to patients with elevated IL10 serum levels. This is also true for patients, treated with Rituximab in addition to chemotherapy, which is the current standard therapy. Therefore, circulating levels of IL10 could be of prognostic relevance for aNHL outcome. In addition, *in vitro* studies showed that IL10 treatment of target cells seems to reduce Rituximab-mediated antibody dependent cellular cytotoxicity (ADCC) but not complement dependent cytotoxicity (CDC).

Furthermore, it was found that homozygous carriers the of IL10$_{-11.668AA}$ far distal *IL10* gene variation, located within an evolutionary conserved sequence, showed a better treatment outcome compared to carriers of the other two genotypes in the RICOVER-60 cohort (OS: HR=0.6; CI= 0.38-0.95; EFS: HR=0.6; CI= 0.41-0.87).
Chromatin immunoprecipitation (ChIP) of modified histones revealed enhancer specific histone modifications around IL10$_{-11.668G/A}$ and other conserved sequences in transformed B cells. Therefore, they seem to be involved in *IL10* gene regulation. Moreover, a very long non-coding RNA has been found to be transcribed from the *IL10* gene locus.

The results of this study confirm an important role for IL10 in the clinical course of aNHL and provide new insight into the structure and regulation of the *IL10* gene.

List of Figures

List of Tables

Abbreviations

Abbreviation	Denotation
acH3	acetylated Histone 3
aNHL	aggressive Non-Hodgkin Lymphoma
ANOVA	analysis of variance
BHK	baby hamster kidney
cDNA	complementary DNA
CNS	conserved noncoding sequences
DiO	3,3′-Dioctadecyloxacarbocyanine perchlorate
DLBCL	Diffuse Large B Cell Lymphoma
DNA	desoxyribonucleic acid
DTT	dithiothreitol
EBV	Epstein-Barr virus
ECL	enhanced chemiluminescence
EDTA	ethylenediaminetetraacetic acid
EFS	event-free survival
ERK	extracellular-regulated kinase
et al.	Lat.: et alteri
FBS	fetal bovine serum
GATA-3	GATA binding protein 3
h	hours
H3K4me1	mono-methylated Lysine 4 at Histone 3
H3K4me3	tri-methylated Lysine 4 at Histone 3
HLA I	human leukocyte antigen class I
IC	immune complexes
IL10	Interleukin 10
IL10R	IL10 Receptor
IPI	International Prognostic Index
kDa	kilo-Dalton
LCL	lymphoblastoid cell line

Abbreviation	Denotation
LD	linkage disequilibrium
LDH	lactate dehydrogenase
LPS	lipopolysaccharide
min	minutes
mRNA	messenger RNA
MTT	(3-(4,5-Dimethyl-2-thiazolyl)-2,5-diphenyl-2H-tetrazolium bromide)
NF-κB	Nuclear factor of kappa B light polypeptide gene enhancer in B cells
OS	overall survival
PBMCs	peripheral blood mononuclear cells
PBS	phosphate buffered saline
PI	propidium iodide
PI3K	phosphoinositide 3-kinase
PKC	protein kinase C
PMA	phorbol-12-myristate-13-acetate
s	seconds
RNA	ribonucleic acid
RT	room temperature
SDS	sodium-dodecyl-sulfate
Th1 cells	T helper 1 cells
Th2 cells	T helper 2 cells
TSS	transcription start site
WHO	World Health Organization
x g	multiple of acceleration of gravity (g = 9.80665 m/s^2)

1 Introduction

Malignant lymphomas comprise a group of hematological malignancies that usually form solid tumors in lymphatic organs due to uncontrolled clonal expansion. They often originate in the lymph node but can also affect other lymphatic tissues, i.e. thymus, spleen and bone marrow. The term Non Hodgkin Lymphoma (NHL) describes any kind of malignant lymphoma other than Hodgkin lymphoma (HL). NHL can be divided into aggressive (fast growing) and indolent (slow growing) types. This thesis concentrates on aggressive NHL (aNHL). Based on morphology, immunology, genetic aberrations and clinical aspects lymphoma entities can be described (Turner et al., 2010). The classification system has been adjusted regularly, based on new diagnostic tools. Today the classification system of the WHO is commonly used (Turner et al., 2010).

In developed countries aNHL is the seventh most cancer diagnosed. The incidence of the disease has been increasing over the last decades (Jemal et al., 2011). This is probably in part caused by demographic changes as well as approved living circumstances and life expectancies in humans in developed countries.

Despite therapeutic advances, many NHL patients do not achieve complete remission or they relapse after conventional chemotherapy and die of the disease. Of 95 new cases (per 1000 of new cancer cases) in men and 84 new cases in women, 37 and 33 deaths have been counted respectively in developed countries in 2008 (Ferlay et al., 2010).

New treatment strategies are required and a vast amount of new drugs has been developed during the last decades, based on an increasing knowledge about molecular mechanisms involved in lymphoma pathogenesis and progression. However, better prognostic factors, which are reliable and clinically applicable, are essential to define patient groups and to adjust individual treatment strategies.

1.1 Non-Hodgkin Lymphoma

Depending on their origination from B or T cells, aNHL is referred B- or T-NHL, whereby in developed countries approximately 90% of aggressive lymphoma are derived from B cells (Murawski and Pfreundschuh, 2010). NHL is found more frequently in men than in women and the relative risk to develop NHL is 10-100 or more times higher in people with immune deficiency due to immune suppressive therapy after transplantation or infection with HIV (Alexander et al., 2007; Grulich and Vajdic, 2005).

The most common subtype of the very heterogeneous group of B-NHL is the diffuse large B cell lymphoma (DLBCL), which comprises approximately 30-40% of all NHL. DLBCL as well as other B-NHL arise from differentiating B cells during the germinal center reaction (1997; Kuppers, 2005). Most DLBCL are composed of cells resembling germinal center centroblasts (Friedberg and Fisher, 2008). A variety of chromosomal alterations, leading to aberrant expression of certain proto-oncogenes have been described for DLBCL, whereby translocations of *BCL-6,* a critical transcriptional repressor during germinal center formation, are the most common (Ci et al., 2008). Two molecular distinct subtypes of DLBCL have been identified via microarray-based gene expression profiling, the germinal center B-like DLBCL (GCB) and activated B-like DLBCL (ABC) (Alizadeh et al., 2000).

Another aNHL is the Burkitt's lymphoma (BL) which accounts for 2% of all NHL (Kuppers, 2005). Characteristic for the BL is a translocation of the proto-oncogene MYC into one of the immunoglobulin gene loci (Hummel et al., 2006). Different variants of BL exist. The endemic form, which is the most common malignancy in children in equatorial Africa, is associated with Epstein-Barr-Virus (EBV) infection. In developed countries the sporadic and the immunodeficiency associated forms of BL are predominant (reviewed in (Bellan et al., 2003)).

T-NHL represent a rare and very heterogeneous group of NHL. T-NHL account for approximately 10% of all NHL, whereby a geographic variation in frequency could be observed for these lymphomas ranging from 1.5% (Vancouver, Canada) to 18.3% (Hong Kong, China). Compared to patients with B-NHL, a more aggressive clinical course and worse treatment outcome for patients with T-NHL is reported in most studies. The only exception is the anaplastic large cell lymphoma (ALCL),

overexpressing anaplastic lymphoma kinase (ALK) (Armitage et al., 2004; Gisselbrecht et al., 1998; Melnyk et al., 1997; Schmitz et al., 2010).

Therapy of aggressive NHL

For more than 25 years the cyclophosphamide, doxorubicin, vincristine and prednisolone (CHOP) has been standard treatment regimen for aNHL (Pfreundschuh et al., 2008). Due to an increasing knowledge about oncogenic pathways and molecules involved in pathogenesis and progression of distinct types of aNHL, obtained via gene expression profiling or other genomic and proteomic technologies, new therapeutic targets have been discovered and a vast amount of new drugs has been developed for the treatment of aNHL during the last decade (Mahadevan and Fisher, 2011; Murawski and Pfreundschuh, 2010). These include cytotoxic drugs, antibodies and other targeted therapies, targeting molecules or pathways characteristic for the lymphoma cells. These targeted therapies are thought to improve treatment responses especially in refractory and relapsed aNHL patients and to decrease side effects on normal tissue, thereby improving quality of life. Targets of these new drugs are for example certain receptor-associated kinases, histone deacetylases or molecules involved in the regulation of apoptosis, angiogenesis and immune modulation (Mahadevan and Fisher, 2011; Murawski and Pfreundschuh, 2010).

Due to these attempts to improve responses to chemotherapy a new standard therapy could be defined. The addition of Rituximab to conventional CHOP therapy significantly improved treatment outcome of young as well as elderly patients with aggressive B-NHL (Coiffier et al., 2002; Murawski and Pfreundschuh, 2010; Pfreundschuh et al., 2008; Pfreundschuh et al., 2006). Rituximab is a monoclonal chimeric antibody specifically targeting CD20 on the surface of normal mature and malignant B cells. How Rituximab mediates effects against malignant cells will be described in chapter 1.4. Several approaches have been undertaken to improve CD20 antibodies by humanization and/or glycoengineering. Antibodies which target other surface molecules than CD20 are also under investigation (Murawski and Pfreundschuh, 2010).

Despite therapeutic advances, many patients with aggressive B-NHL do not achieve a complete remission with the so far best treatment regimen (Friedberg and Fisher, 2008; Mahadevan and Fisher, 2011).

Treatment of T-NHL remains a therapeutic challenge. Promising treatment strategies for B-NHL do not improve therapy of T-NHL patients (Nickelsen et al., 2009). Several new agents have been introduced in combination with CHOP therapy and/or stem cell transplantation, but most of them still need to be assessed in prospective clinical trials. In younger T-NHL patients the addition of etoposide to standard CHOP therapy (cyclohexamide, doxorubicin, vincristine, prednisolone), improved response rates (Schmitz et al., 2010). However, a more effective standard therapy for T-NHL has yet to be defined (O'Leary and Savage, 2008; Reimer et al., 2009).

Good prognostic markers are essential to improve treatment strategies, to define patient subgroups and to compare different clinical trials. Today the International Prognostic Index (IPI), including the clinically relevant factors age, elevated lactate dehydrogenase (LDH), Ann Arbor stage, performance status and the involvement of extranodal sites is used to predict the outcome of NHL patients. Nevertheless, there is still a strong need to identify better prognostic markers in order to improve treatment strategies.

Cytokines in aNHL

Increasing evidence exists that the initiation or progression of aNHL is supported by certain cytokines, chemokines or their soluble receptors. Cytokines are important soluble mediators of low molecular weight, essential for the regulation magnitude and profile of innate and adaptive immune responses. They are produced by immune cells and facilitate communication between these cells. Cytokines can act in an autocrine, paracrine or endocrine fashion. They have pleiotropic properties, since they can affect the activity of many different cell types via binding to the respective receptors on the cell surface.

Certain cytokines produced in the tumor microenvironment or by tumor cells can promote an enhanced tumor progression, invasion and metastasis for example by promoting inflammatory processes or by acting as paracrine or autocrine growth factors (Dranoff, 2004; Lin and Karin, 2007; Voorzanger et al., 1996). Context dependent certain cytokines also have the capacity to inhibit tumor development and progression (Dranoff, 2004).

Inherited gene variations or elevated secretion of certain cytokines have been frequently associated with susceptibility or disease outcome of aNHL and could therefore serve as prognostic factors in the future. In this context, pro- and anti-inflammatory molecules such as TNF, Interleukin (IL)-4, IL6 or IL10 or their receptors are under investigation (Goto et al., 2006; Habermann et al., 2008; Hackstein et al., 2001; Kube et al., 2008; Lech-Maranda et al., 2006; Skibola et al., 2007). Of particular interest for this thesis is the cytokine IL10. Therefore, it will be introduced in more detail in chapter 1.2.

1.2 The cytokine Interleukin 10

The active IL10 protein is a homodimer and each subunit consists of 178 amino acids and approximately 18kDa. IL10 is a highly conserved protein. 78% identity between the human and the mouse IL10 amino acid sequence can be observed. IL10 exhibits potent immunosuppressive and anti-inflammatory activity, repressing the expression of inflammatory cytokines such as TNF-α (tumor necrosis factor-alpha), IL6 and IL1 by macrophages (Fiorentino et al., 1991). In addition to this, IL10 induces the production of anti-inflammatory molecules. Therefore, IL10 is a cytokine with immune-modulatory functions, limiting inflammatory responses of the host (Moore et al., 2001). IL10 is secreted by a variety of immune cells including monocytes and macrophages, certain T cell subsets and B cells (Moore et al., 2001; Shoemaker et al., 2006). IL10 was first described as cytokine synthesis inhibitory factor (CSIF), due to its ability to inhibit activation of Th1 cells as well as production of cytokines like IFN-γ (Interferon-gamma) and TNF-α by Th1 cells. This also lead to the characterization of IL10 as a Th2 (T helper 2 cells) cytokine, shifting the immune response from Th1 or T cell-mediated to a Th2 or humoral immune response (Mocellin et al., 2005). However, the down-regulation of cytokine production by T cells and also natural killer cells (NK cells) seems to be an indirect effect, mediated by inhibition of accessory cells like macrophages and monocytes (Moore et al., 2001).

IL10 is a potent growth factor for B cells by increasing the expression of the anti-apoptotic gene Bcl-2 or by acting as a cofactor for proliferation of B cells after BCR or CD40 crosslink (Levy and Brouet, 1994; Rousset et al., 1992).

IL10 is thought to be involved in infectious and autoimmune diseases, transplantation tolerance and tumorigenesis (Moore et al., 2001). Due to its immunosuppressive properties or by stimulating cell proliferation and inhibition of apoptosis, it can promote tumor development and progression (Alas et al., 2001; Lu et al., 1995; Masood et al., 1995; Voorzanger et al., 1996).

IL10 mRNA expression for example has been shown in tumor tissue samples derived from NHL patients an exogenous IL10 promoted proliferation of purified tumor cell preparations (Voorzanger et al., 1996). On the other hand, IL10 possesses immunostimulatory anticancer properties or inhibits angiogenesis (Cervenak et al., 2000; Mocellin et al., 2005).

IL10 signals through the IL10 receptor (IL10R). Two ligand binding subunits (IL10Rα) and two accessory subunits for signaling (IL10Rβ) form a functional IL10R. Binding of IL10 to the receptor leads to phosphorylation and activation of two receptor-associated janus kinases, Janus Kinase-1 (JAK1) and Tyrosine Kinase-2 (TYK2), which in turn phosphorylates two tyrosine residues in the cytoplasmic tail of IL10Rα. Upon phosphorylation they form temporary docking sites for Signal Transducer and Activator of Transcription-3 (STAT3). STAT-3 binds via its Src Homology-2 (SH2) domain to the receptor and becomes phosphorylated by JAK1 and TYK2. STAT3 forms homodimer, which translocate to the nucleus, where it binds to promoters of IL10 responsive genes (Donnelly et al., 1999). Therefore, phosphorylated STAT3 is the main transcription factor mediating IL10-induced signals.

1.2.1 The *IL10* gene locus and its regulation in immune cells

The gene coding for IL10 is located on chromosome 1q31/32 and consists of 5 exons (Eskdale et al., 1997). Cytokine or cytokine receptor genes, as well as the *IL10* gene, are frequently found in highly polymorphic „gene clusters“ (Keen, 2002). However, some regions within the *IL10* gene locus show a high homology between species (Figure 1-1). Because these sequences are located within noncoding regions they are termed conserved noncoding sequences (CNS). This high conservation generally indicates a potential role of these sequences for regulatory processes.

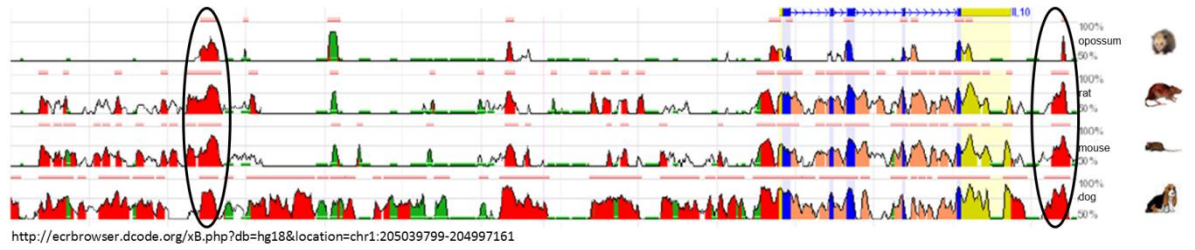

Figure 1-1 Evolutionary conserved noncoding sequences are located in the *IL10* gene locus

A comparison of the human *IL10* gene locus (x-axis) and the opossum, rat, mouse and dog *IL10* gene loci (y-axis) is shown. This comparison has been calculated using the browser for evolutionary conserved regions (ECR) (http://ecrbrowser.dcode.org). Sequences of similarity are marked by the height of the curves. A vertical axis cut-off of 50% to 100% identity is utilized to visualize only the significant alignments. Annotated genes (*IL10*) are depicted as a horizontal line above the graph. ECRs (pink rectangles on top of the plot), coding exons (blue), intronic regions (salmon-pink), transposons and simple repeats (green) and intergenic regions (red) are indicated. The CNS-12 and CNS+6 are indicated with black ovals.

In addition, several single nucleotide polymorphisms (SNPs), microsatellites and one insertion/deletion variation have been described to be located within the *IL10* gene locus (Figure 1-2). SNPs can be coding if they are located within the coding region, leading to an amino acid exchange or they can be regulatory (non-coding), if they are located within 5'- or 3'-regions or within introns of genes.

Regulatory gene variations in the *IL10* promoter are thought to influence the expression level of the cytokine, for example if they lie within transcription factor binding sites. This will be described in more detail in chapter 1.2.2. Moreover, certain *IL10* gene variations have been associated with the outcome of aNHL and might be useful prognostic factors in addition to the IPI factors. This issue will be addressed in chapter 1.3.

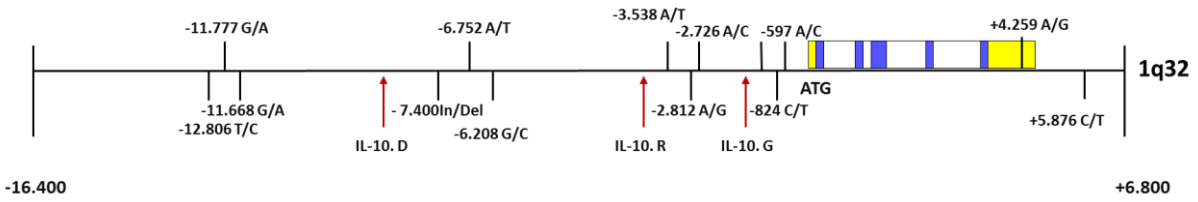

Figure 1-2 Scheme of the *IL10* gene locus

The human *IL10* gene locus from -16.400bp till +6800bp on chromosome 1q31/32 is shown. Single nucleotide polymorphisms (SNP) and the insertion/deletion variation at -7400bp are indicated. In addition, the locations of two dinucleotide repeats IL10.R and IL10.G as well as one complex repetitive sequence, the IL10.D are indicated by red arrows. The *IL10* gene and the position of the ATG are shown. UTR (yellow), exons (dark blue) and introns (white) are displayed.

Molecular mechanisms that contribute to the regulation of *IL10* expression are still under investigation. Several studies examined these mechanisms in macrophages and DC (Dendritic cells) or T cells from mice. Thereby mechanisms have been revealed that are exclusive for one cell type, while others are common to all cell types investigated. For B cells the exact involved signaling pathways and molecular mechanisms remain elusive.

IL10 expression in macrophages can be induced via inflammatory signals like the stimulation with LPS, whereas in T cells proliferative signals like the stimulation with PMA lead to *IL10* expression. Notably, the induction of IL10 takes several hours (4-6) in both cell types. *IL10* expression in macrophages and DC is induced via the activation of the extracellular signal-regulated kinase (ERK), p38 or nuclear factor-κB (NF-κB) pathways (Boonstra et al., 2006; Dillon et al., 2004; Yi et al., 2002). ERK and p38 signals are mediated via the transcription factors CREB and AP1. *IL10* expression in different subsets of T cells is also ERK- but not p38-dependent and involves distinct signal transducer of activation (STAT) pathways. *IL10* expression has been found to be accompanied by, and in the case of memory Th1 and Th2 cells, also conditional on the expression of those cytokines characteristic for the respective subset (Chang et al., 2007; Saraiva et al., 2009; Shoemaker et al., 2006). IL10 itself provides a negative feedback loop controlling its own production (Hammer et al., 2005).

In both macrophages and T cells many different transcription factors have been identified via mutagenesis or chromatin immunoprecipitation (ChIP). However, remodeling of the *IL10* locus has been found to be required for transcription factor binding (Lucas et al., 2005; Shoemaker et al., 2006; Zhang et al., 2006).

In eukaryotes DNA of the cell is found in the nucleus organized on separate chromosomes. In non-dividing cells the chromatin seems to be distributed throughout the nucleus and is organized into heterochromatin or condensed chromatin and the euchromatin, which resembles the more open confirmation (Felsenfeld and Groudine, 2003). Chromatin is organized in nucleosomes, each containing 147bp of DNA wrapped around an octamer of the core histones (2xhistone 2A (H2A), 2xH2B, 2xH3 and 2xH4), linked by 10-60bp of linker DNA. This “beads on a string” arrangement is folded into more condensed fibers of chromatin and stabilized by linker histones (H1 and H5). Due to this organization of DNA into condensed fibers, posttranslational

modifications are necessary to make the DNA sequence accessible for other proteins like transcription factors. These posttranslational modifications include acetylation, methylation as well as phosphorylation of certain amino acids within the amino- or carboxy-terminal residues of the histones. Thereby, it seems that a pattern of histone marks determines whether these posttranslational modifications are associated with transcriptional activation or repression (Peterson and Laniel, 2004).

By identification of DNaseI- hypersensitive sites (HSS), studies on *IL10* regulation in T cells and macrophages revealed that the chromatin at the *IL10* locus is remodeled in IL10 producing cells. These HSS can be inducible or constitutive (Im et al., 2004; Lucas et al., 2005; Wang et al., 2006). Most HSS are common to differentiated Th1, Th2 cells (but not naïve T cells) and macrophages, while others are unique to one cell type. HSS-4.5 for example is only found in macrophages and inducible by LPS stimulation. It is hyperacetylated upon LPS stimulation and comprises a binding site for NF-κB (p65). Acetylation of certain amino acids within the amino-terminal residues of H3 and H4 is often associated with transcriptional activation (Li et al., 2007; Peterson and Laniel, 2004). Inhibition of NF-κB leads to reduction in *IL10* mRNA (Saraiva et al., 2005).

Some of the HSS correlate with CNS (Figure 1-1). Several of these CNS function as enhancer elements in Th2 cells as shown by Jones and Flavell (Jones and Flavell, 2005). The same group could show that some CNS possess promoter function and transcribe intergenic RNA in Th2 cells and in most cases also in Th1 cells, whereby the exact role of these RNAs for *IL10* gene regulation remains to be elucidated. Two CNS, CNS-9 and CNS+6.45 were repeatedly emphasized not only by Jones and Flavell. CNS+6.45 for example has been shown to bind AP1 in Th2 cells. Later on, NFAT1 and IRF4 were shown to bind to CNS-9, preferentially in Th2 cells (Lee et al., 2009a). CNS-9 is located 12kb downstream of the *IL10* TSS (transcription start site) in the human genome and will therefore be referred to as CNS-12 for the human *IL10* gene in this dissertation. CNS+6.45 is located around 6kb upstream of the TSS and will be referred CNS+6 for the human *IL10* gene (Figure 1-1).

GATA binding protein 3 (GATA-3), a key main transcription factor needed for Th2 differentiation, was found to regulate *IL10* expression in Th2 cells. One binding site is located in CNS+6.45, and binding of GATA3 induces chromatin remodeling and histone acetylation at the *IL10* locus (Shoemaker et al., 2006). For the induction of

IL10 expression additional stimuli are necessary, thus GATA-3 induces changes in chromatin structure at the *IL10* locus, which are required for other transcription factors to bind to the DNA and induce *IL10* expression.

Similar mechanisms have been found to contribute to *IL10* gene regulation in macrophages. Two stimuli are needed for full induction of *IL10* expression. Fc-γR ligation with immune complexes leads to activation of the mitogen activated protein kinases (MAPK) ERK and p38. This induces chromatin remodeling at *IL10* gene locus, transient phosphorylation of histone 3 (H3) and increased accessibility, shown by DNAse I HSS. LPS stimulation then leads to activation of other transcription factors (Sp1 and STAT3), which are now able to bind to the *IL10* promoter and to induce *IL10* expression. Fc-γR ligation alone does not induce *IL10* expression (Lucas et al., 2005; Zhang et al., 2006).

Therefore, one can conclude that both T cells and macrophages need two signals for IL10 induction. One signal that leads to an open chromatin confirmation and a second one that induces transcription factors (Lucas et al., 2005; Shoemaker et al., 2006; Zhang et al., 2006) In macrophages the first signal seems to be provided by ligation of immune complexes to Fc-γR, while the second signal is transmitted by inflammatory signals (Lucas et al., 2005; Zhang et al., 2006). In T cells the differentiation into Th2 or regulatory T cells (Treg) resembles the first signal. The second one is provided by signals inducing proliferation like PMA/Ionomycin stimulation (Jones and Flavell, 2005; Shoemaker et al., 2006). Nevertheless, even beside the nature of the two signals, there seem to be differences in *IL10* regulation in T cells and macrophages.

Little is known about the molecular mechanisms of *IL10* regulation in B cells, even though IRF-1 and STAT3 seem to be involved in these processes (Benkhart et al., 2000; Ziegler-Heitbrock et al., 2003). STAT3 is thought to be responsible for the induction of *IL10* expression after LPS or INF-α stimulation of the RPMI8226.1 B cell line, whereas IRF-1 is only induced after INF-α stimulation of the same cell line. No other B cell lines were tested (Benkhart et al., 2000; Ziegler-Heitbrock et al., 2003). INF-γ down-regulates *IL10* expression via STAT1 induction, which leads to a displacement of STAT3. Nothing is known about these mechanisms in other B cell lines.

In the past it has been observed that the fact that several Burkitt's lymphoma cell lines were positive for EBV (Epstein-Barr virus) is correlated to some extent with *IL10* expression and that one mechanism to induce *IL10* expression in normal human B cells is by immortalization of these cells via *in vitro* EBV infection (Benjamin et al., 1992; Burdin et al., 1993). B cells immortalized *in vitro* with EBV are termed LCLs (Lymphoblastoid cell lines). As a consequence of EBV infection, LCLs express several proteins, among them LMP1 (latent membrane protein 1), a protein significantly contributing to transformation and immortalization of B cells (Kaye et al., 1993; Kilger et al., 1998). LMP1 activates NF-κB, AP1 and mimics B cell activation processes which are physiologically triggered by CD40 signaling (Kieser et al., 1997; Kilger et al., 1998). Moreover, LMP1 has been shown to activate *IL10* expression in Burkitt's lymphoma cell lines through p38 activation but not in cell lines derived from other NHL or HL (Vockerodt et al., 2001). Reporter assays revealed positive and negative regulatory regions within the first 1100bp of the *IL10* promoter in EBV positive Burkitt lymphoma cell lines (Kube et al., 1995). These regions seem to differ between EBV positive and negative cell lines with constitutive *IL10* expression (Kube et al., 1999).

As aNHL originates in 90% from B cells, knowledge about the regulation of *IL10* gene expression and pathways involved in these processes in this cell type would be of great importance for the development of future therapeutic targets. So far, nothing is known about chromatin modification processes involved in *IL10* gene regulation.

1.2.2 Interindividual differences in IL10 production

Twin studies indicated that 50 to 75% of interindividual differences in IL10 production are heritable (Reuss et al., 2002; Westendorp et al., 1997). Based on data obtained from *in vitro* studies of whole blood cultures or PBMCs stimulated with different agents, differences in interindividual IL10 production have been attributed to genetic variations, including the *IL10* microsatellite alleles as well as SNPs or haplotypes formed by these gene variations in the 5'-region of *IL10* (Crawley et al., 1999; Eskdale et al., 1998; Gibson et al., 2001; Mormann et al., 2004; Rieth et al., 2004; Turner et al., 1997).

Some of the best studied gene variations are the SNPs IL10-1087A/G, IL10-824C/T, IL10-597A/C forming only three different haplotypes in Caucasian populations, ATA,

ACC and GCC (compare to Figure 1-1 and 1-3). Donors of the ATA haplotype (IL10-1087A, -824T, -597A) for example were described as „low IL10 producers", while carriers of the GCC haplotype (IL10-1087G, -824C, -597C) have been considered as "high IL10 producers", which is supported by studies of whole blood cultures and PBMCs as well as transient transfection studies (Crawley et al., 1999; Turner et al., 1997). This has been explained by the authors with data indicating that IL10-1087A/G occurs within a putative binding site for transcription factors from the Ets (E-twenty six) family of transcription factors. The other two polymorphisms lie in putative positive and negative regulatory regions, respectively and IL10-597A/C lies within a putative STAT3 binding site (Crawley et al., 1999; Kube et al., 1995).

Later on, gene variations in the more distal parts of the *IL10* gene have been proposed to be of higher importance (Gibson et al., 2001). The A-G/A-A haplotypes, formed by IL10-3538A/T, IL10-2812G/A and IL10-2726C/A showed lower IL10 production in whole blood cultures stimulated with LPS compared to the TGC haplotype (red box in Figure 1-3). Moreover, the GCC haplotype (IL10-1087G, -824C, -597C) was present in combination with A-G/A-A as well as TGC haplotype and not associated with high or low production of IL10 (green box in Figure 1-3).

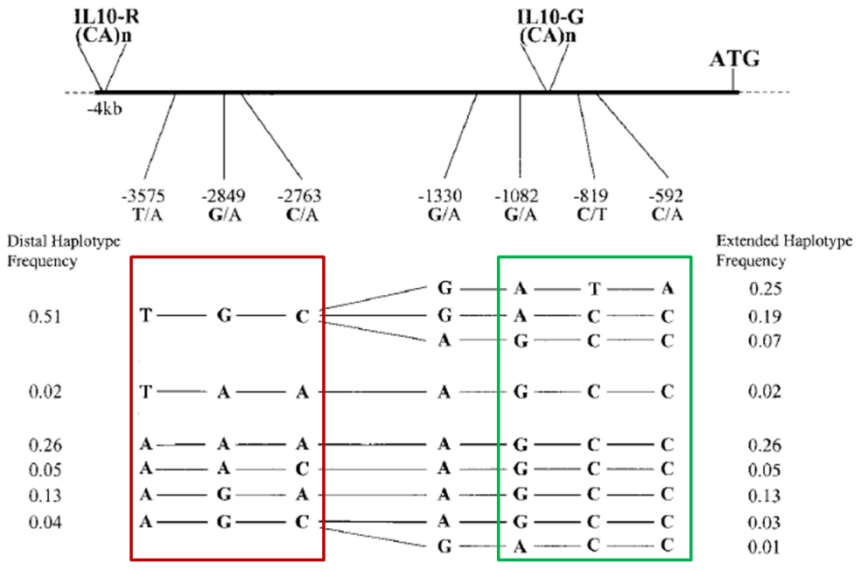

Figure 1-3 Distal *IL10* haplotypes defined by Gibson et al.

IL10 haplotype frequencies were defined in 52 Caucasian normal blood donors by Gibson et al. A scheme of the *IL10* 5'region is shown. The 7 SNPs genotyped in the blood donors as well as the two dinucleotide repeats IL10.R and IL10.D are indicated. The translation start site of the *IL10* gene is indicated by ATG. Beneath the scheme the estimated haplotypes are shown. Frequencies are given for distal (red box) and extended haplotypes. The proximal haplotypes originally found to influence *IL10* expression are emphasized by the green box. The figure is taken and modified from Gibson et al. 2001 (Gibson et al., 2001).

However, depending on the stimulus used for the induction of IL10, different *IL10* gene variations seem to be of importance (Mormann et al., 2004). In line with this, homozygous carriers of the deletion of the insertion/deletion gene variation at position -7400 (IL10-7400In/Del, see Figure 1-2) were characterized by a significantly higher IL10 production capacity compared to the other two genotypes in PBMCs stimulated with LPS (Rieth et al., 2004). The same trend has been observed for cAMP stimulated PBMCs or EBV immortalization (LCLs). However, in these groups the trend was not significant, which might be due to the rare number of homozygous carriers of the deletion. Notably, the IL10-7400Del allele is in strong linkage disequilibrium to the IL10-1087G allele. Both have been described to be associated with high IL10 production.

Taken together, the results of the implemented studies described above illustrate that regulatory gene variations within the *IL10* promoter could influence interindividual differences in IL10 production. However, data are still incomplete and an ultimate answer to the question which gene variations and haplotypes influence IL10 production under which conditions does not exist.

Interindividual differences in IL10 production and therefore *IL10* gene variations are thought to play a role for the establishment and outcome of certain diseases including aNHL. Therefore, a better knowledge and understanding of the influence of gene variations within the *IL10* gene locus on interindividual IL10 production is mandatory for the interpretation of survival analyses revealing associations between certain gene variation and the outcome of aNHL. The role of *IL10* gene variations as prognostic factors for aNHL outcome will be handled in the following chapter.

1.3 Gene variations and serum levels of IL10 as prognostic factors for NHL outcome

In recent years numerous studies have been undertaken to elucidate the role of gene variations in cytokine and cytokine receptor genes, possibly influencing the interindividual expression levels of the respective cytokine, for the susceptibility and the clinical course of malignant lymphoma as well as other types of cancer, autoimmune diseases or transplantation tolerance. Thereby numerous associations of gene variations with disease outcome have been reported.

In this context, the cytokine IL10 has been in the focus of a number of studies. Some reports provided evidence that the risk to develop lymphomas as well as the clinical outcome of aNHL patients could be related to some extent to defined *IL10* gene variations. (Breen et al., 2003; Cunningham et al., 2003; Habermann et al., 2008; Kube et al., 2008; Lech-Maranda et al., 2004; Rothman et al., 2006). The IL10-1087G allele has been found to be associated with a superior clinical outcome in DLBCL patients (Domingo-Domenech et al., 2007; Lech-Maranda et al., 2004), which could not be confirmed in two independent aNHL patient cohorts (Berglund et al., 2005; Kube et al., 2007). Moreover, the TGCC haplotype formed by IL10-3538T, IL10-1087G, IL10-824C and IL10-597C has been associated with a 2.4 enhanced relative risk of shorter overall survival (OS) (Habermann et al., 2008). In 2006 two controversial studies related to the IL10-3538A/T gene variation were published. A report from the InterLymph consortium found the IL10-3538A allele to be associated with an increased susceptibility to aNHL and in particular to DLBCL (Rothman et al., 2006). The same effect could not be detected in another study of 710 lymphoma patients in comparison to 710 healthy controls from a German study cohort (Nieters et al., 2006). These controversial results are probably caused by differences between the studied patient cohorts. They differed for example in study size, origin of population, histological subtypes and median age or other relevant clinical characteristics like an elevated LDH levels. This emphasizes the strong need for good, large prospective clinical trials to elucidate the role of *IL10* gene variations for aNHL outcome. Furthermore, it is not clear whether the studies conducted so far focused on the "right" *IL10* gene variations or if there might be other gene variations in linkage disequilibrium to the examined ones, bearing a higher value of information.

In the most recent study of the working group in which this thesis was conducted, an increased risk for patients suffering from aNHL and carrying gene variation IL10-7400DelDel for a worse clinical outcome has been observed. This was estimated by a significantly shorter OS in a cohort of 500 equally treated aNHL patients (Kube et al., 2008). The number of homozygous carriers of IL10-7400DelDel was very low. Therefore, more distal gene variations of *IL10*, located in putative regulatory regions like the CNS, with a higher frequency might be more informative in terms of treatment outcome prediction.

Little investigation has been conducted in the field of T-NHL, a very heterogeneous and very aggressive subgroup of NHL. Recently, significant associations between

IL10 gene variations and clinical outcome have been shown in an Asian cohort of 108 T-NHL patients (Lee et al., 2007). Patients carrying at least one allele of the ATA haplotype (IL10-1087AG,-824CT,-597AC) showed better overall survival (OS) and failure-free survival compared to those without ATA haplotype. The authors stated that even though a definite association with the response to chemotherapy was not proven, their data imply that IL10 may have some impact on the prognosis of T-NHL. This is a further crucial question, which should be answered in order to improve treatment strategies for this very aggressive NHL entity.

In addition to *IL10* gene variations the effects of IL10 serum levels prior to treatment has been assessed. In several studies, high levels of IL10 were associated with a poor outcome of lymphoma patients (Blay et al., 1993; Bohlen et al., 2000; Lech-Maranda et al., 2006). Whereby, in other studies on NHL patients the same effect could not be observed (Cortes et al., 1995; Ozdemir et al., 2004; Stasi et al., 1994). Notably, the opposite effect of a better treatment outcome associated with elevated IL10 serum levels has not been reported. The studies differed with respect to histological subtypes of included lymphoma, the number of patients as well as the assay used for the detection of IL10 serum levels. Elder studies could not discriminate between viral IL10 and human IL10 and the detection limit of those assays was very high (Cortes and Kurzrock, 1997). Moreover, the study sizes were relatively small by today's standards. Therefore larger trials are necessary to confirm the observation that elevated IL10 serum levels are associated with worse treatment outcome. Thereby, the question could be answered whether elevated IL10 serum levels could be used as clinically applicable prognostic markers for the outcome of aNHL or certain a NHL subtypes.

As described in detail below (chapter 1.4) the CD20 antibody Rituximab has the potential to directly down regulate IL10 and therefore Bcl-2 (Alas et al., 2001). This raises the possibility that Rituximab could overcome the adverse prognostic features of elevated IL10 serum levels. As Rituximab together with CHOP is the current standard therapy it would be highly interesting to asses this question. So far studies analyzing the effects of *IL10* gene variations or serum levels in patients treated with Rituximab are lacking.

1.4 Rituximab-mediated effects on immune responses against malignant cells

The effects of Rituximab are mediated by various immune responses against the malignant cells, complement-dependent cytotoxicity (CDC), antibody dependent cellular cytotoxicity (ADCC) (Reff et al., 1994) or antibody dependent cellular phagocytosis (ADCP) as well as direct apoptosis through CD20 crosslinking (Glennie et al., 2007; Shan et al., 2000).

CDC, ADCC and ADCP involve the binding of Fc-γR to Rituximab antibodies bound to CD20 on the surface of B cells. In CDC Rituximab activates the complement cascade, leading to the generation of a membrane attack complex that results in cell lysis.

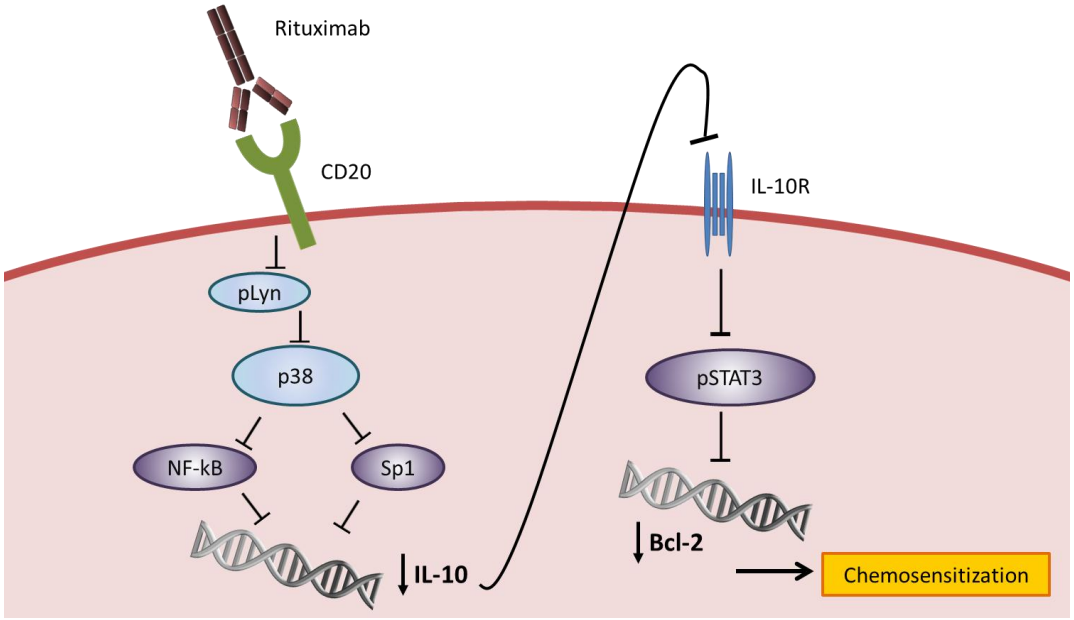

Figure 1-4 Rituximab-mediated inhibition of p38 and IL10 induces chemosensitization

The effects of rituximab treatment on inhibition of p38 MAPK activity and *IL10* transcription and secretion in 2F7 AIDS derived DLBCL cell line are shown. CD20 crosslink by Rituximab antibody leads to inhibition of constitutively active Lyn kinase and p38 MAPK, resulting in down-regulation of *IL10* expression via inhibition of SP1 and NF-κB. Decreased expression of *IL10* leads to inhibition of constitutively active STAT3, through IL10 - IL10R interactions, and therefore inhibition of Bcl-2 expression. This results in enhanced drug-induced apoptosis of the 2F7 cells. Lines ending in bars indicate inhibition. Arrows pointing downwards indicate down-regulation and arrow indicates activation. Figure was taken and modified from Bonavida et al. 2006 (Bonavida, 2006).

In ADCC the Fc-γR of NK cells binds to the Rituximab antibody attached to the tumor cell. By monitoring human leukocyte antigen class I (HLA class I) expression on the surface of target cells, NK cells discriminate between self and non-self. The release of granules containing pore-forming perforin and the cytotoxic granzymes A and B is activated by the absence of inhibitory signals due to an altered or absent HLA class I on transformed cells. This leads to the destruction of the tumor cells. Inhibitory signals are mediated by interactions of killer immunoglobulin-like receptors (KIR) on the NK cell with HLA class I molecules (Vilches and Parham, 2002). In ADCP the Rituximab antibody is bound by Fc-γR on the surface of monocytes and macrophages, which results in the engulfment of the antibody coated tumor cell (Ljunggren and Karre, 1990).

Studies on a DLBCL cell line indicated that Rituximab treatment leads to an enhanced sensitivity to chemotherapeutic drugs in drug-resistant tumors (Demidem et al., 1997). Later on Bonavida and colleagues could show that Rituximab mediates inhibition of the p38 MAPK, ERK1/2 and Akt signaling pathways, leading to down-regulation of the anti-apoptotic molecules Bcl-2 and Bcl-$_{xl}$ (Alas and Bonavida, 2001; Alas et al., 2001; Jazirehi et al., 2004; Suzuki et al., 2007; Vega et al., 2004). Inhibition of p38 MAPK signaling pathway, a pathway that induces IL10 via the Sp1 transcription factor, resulted in inhibition of *IL10* transcription and IL10 secretion in an AIDS related lymphoma cell line (Figure 1-4) (Vega et al., 2004). Inhibition of *IL10* expression leads to reduction of STAT3 phosphorylation and Bcl-2 expression (Alas and Bonavida, 2001; Alas et al., 2001). Notably, the same effect could not be observed in Ramos and Daudi cell lines (both human Burkitt's lymphoma). In these cell lines Rituximab inhibits the ERK as well as the PI3K-Akt pathway, leading to a down-regulation of anti-apoptotic Bcl-$_{xl}$ (Jazirehi et al., 2004; Suzuki et al., 2007). Both of these pathways also seem to be involved in *IL10* regulation (observation in macrophages). Due to the fact that the Ramos cell line does not express *IL10* without prior stimulation (observation of working group) and Daudi cells express only very low levels of IL10 (Samanta et al., 2008), the effects on *IL10* expression could not be assessed in these cell lines.

Aims of the Study

In order to adjust individual treatment strategies of aNHL patients, reliable and clinically applicable prognostic markers are needed, which improve the prognostic value of the IPI factors.

Previous studies suggested that the initiation or progression of lymphomas is supported by certain cytokines and their receptors, produced by lymphoma cells and/or cells in the tumor microenvironment. A number of studies have been performed to estimate the impact of inherited gene variations in cytokine or cytokine receptor genes on the susceptibility as well as clinical outcome of aNHL. In this context the anti-inflammatory cytokine IL10 has been investigated. Approximately 90% of aNHL originate from B cells, on which IL10 acts as a potent autocrine growth factor. Associations of *IL10* gene variations or elevated IL10 serum levels with the clinical outcome of aNHL have been assessed. However, results of these studies are controversial.

The fundamental questions arising from these studies are whether *IL10* gene variations and serum levels are predictive only for the clinical outcome of aNHL patients treated with CHOP or if they are also predictive for patients treated with Rituximab in addition to CHOP. Inherited *IL10* gene variations, located in distal conserved regions of the *IL10* gene locus, might be of prognostic relevance for treatment outcome. These gene variations might cause differences in interindividual IL10 production. Mechanisms contributing to *IL10* gene regulation in B cells have not gained much attention in studies conducted so far.

Therefore, this thesis aimed at answering the following questions:

- What is the prognostic relevance of *IL10* gene variations and IL10 serum levels for the outcome of aNHL in independent patient cohorts?
- Does the addition of Rituximab to CHOP therapy overcome adverse prognostic features reported for elevated IL10 serum levels?
- What is the effect of IL10 on lymphoma cells in Rituximab-mediated target cell killing?
- How do *IL10* gene variations affect interindividual IL10 production?

- Which molecular mechanisms contribute to the regulation of *IL10* gene expression in human B cells?

In order to answer these questions, DNA of aNHL patients derived from three different cohorts has to be genotyped on *IL10* gene variations, including gene variations within putative regulatory regions shown to be located in conserved noncoding sequences (CNS). The obtained data have to be compared to respective clinical parameters. In addition, this study aims in assessing the prognostic relevance of IL10 serum levels for patients treated with or without Rituximab.

EBV infected, immortalized lymphoblastoid cell lines (LCL) are characterized by different IL10 production. Therefore, this study examines the influence of *IL10* gene variations on interindividual IL10 production using LCLs.

To acquire a deeper knowledge about molecular mechanisms of *IL10* gene regulation, different B cell lines with inducible or constitutive *IL10* expression will be used for chromatin immunoprecipitation (ChIP) experiments. In addition to this, transcription of ncRNA from CNS will be examined.

Moreover, this study aims in examining the influence of IL10 on lymphoma cells in Rituximab-mediated CDC and ADCC after preincubation with IL10 as well as in cells with different *IL10* expression levels.

2 Material and Methods

2.1 Biological Material

2.1.1 cell lines

Cell lines used for this thesis are listed in table 2-1.

Table 2-1 Cell lines

Cell line	Source	Reference
Balm3	B cell, diffuse lymphocytic lymphoma (EBV negative)	(Lok et al., 1979)
BHK	baby (Syrian) hamster kidney cells	(Macpherson and Stoker, 1962)
BHK-CD40L	BHK, stably transfected with CD40L expression plasmid	(Macpherson and Stoker, 1962)
BJAB	B cell, Burkitt's lymphoma (EBV negative)	(Menezes et al., 1975)
BL2	B cell, Burkitt Lymphoma (EBV negative)	(Kube et al., 1995; Nilsson and Ponten, 1975)
Karpas422	B cell, Diffuse Large B cell lymphoma	(Dyer et al., 1990)
L428	Hodgkin lymphoma	(Schaadt et al., 1979)
MC116	B cell, lymphoma undifferentiated	(Magrath et al., 1980)
Ramos	B cell, Burkitt Lymphoma (EBV negative)	(Klein et al., 1975)
SuDHL4	B cell, Diffuse Large B cell lymphoma	(Epstein et al., 1976)
OCI Ly1	B cell, Diffuse Large B cell lymphoma	(Epstein et al., 1978)
OCI Ly3	B cell, Diffuse Large B cell lymphoma	(Tweeddale et al., 1989)

Lymphoblastoid cell lines (LCL) were obtained via immortalization of B cells with EBV using supernatant of the marmoset cell line B95-8 cell line as described in 2.9.2. Approximately 130 LCLs have been established in the context of previous studies from Prof. Dr. Kube (numbered 4/1-183/8). In addition 8 LCLs from the HapMap project were provided by Dr. Mladen Tzvetkov and 6 LCL were established during this thesis (numbered 191-202).

2.1.2 Lymphoma Patients

For the analysis of the *IL10* gene variations, DNA of aNHL patients from different trials conducted by the DSHNHL has been used. The NHL-B trial (Pfreundschuh et al., 2004a; Pfreundschuh et al., 2004b), The RICOVER-60 trial (Pfreundschuh et al., 2008) and the MInT trial (Pfreundschuh et al., 2006). The study was conducted in accordance with the Declaration of Helsinki. The protocol was approved by the ethics review committee of each participating center. Patients were eligible if they had previously untreated, biopsy-confirmed aggressive non-Hodgkin lymphoma according to the Revised European-American Lymphoma Classification (translated into the World Health Organization [WHO] classification).

The NHL-B trial can be divided into the NHL-B1 and NHL-B2 trial which aimed in elucidating whether the addition of etoposide to CHOP therapy improved treatment response in young (age≤60) or elderly (age>60) aNHL patients respectively. The RICOVER-60 trial aimed in elucidating the effect of the addition of Rituximab to CHOP therapy in elderly patients (age>60), while the MInT trial assessed the same question in young patients (age≤60). The patient cohorts used for genotyping analyses followed by survival analyses were representative for the complete trials in terms of clinical (table 3-1A and 3-1B) and histological (table A-1A and A-1B) characteristics. For this thesis the terms “trial” or “complete” are used for patients from the original trial and the terms “cohort” or “included” refer to patients included into the described analyses. A total number of 1724 patient DNA samples have been genotyped for *IL10* gene variations. 942 patients included into these analyses were from the NHL-B; thereof 477 were from the NHL-B1 and 465 from the NHL-B2 trial. 498 patients derived from the NHL-B trial have been analysed previously with respect to *IL10* gene variations (Kube et al., 2008). The remaining 444 patients are described here as NHL-B_CCR-excluded cohort. 604 patients were from the RICOVER-60 trial and thereof 301 patients have been treated with CHOP and 303 have been treated with R-CHOP. In addition 178 patient DNA samples from the MInT trial have been analysed.

Patients included into the analysis of T-NHL patients were from the NHL-B and RICOVER-60 trials. 197 patients with mature nodal or extranodal biopsy-confirmed T cell or NK cell lymphoma were included within prospective clinical trials of the DSHNHL as described recently (Pfreundschuh et al., 2008; Pfreundschuh et al.,

2004a; Pfreundschuh et al., 2004b; Schmitz et al., 2010). Based on quality and availability of respective material 117 patients have been included into this study. Clinical and histological characteristics of the patients eligible for this study are shown in Table A-2.

2.2 Chemicals and Consumable supplies

Chemicals are listed in table 2-2. Chemical inhibitors are listed in table 2-3 and Consumables are listed in table 2-3.

Table 2-2 Chemicals

Chemical	Manufacturer
4-IPBA	Sigma-Aldrich, Munich GER
Agarose	Sigma-Aldrich, Munich GER
Acrylamid/Bisacrylamid 40%	BioRad, Munich GER
Ammonium sulfate	Merck, Darmstadt GER
Bradford solution	RothiQuant-Roth, Karlsruhe GER
Bromphenol Blue	Sigma-Aldrich, Munich GER
BSA	Serva, Heidelberg GER
Chelex 100	BioRad, Munich GER
Cyclosporin A	Bayer, Leverkusen GER
DEPC	Roth, Karlsruhe GER
3,3′-Dioctadecyloxacarbocyanine perchlorate (DiO)	Sigma-Aldrich, Munich GER
DMSO	Sigma-Aldrich, Munich GER
dNTP (dATP, dCTP, dGTP, dTTP)	Primetech LTD, Minsk Belarus
Ethanol (100%)	J.T. Baker, Deventer NL
Ethidiumbromid	Sigma-Aldrich, Munich GER
EDTA	Riedel-de Haën, Seelze GER
Fetal bovine serum (FBS) for cell culture medium A,C,D	Sigma-Aldrich, Munich GER
FBS for cell culture medium B	Sigma-Aldrich, Munich GER
Ficoll separating solution	Invitrogen, Karlsruhe GER
Full Range Rainbow Molecular Weight Markers RPN800	GE Healthcare, Munich GER
Formaldehyde	Sigma-Aldrich, Munich GER

Chemical	Manufacturer
Formic acid	Merck, Darmstadt, GER
G418	Roche, Mannheim GER
Glycerol	Roth, Karlsruhe GER
Glycin	Roth, Karlsruhe GER
Glyco Blue™	Applied Biosystems, Foster City USA
HEPES	Sigma-Aldrich, Munich GER
HiDi - Formamid	Applied Biosystems, Foster City USA
Iscove's modified Dulbecco's medium (IMDM)	Pan Biotech, Aidenbach GER
Isopropanol	Sigma-Aldrich, Munich GER
L-Glutamine	Sigma-Aldrich, Munich GER
Luminol	Sigma-Aldrich, Munich GER
LymphoPrep (Ficoll)	PROGEN Biotechnik GmbH, Heidelberg GER
Methanol 100% (p.a.)	J.T. Baker, Deventer NL
Milk powder	Roth, Karlsruhe GER
MTT (3-(4,5-Dimethyl-2-thiazolyl)-2,5-diphenyl-2H-tetrazolium bromide)	Sigma-Aldrich, Munich GER
Nonidet P-40 (Igepal)	Sigma-Aldrich, Munich GER
Penicillin/Streptomycin	Sigma-Aldrich, Munich GER
Phorbol 12-myristate 13-acetate (PMA) (Approx. 99% TLC)	Sigma-Aldrich, Munich GER
Phosphatase inhibitor Phospho- STOP	Roche, Mannheim GER
PMSF	Sigma-Aldrich, Munich GER
Ponceau S	Sigma-Aldrich, Munich GER
Protein A Sepharose	GE Healthcare, Munich GER
Propidium iodide	Sigma-Aldrich, Munich GER
Proteaseinhibitor-Mix Complete™	Santa Cruz biotechnology, Heidelberg GER
RPMI	Lonza, Basel CH
SDS	Merck, Darmstadt, GER
Sodium butyrat	Sigma-Aldrich, Munich GER
Sodium chloride	Merck, Darmstadt, GER
Sodium deoxycholat	Merck, Darmstadt, GER

Chemical	Manufacturer
Sodium pyruvate	Sigma-Aldrich, Munich GER
Sodium vanadate	Sigma-Aldrich, Munich GER
Spectra Multicolor Broad Range Protein Ladder	Fermentas, Frankfurt GER
SybrGreen	Roche, Grenzach GER
TEMED	Sigma-Aldrich, Munich GER
Thymidin-5'-^{3}H	GE Healthcare, Munich GER
Trehalose	Roth, Karlsruhe GER
Trisbase	Sigma-Aldrich, Munich GER
Triton-X-100	Roth, Karlsruhe Germany
Trypanblue 0.4% in PBS	GIBCO BRL, Life Technologies, Eggenstein GER
Tween-20	Merck, Darmstadt GER
Water HPLC grade	Merck, Darmstadt GER

Table 2-3 Chemical Inhibitors and Recombinant Proteins and Enzymes

Description	Manufacturer	Working concentration
Chemical Inhibitors		
Bisindolylmaleimide I (PKC)	Calbiochem/Merck, Darmstadt, GER	10nM
Ly294002 (PI3K)	Calbiochem/Merck, Darmstadt, GER	10µM
U0126 (ERK1/2)	Sigma-Aldrich, Munich GER	10µM
Recombinant Proteins		
recombinant human IL10	Peprotech, Hamburg GER	100ng/ml
Enzymes		
EcoRV	New England BioLabs, Frankfurt am Main GER	
HOT FIREPol (Hotstart DNA Polymerase) (5U/µl)	Solis Biodyne, Tartu Estonia	
Taq Polymerase (5U/µl)	Invitrogen, Karlsruhe GER	0.5 U/25µl
Taq Polymerase (5U/µl)	Primetech LTD, Misk Belarus	0.5 U/25µl
PlatinumTaq Polymerase (5U/µl)	Invitrogen, Karlsruhe GER	0.5 U/25µl
Proteinase K	Invitrogen, Karlsruhe GER	20µg/ml

Table 2-4 Consumables

Consumable	Manufacturer
ABI PRISM® 384-well clear optical reaction plate	Applied Biosystems, Foster City USA
ABI PRISM® 384-well reaction plate	Applied Biosystems, Foster City USA
ABI PRISM® Optical Adhesive Covers	Applied Biosystems, Foster City USA
Cell culture flasks	Sarstedt, Nümbrecht GER
Cryo Box	Nunc, Wiesbaden GER
Cryotubes	Nunc, Wiesbaden GER
Diethylaminoethyl-Cellulose	Whatman®, International Ltd UK
Falcon Tubes 15 ml	Sarstedt, Nümbrecht GER
Falcon Tubes 50 ml	Sarstedt, Nümbrecht GER
Filter Tips, 10 µl, 100 µl, 200µl, 1000 µl	Starlab, Ahrensburg GER
Flat bottom tube (screw cap)	Nunc, Wiesbaden GER
Heparin Monovettes	Sarstedt, Nümbrecht GER
MicroAmp Optical 96-well reaction plate	Applied Biosystems, Foster City USA
Sterling Nitrile Powder-Free Examination Gloves	Kimberly-Clark, Zaventem, Belgium
Pasteurpipettes	Sarstedt, Nümbrecht GER
Pipette Tips (wo filters) 100µl, 1000µl	Sarstedt, Nümbrecht GER
Plate septa 96-well	Applied Biosystems, Foster City USA
Reactiontubes 0.5ml	Sarstedt, Nümbrecht GER
Reactiontubes 1.5ml	Sarstedt, Nümbrecht GER
Reactiontubes 2.0ml	Sarstedt, Nümbrecht GER
Serological pipettes 5 ml	Sarstedt, Nümbrecht GER
Serological pipettes 10 ml	Sarstedt, Nümbrecht GER
Serological pipettes 25 ml	Sarstedt, Nümbrecht GER
Tissue culture plates, 6 well	Nunc, Wiesbaden GER
Tissue culture plates, 12 well	Nunc, Wiesbaden GER
Tissue culture plates, 24 well	Nunc, Wiesbaden GER
Tissue culture plates, 96 well, round bottom	Nunc, Wiesbaden GER
Tissue culture plates, 96 well, flat bottom	Nunc, Wiesbaden GER

2.3 Buffers, Solutions and Media

Buffers, solutions and media used for this work are listed in table 2-5.

Table 2-5 Buffers, Solutions and Media

Buffers, solutions and media	Receipt / Manufacturer
1x TE	10mM Tris/HCl (pH 7.4) 1mM EDTA
2x SDS loading dye	4% SDS 0.12 M Tris/HCl (pH 6.8) 200mM DTT Pipette Tip of 1% Bromphenolblue
4x loading buffer Roti®-Load	Roth, Karlsruhe GER
Cell culture medium A (Balm3, BHK, BJAB, Karpas422, LCLs, MC116)	RPMI-1640 10% (v/v) FBS 200U/ml Penicillin + 200µg/ml Streptomycin 4mM L-Glutamine
Cell culture medium A for BHK-CD40L	Cell culture medium A supplemented with 100µg/ml G418
Cell culture medium B (L428)	RPMI-1640 10% (v/v) FBS 200U/ml Penicillin + 200µg/ml Streptomycin 4mM L-Glutamine
Cell culture medium C (Ramos, Bl2)	RPMI-1640 10% (v/v) FBS 200U/ml Penicillin + 200µg/ml Streptomycin 4mM L-Glutamine 50 µM α-Thiolglycerol 20 nM BCS, 1 mM Sodium pyruvat
Cell culture medium D (OCI Ly 1 and OCI Ly 3)	IMDM 10% (v/v) FBS for OCI Ly 1 20% FBS for OCI Ly 3 200U/ml Penicillin + 200µg/ml Streptomycin 4mM L-Glutamine
ChIP Nelson buffer modified	50mM Tris/HCl (pH 7,5) 150mM NaCl 20mM EDTA (pH 8) 0.5% NP-40 (IGEPAL) 1% Triton-X-100 20mM NaF (only necessary for phosphorylation) add 0.5mM DTT fresh add Roche Protease inhibitor cocktail fresh add inhibitors fresh
ChIP Gomes Lysis buffer	50mM Tris/HCl (pH 8) 150mM NaCl 20mM EDTA (pH 8) 1% v/v NP-40 (IGEPAL) 0.5% w/v sodium deoxycholate 0,1% w/v SDS 20mM NaF (only necessary for phosphorylation) add Roche Protease inhibitor cocktail fresh add inhibitors fresh

Buffers, solutions and media	Receipt / Manufacturer
ChIP Gomes Wash buffer	100mM Tris/HCl (pH 8.5) 500mM LiCl 20mM EDTA (pH 8) 1% v/v NP-40 (IGEPAL) 1% w/v sodium deoxycholate 20mM NaF (only necessary for phosphorylation)
ChIP SDS-Lysis buffer	50mM Tris/HCl (pH 8.1) 10mM EDTA 1% w/v SDS add Roche Protease inhibitor cocktail fresh add inhibitors fresh
Enhanced Chemiluminescence solution (ECL), self-made	Luminol-solution+ Peroxide-solution (1:1)
EDTA cell culture grade	0.5 M, Sigma-Aldrich, Munich GER
Freezing medium	90% (v/v) FBS (Biochrom, Berlin GER) 10% (v/v) DMSO (Sigma-Aldrich, Munich GER)
LB-agar	1.5% (w/v) Agar in LB-medium
LB-Medium	0.5% (w/v) Sodium Chloride 0.5% (w/v) Yeast Extract 1% (w/v) Bacto-Trypton 100µg/ml Ampicillin
Laemmli buffer (2x)	187.5 mM Tris/HCl (pH 6.8) 6.0% (w/v) SDS 30.0% (v/v) Glycerin 0.01% (w/v) Bromphenolblue 10% (v/v) ß-Mercaptoethanol
Luminol-solution (for ECL)	100mM Tris/HCl (pH 8.8) 2.5mM Luminol 4mM 4-IPBA, dark 4°C
MTT solution I	5mg/ml MTT in PBS store at 4°C, dark
MTT solution II	33% DMSO 5% formic acid 62% Isopropanol store at RT, dark
PBS pH 7.4 (cell culture grade)	Lonza, Basel CH
Peroxide-solution (for ECL)	100mM Tris/HCl (pH 8.8) 10.6mM H_2O_2, dark 4°C
Ponceau-S	5 % (v/v) glacial acetic acid 0.5 % (w/v) Ponceau-S
RIPA buffer	1x PBS pH 7.4 1% (v/v) Igepal 0.5% (w/v) Sodium-deoxycholat mg/ml PMSF (solved in isopropanol) 1 mM Soduim-Orthovanadat Complete-Solution (40 µl stock solutiuon for 1 ml RIPA; stock solution: 1 tablet for 1.5ml H_2O,
Running buffer (1x):	25mM Tris-Base 192mM Glycin 34.67 mM SDS
Separation Gel Mix	31.3 % (v/v) Acrylamid/Bisacrylamide Solution (40 %) 332 mM Tris Base, pH 8,9 3.33 mM EDTA

Buffers, solutions and media	Receipt / Manufacturer
Stacking Gel Mix	15 % (v/v) Acrylamid/Bisacrylamid Solution (40 %) 125 mM Tris Base pH 6.8 0.1 % (w/v) SDS 5 mM EDTA
SYBR Green Mix	1x SYBR Green PCR buffer 3mM MgCl2 (supplied with HOT FIREPol®) 1:80000 SybrGreen 0.2 mM dNTP each 20 U/ml Hot FIREPol® 0.25 % TritonX-100 0.5 mM Trehalose, in 10mM Tris-HCl pH 8,0
SYBR Green PCR-buffer 10x	750 mM Tris-HCl pH 8.8 200 mM Ammonium sulfate 0.1% Tween-20 in depc water
TAE (10x)	400mM Tris 0.01M EDTA (pH 8.3)
TBS (1x)	20mM Tris-Base, 137mM Sodium Chloride (pH 7.6)
TBS-T	1x TBS 0.1% (v/v) Tween-20
Transfer buffer	25mM Tris-Base 192mM Glycin 15% (v/v) MeOH

2.4 Equipment

Table 2-6 Equipment

Instrument	Manufacturer
Genetic Analyser 3130	Applied Biosystems, Foster City USA
ABI PRISM 7900HT	Applied Biosystems, Foster City USA
Accu-jet	Brand, Hamburg GER
Biofuge Pico	Heraeus Instruments, Hanau GER
Biorupter™ Next Gen	Diagnode, Liège, Belgium
Biometra TI 3	INTAS, Göttingen GER
Electrophoresis Power Supply	Invitrogen, Karlsruhe GER
FACSCanto™ Flow Cytometer	Becton Dickinson, Heidelberg GER
Freezer -20	Liebherr GER
Freezer -150 Ultra low VIP+	Sanyo, San Diego USA
Fridge 4°C	Linder
IKA KS 260 shaker	IKA, Staufen GER
IKAMAG RCT magnetic stirrer	IKA, Staufen GER
Incubator Heracell	Heraeus Instruments, Hanau GER

Instrument	Manufacturer
Incudrive incubator	Schütt Labortechnik, Göttingen GER
Inotech Cell Harvester,	Wallac Distribution Freiburg
LAS-4000 Image Reader	Fujfilm, Düsseldorf GER
Microcoolcentrifuge 1-15k	Sigma, Munich GER
Multifuge 3 L-R	Heraeus Instruments, Hanau GER
NanoDrop™	ND-1000 UV/Vis-Spektralphotometer, Wilmington USA
Neubauer Counting Chamber Improved	Lo Labor Optik, Friedrichsdorf GER
Power Pac 300 Power Supply	Bio-Rad, München GER
Robocycler Gradient 96	Agilent Technologies, Waldbronn GER
Roller Mixer RM5	Hecht Assistant, Sondheim GER
Stuart SRT 6 horizontal roller	Sigma-Aldrich, Munich GER
Sunrise^{TM} Microplate Reader	Tecan, Crailsheim GER
Televal 31 inverse light optical microscope	Zeiss, Jena GER
MaterCycler Eppendorf 384-well gradient	Eppendorf, Hamburg GER
Thermocycler T3000	Biometra, Göttingen GER
Thermomixer Compact	Eppendorf, Hamburg GER
Vortex Genie 2	Schütt Labortechnik, Göttingen GER
Water bath	Köttermann Labortechnik, Hänigsen GER

2.5 Oligonucleotides

Primers used for qRT-PCR are listed in Table 2-7 (chapter 2.5). Primers used for Taqman assay are listed in Table 2-8. Primers used for Snap-shot are listed in Table 2-9.

Table 2-7 Primers for qRT-PCR

Gene	Oligonucleotide
abl	fwd 5´-AGCCTGGCCTACAACAAGTTCTC-3´
	rev 5´-GACATGCCATAGGTAGCAATTTCC-3´
ACTB-TSS	fwd 5'-CGTTCCGAAAGTTGCCTTTT-3'
	rev 5'-CCGCTGGGTTTTATAGGGC-3'

Gene	Oligonucleotide
beta2 microglobulin (β2m)	fwd 5´-CTATCCAGCGTACTCCAAAGATTCA-3´
	rev 5´-TCTCTGCTGGATGACGTGAGTAAA-3´
ChIP_IL10+6800	fwd 5′-AGCAATAAGATGGCATTATTGCTGT-3′
	rev 5′-TGACTATCAGCTTCCTCTTGGAGAA-3′
ChIP_IL10-AP1(+6000bp)	fwd 5'-CAGGCTGTGGTCAGTTTTTCAGT-3'
	rev 5'-GTTTCCCACTTCCTTCCTATGGTTA-3'
ChIP_IL10+5876fwd	fwd 5'-AGCCCCGTGACTTAGAGGAGAG-3'
	rev 5'-TACTGAAAAACTGACCACAGCCTG-3'
ChIP_IL10+1020	fwd 5'-GCAAATGAAGGATCAGCTGGGAC-3'
	rev 5'-CCTCCAGCAAGGACTCCTTTAAC-3'
ChIP_IL10_TATA	fwd 5'-TGGCTTTTTAATGAATGAAGAGGC-3'
	rev 5'-TGTAGACCTTCACCTCTCTGTCCC-3'
ChIP_IL10-TSS	fwd5'-AAAAGGGGGACAGAGAGGTG-3'
	rev 5'-TCACCCCAGTCAGGAGGAC-3'
ChIP_IL10-597	fwd 5'-GAGCCTGGAACACATCCTGTG-3'
	rev 5'-CCCTTCCATTTTACTTTCCAGAGAC-3'
ChIP_IL10-SP1 (-1000bp)	fwd 5'-CACACAAATCCAAGACAACACTACTAAG-3'
	rev 5'-AGAAGTTGAAATAACAAGGAAAAGAAGTC-3'
ChIP_IL10-1087	fwd 5'-GCTCCCCTTACCTTCTACACACAC-3'
	rev 5'-GGAGGTCCCTTACTTTCCTCTTACC-3'
ChIP_IL10-2812	fwd 5'-GTGGCTCATGCCTGTAATCTCAG-3'
	rev 5'-GTTAACCAGGATGGTCTCGATCTC-3'
ChIP_IL10-3538	fwd 5'-GGGATGGAAGAAGAGAGGTATTCC-3'
	rev 5'-CAAGCCCAGATGCATAGTAGGC3'
ChIP_IL10-HSS4.5	fwd 5'-GCCTGATTTGGTGCCATAGTTG-3'
	rev 5'-TGATCTTTGGGCAGCCAATG-3'
ChIP_IL10-7400fwd	fwd 5'-GAAGGAACATCTGAGCTGAGAGCT-3'
	rev 5'-TACATTGCACCAGCCACTATGC-3'
ChIP_IL10-11668fwd	fwd 5'-CCTCCTAAATGCCTGAGCCAG-3'
	rev 5'-GGATCTGAAGACTTGGAACAGACC-3'

Gene	Oligonucleotide
ChIP_IL10-11777fwd	fwd 5'-GGGCATTAGCTTTGGAAATCTTC-3' rev 5'-CAGCCCTGGACCTTCTACTATGAG-3'
ChIP_IL10-12806fwd	fwd 5'-CAATGGTTGCCACTCAAGTCC-3' rev 5'-CTTGGATCCTTGAAGGAGGGTC-3'
ChIP_IL10_CNS-12	fwd 5'-GATTGCGAGAAGGAAATACAGGTG-3' rev 5'-AGCTCATAGCTTCTGCCCAGC-3'
ChIP_IL10-14.300	fwd 5'-ATATGAAGAGCTCAGCATCCCTTG-3' rev 5'-AACTTGCTTCTCTATTGGCTGCA-3'
ChIP_IL10-16.400	fwd 5'-CATCCTCAACTTTCTGGAATCTGTG-3' rev 5'-TGTCTCAACCTAAGGCAGTGCA-3'
hIL10_9133	fwd 5'-GAGGAAGCAACTGCATCTTCATG-3' rev 5'-TCATCCTGCCCATTCTGGTC-3'
hIL10_8583	fwd 5'-ACACTGTGACACTCATGGATCAGAG-3' rev 5'-GAATTGGGAATGATAGTGAGGGTG-3'
qRT-IL10-e1-2	fwd 5'-AACCTGCCTAACATGCTTCGAG-3' rev 5'-AACAAGTTGTCCAGCTGATCCTTC-3'
-7400forward IL10 -7400reverse neu	fwd 5'-GAAGGAACATCTGAGCTGAGAGCT-3' rev 5'-TTGAACTCCTAGGCTCAAGTAATCCT-3'

Table 2-8 Primers used for Taqman genotyping assay

gene variation	rs-number	Allels	Assay details / Primers	
IL10-6752	rs6676671	T=Vic; A=Fam	FW: AGCTCAGGGCCTTTGCA REV: TGAGAAAAGACAAGTTAAGGGTGCAT Vic-Probe: CATACCAGTGATGGCCCA Fam-Probe: ATACCAGTGTTGGCCCA	*
IL10-6208	rs10494879	G=Vic; C=Fam	C__26593071_10	**
IL10-3538	rs1800890	T=Vic; A=Fam	C___8828790_10	**
IL10-1087	rs1800896	A=Vic; G=Fam	C___1747360_10	**

IL10-824	rs1800871	C=Vic T=Fam	FW: GAGGAAACCAAATTCTCAGTTAGCA Rev: TTATAGTGAGCAAACTGAGGCACAG Vic-Probe: AGGTGATGTAACATCT Fam-Probe: AGGTGATGTAATATCT	***
IL10-597	rs1800872	A=Vic; C=Fam	FW: GGTAAAGGAGCCTGGAACACATC REV: GCCCTTCCATTTTACTTTCCAGAG Vic-Probe: CTGGCTTCCTACAGTAC Fam-Probe: TGGCTTCCTACAGGAC	***

* Applied Biosystems Darmstadt Germany; Custom made assay,
** Applied Biosystems Darmstadt Germany; Validated assay,
*** Eurogentec Seraine Belgium

Table 2-9 Primers used for SNaPshot assay

gene variation	rs-number	alleles	Assay details / Primers	
IL10 -12 kb	rs17015865 rs4072227 rs4072226		fwd: 5'-CTGTCCCAGCTCACAGATCA-3' rev: 5'-GTTTCACGAAAGCGGCTAAG-3'	*
IL10 -3 kb	rs1800890 rs6703630 rs6693899		fwd: 5'-TATTTTGGAGCAGGGATGGA-3' rev: 5'-ATGTCAGGGAGAAGGGAGGT-3'	*
IL10+4 kb	rs3024498 rs3024505		fwd: 5'-AAGCCTGACCACGCTTTCTA-3' rev: 5'-AAACTGACCACAGCCTGTCC-3'	*
IL10-12806	rs17015865	C=black T=red	Primer 5' 5'-GACTAGATCGATCGATCGATTATGTTTGTGTTCCATGGGT(C/T) -3'	**
IL10-11777	rs4072227	A=green G=blue	Primer 5' 5'-AGCCCTTGGATTATTGATGCAGCCCTTGGATTATTGATGC(A/G) -3'	**
IL10-11668	rs4072226	A=green G=blue	Primer 5' 5'-GATCGATCGATCGATCGATCGATCAGCCTGAGCCAGTCAGTCTTTCTACT(A/G) -3'	**
IL10-3538	rs1800890	A=green T=red	Primer 5' 5'-GATCGATCGATCGATCCAGTACATCCCCCACTGGAAAAAT-3'	**
IL10-2812	rs6703630	A=red G=black	Primer 3' 5'-GATCGGTCTCGATCTCCTGACCTTATGATC-3'	**
IL10-2726	rs6693899	A=red C=blue	Primer 3' 5'-GATCGATCGATCGATCGATCGATCAGGCGCCTGGCACCACGCCCGGCTAA-3'	**
IL10+4259	rs3024498	A=red G=black	Primer 3' 5'-GATCCTGGTTTCTCTTCCTAAGAGTATTTG(T/C)-3'	**

*IBA Göttingen Germany
**MWG Ebersberg Germany

2.6 Antibodies

Antibodies used for Immunoblot analysis, ChIP and FACS are listed in Table 2.10.

Table 2-10 Antibodies

Antibody	Manufacturer	Working Dilution
ChIP		
anti IgG ChIP grade (ab46540)	abcam, Cambridge UK	2µg/IP
anti acH3 ChIP grade (06-599)	Millipore, Schwalbach GER	2µg/IP
anti H3K4me1 ChIP grade (ab8895)	abcam, Cambridge UK	2µg/IP
anti-H3K4me3 (07-473)	Millipore, Schwalbach GER	2µg/IP
Immunoblot		
mouse monoclonal anti-tubulin (#05-829)	Upstate/Millipore, Schwalbach GER	1:5000 in 3% milkpowder in TBS-T
rabbit anti p-STAT3 (Ser727) (#9134)	Cell Signalling/ New England Biolabs, Frankfurt am Main GER	1:1000 in 3% BSA in TBS-T
rabbit anti-STAT3 (#9132)	Cell Signalling/ New England Biolabs, Frankfurt am Main GER	1:1000 in 3% BSA in TBS-T
anti-LMP1	Cell Signalling/ New England Biolabs, Frankfurt am Main GER	1:1000 in 3% BSA in TBS-T
FACS		
anti-mouse HRP polyclonal goat (D1609)	Santa Cruz, Heidelberg GER	1:5000 in 3% milkpowder in TBS-T
anti-rabbit HRP polyclonal goat (E1710)	Santa Cruz, Heidelberg GER	1:1000 in 3% BSA in TBS-T
anti-CD20 FITC	Becton Dickinson, Heidelberg GER	1:20 in Medium
anti-CD56	BD Biosciences Heidelberg GER	1:20 in Medium
anti-CD3 PE	Beckmann Coulter, Krefeld GER	1:20 in Medium
anti-CD16 PE	BD Biosciences Heidelberg GER	1:20 in Medium
anti-HLA PE, Monoclonal Mouse Anti Human HLA-ABC Antigen/RPE clone W6/32	Dako, Stockport UK	1:20 in Medium

2.7 Plasmids

Plasmids used for qRT-PCR as Standards are listed in Table 2-11.

Table 2-11 Plasmids

Plasmid	Description
pCR2.1 Topo-IL10e1-2	control vector for qRT-PCR containing PCR product of qRT-IL10-e1-2
pCR2.1 Topo-β2m	control vector for qRT-PCR containing PCR product of β2m primers

2.8 Ready to use Reaction Systems

In Table 2-12 the used ready to use reaction systems are listed.

Table 2-12 Ready to use reaction systems

Description	Manufacturer
BigDye Terminator Cycle Sequencing-Kit v1.1,	Applied Biosystems, Foster City USA
EndoFree® Plasmid Maxi Kit	Qiagen, Hilden GER
Human IL10 ELI PAIR	Diaclone, Giessen GER
innuPREP DYEpure Kit	Analytik Jena, Jena GER
NK cell isolation Kit II	Miltenyi Biotec, Bergisch Gladbach GER
Nucleo Spin RNA II	Machery+Nagel, Düren GER
Rneasy® Plus Mini Kit	Qiagen, Hilden GER
Superscript II™ RT Kit	Invitrogen, Karlsruhe GER
TOPO TA cloning® Kit	Invitrogen, Karlsruhe GER
QIAamp® DNA Mini Kit	Qiagen, Hilden GER
QIAEX II Agarose Gel Extraction Kit	Qiagen, Hilden GER
QIAGEN Plasmid Mini Kit	Qiagen, Hilden GER
QIAshredder	Qiagen, Hilden GER
QIAquick PCR purification Kit	Qiagen, Hilden GER

2.9 Cell Biology

2.9.1 Cell culture techniques

All cell lines were cultured at 37°C, 5% CO_2 and were splitted every second day according to proliferation rate, observed via cell density. If not otherwise indicated B cell lines were cultured in cell culture medium A (for detail see table 2-5) in a density between $5x10^5$/ml- $1x10^6$/ml. The Hodgkin cell line L428 was cultured in cell culture medium B in a density between $5x10^5$/ml- $1x10^6$/ml. Burkitt's lymphoma cell lines were cultured in cell culture medium C in a density of $3x10^5$/ml- $1x10^6$/ml. OCI Ly1 and OCI Ly3 were cultured in cell culture medium D supplemented with 10% FBS or 20% FBS respectively in a density between $5x10^5$/ml- $1x10^6$/ml. The adhesive cell line BHK was cultured in cell culture medium A, supplemented with 100µg/ml G418 for BHK-CD40L for selectively culturing neomycin resistant cells. Cells were counted in a Neubauer counting chamber diluted 1:1 with PBS 0.4% Trypanblue.

To freeze cells, approximately $1x10^7$cells were sedimented (centrifugation 250xg/8min/RT) and resuspended in 1ml freezing medium. Cryo boxes containing isopropanol were used for a constant cooling of 1°C/min till -80°C. Frozen aliquots were stored at -150°C. To thaw cells for cultivation, a frozen aliquot was thawed and washed in 10ml of RT cell culture medium. The cells were sedimented as described above and resuspended in 5-10ml of the respective cell culture medium.

2.9.2 EBV immortalization of B cells

For the establishment of lymphoblastoid cell lines (LCLs), peripheral blood mononuclear cells (PBMCs) were isolated from peripheral blood of voluntary donors (buffy coats) and immortalized by EBV infection. Peripheral blood of voluntary donors (50ml) was separated by centrifugation (1300xg/10min). PBMCs interphase (white ring) were transferred to a new tube and diluted with 0.9% sodium chloride. 15ml ficoll separating solution was overlayed carefully with 35ml diluted PBMCs and centrifuged at 850xg for 20 min. The interphase, containing PBMCs was transferred to a new tube (without toxic ficoll). After centrifugation at 90xg for 10min the supernatant was discarded and the cells were washed twice in 35ml 0.9% sodium chloride. In a final step the cells were resuspended in cell culture medium A in a density of $1x10^6$ cells/ml. 1ml of PBMCs suspension was placed into a flat bottom

tube and 1ml of sterile filtered (0.2µm) Epstein-Barr-Virus (EBV) supernatant from a B95-8 marmoset cell line was added (incubation at 37°C, 5% CO_2 overnight).

On the next day 1.4ml fresh cell culture medium A, supplemented with 2µg/ml of Cyclosporin A was added for 7 days culture. Cyclosporin A suppresses T cell growth, preventing the elimination of EBV infected B cells. Approximately after 7 days half of the supernatant was discarded and filled up with fresh cell culture medium A supplemented with 1µg/ml of Cyclosporin A. As soon as LCLs formed clusters and grew densely, they were transferred into 25 cm^2 culture flasks. Cultivation continued for several weeks by using cell culture medium A.

2ml of the peripheral blood were used for DNA preparation (2.11.1).

2.9.3 Stimulation of L428 cell line with PMA

PMA (powder) had to be dissolved in 100% Ethanol with a final concentration of 1mg/ml and aliquots were stored at -20°C. Directly prior to stimulation PMA was diluted 1:100 in respective cell culture medium (10ng/µl).

24h prior to stimulation, cells were seeded in an optimal cell density in fresh cell culture medium. This was $5x10^5$ for L428 in cell culture medium B (incubation 37°C, 5% CO_2). After 24h cells were sedimented (centrifugation 250xg/8min/RT), counted and adjusted to a density of $5x10^5$/ml in fresh medium. A respective amount of cells (i.e. $1x10^6$ cells for RNA preparation) was stimulated with 2µl PMA/ml cells (20ng PMA/ml cells) or left untreated for control. Enough cells for each required time point had to be stimulated. In case of chromatin immunoprecipitation (chapter 2.11.10) stimulation was conducted in separate flasks. The cells were incubated for 1h at 37°C and 5% CO_2. Subsequently, they were sedimented (centrifugation 250xg/8min/RT) and resuspended in fresh medium in a density of $5x10^5$/ml. If very high amount of cells were used, the control samples were resuspended in (1h) old medium. This was followed by cultivation of cells for indicated times (counted from stimulation of the cells). Subsequently, cells were harvested according to the respective application.

2.9.4 CD40 crosslink using BHK-CD40L

BHK cells were cultivated in Cell culture medium A, supplemented with 100µg/ml G418 for BHK-CD40L. In this medium, only stably transfected cells with neomycin resistance were able to proliferate. Prior to usage of BHK-CD40L cells for stimulation, two passages without G418 should have been done. Adherent BHK cells were splitted by adding 1ml 5mM EDTA in PBS to cells, after taking away all cell culture medium. Cells were incubated approximately 1min at 37°C and rinsed from the bottom of the cell culture flask with 10ml PBS. After sedimentation (300xg/5min/RT) cells were resuspended in 10ml cell culture medium. A respective amount of cells was seeded into a fresh cell culture flask.

For stimulation, $5x10^5$ cells were seeded on 6 well plates in 3ml of cell culture medium A, 24h prior to stimulation. At the same time point, cell lines that had to be stimulated were seeded in an optimal cell density in fresh medium. This was $3x10^5$/ml for Ramos. On the next day medium was taken away from BHK cells carefully and $1x10^6$ Ramos cells were added in 3ml fresh cell culture medium B. Cells were harvested for RNA preparation (2.11.6) after the indicated time points.

2.9.5 Inhibitor treatment

For analyses of pathways involved in *IL10* gene regulation in L428, cells were treated with inhibitors listed in table 2-3.

24h prior to stimulation, L428 cells were seeded in a density of $5x10^5$/ml. On the next day, 3ml L428 in a density of $5x10^5$/ml were treated with 10nM (1:242) Bisindolylmaleimide I (PKC Inhibitor), 10µM U0126 (ERK Inhibitor) or Ly294002 (PI3K Inhibitor) or respective dilutions of the solvent DMSO as a control for 3 h prior to PMA stimulation. Cells were stimulated with PMA and washed after one our according to procedure described in 2.9.3. After the washing step, fresh inhibitor and DMSO were added to the cells. After 12h PMA stimulation, cells were harvested for RNA preparation (2.11.6) and Immunoblot analyses (2.10.3) to check pathway activity.

2.9.6 Treatment with IL10

24h prior to stimulation with IL10, cells have been seeded in an optimal cell density ($3x10^5$/ml for Burkitt's lymphoma cell lines, $5x10^5$/ml for DLBCL cell lines) in fresh cell culture medium. For IL10 stimulation cells have been sedimented (centrifugation 250xg/8min/RT), resuspended in fresh medium in required densities and stimulated with 100ng IL10/ml cells (stock 5ng/µl).

2.9.7 Rituximab treatment of B cell lines

24h prior to stimulation with Rituximab, cells have been seeded in an optimal cell density ($3x10^5$/ml for Burkitt's lymphoma cell lines, $5x10^5$/ml for DLBCL cell lines) in fresh cell culture medium. For Rituximab stimulation, the cells have been sedimented (centrifugation 250xg/8min/RT), resuspended in fresh medium in required densities and stimulated with indicated amounts of Rituximab (stock 10mg/ml). If necessary, Rituximab has been diluted in the respective cell culture medium prior to use.

2.9.8 MTT viability assay

MTT is a colorimetric assay for measuring the activity of enzymes that reduce MTT in living (viable) cells. 24h prior to MTT assay cells were seeded in optimal densities ($3x10^5$ Burkitt's lymphoma cell lines and $5x10^5$/ml for all other cell lines). On the next day cells were sedimented (centrifugation 250xg/ 8min/ RT) counted and $5x10^5$cells/ml were resuspended in respective cell culture medium. Respective cell culture medium was supplemented with human serum instead of FBS. 100µl cells were seeded on a round bottom 96-well plate. 100ng/ml of IL10 was added to respective samples as indicated (see 2.9.6). Indicated amounts of Rituximab were added (see 2.9.7). Plates were incubated at 37°C and 5% CO_2. 20h, 44h and 68h later 10µl MTT solution I was added to all samples and plates were incubated for another 4h at 37°C and 5% CO_2. During this time the yellow MTT was converted into blue formazan by mitochondrial reductases. Subsequently, the plates were centrifuged to pellet the cells and supernatant was removed carefully. 100µl of MTT solution II were added to each well. Plates were rocked until all cell agglutinations were solved. Viability of cells was determined by measuring the absorbance in SunriseTM Microplate Reader at 540nm with reference of 655nm.

2.9.9 Proliferation assay

The proliferation of cells has been determined using the ^{3}H-thymidin incorporation method. The radioactive nucleoside ^{3}H-thymidin is incorporated into new strands of chromosomal DNA during replication. Therefore radioactivity is proportional to the number of proliferating cells.

Cells have been prepared as for the MTT (see 2.9.8) but instead of a round bottom 96-well plate a flat bottom 96-well plate was used (incubation 37°C, 5% CO_2). 16h before the end of incubation 0,5µCi Thymidin-5'-^{3}H in 30µl cell culture medium have been added to each well. For harvesting the cells have been transferred on a filter paper, which was dried subsequently for 1h at 60°C. Radioactivity was estimated using a Liquid Scintillation-Counter.

2.9.10 Flow cytometry

Flow cytometry is used to analyse properties of cells. A laser beam of a specific wavelength is directed onto the single cells within a carrier liquid. The emitted fluorescent of each single cell is measured by detectors. The size of the cell is determined by the forward scatter and the granularity by the sideward scatter. Fluorescent dyes bound to the cell via specifically labeled antibodies can be excited and emit light of a specific wavelength. Fluorescent dyes used were Fluorescein (FITC; absorption maximum at 494nm; emission maximum of 521nm) and Phycoerythrin (PE; absorption maximum at 495nm; emission maximum at 575nm).

For the characterization of cell populations prior to ADCC, the cells were stained with respective antibodies (see table 2-10). 5µl antibody was added to 100µl cells ($5x10^5$/ml for cell lines, $1x10^6$/ml for NK cells). For ADCC propidium iodide (PI 0.1µg/ml) was added to the cells to detect lysed/dead cells.

2.9.11 ADCC

NK cell purification

$CD56^+$ and $CD3^-$ NK cells have been purified from peripheral blood of voluntary donors. NK cells were immunomagnetically selected using the NK cell Isolation Kit II. By use of this kit non-NK cells, i.e., T cells, B cells, stem cells, dendritic cells, monocytes, granulocytes, and erythroid cells, are magnetically labeled by using a

cocktail of biotin-conjugated antibodies and the NK Cell MicroBead Cocktail. Isolation of highly pure NK cells is achieved by depletion of magnetically labeled cells.

Therefore, peripheral blood was diluted 1:1 with PBS. Leukocytes were obtained via Ficoll (LymphoPrep) separation. Peripheral blood/PBS was given to the same amount of Ficoll and centrifuged 800xg, 20min without brake. The Phase containing leukocytes was taken off and washed once with PBS (centrifugation 250xg/10min) and MACS buffer (300xg/10min). $1x10^8$cells were resuspended in 400µl MACS buffer. 75µl of biotin-conjugated antibody mixture from the Kit was added to the cells and binds to all non-NK cells (rock 10min/ 4°C). 300µl MACS buffer together with 150µl magnetic-beats (Kit) were added (rock 15min/ 4°C). Mixture was washed with 25ml of MACS buffer meanwhile the column (LS. Kit) was equilibrated with MACS-buffer. Sample was diluted in 500µl MACS buffer and added on the column. Elution of NK cells was done three times with 3.5ml MACS-buffer. NK cells were sedimented and resuspended in cell culture medium in a density of $5x10^6$/ml. To increase cytotoxic activity of NK cells, they were cultivated with 5µl IL2/ml cells overnight (37°C, 5% CO_2). Purity of NK cells has been assessed by Flow cytometry (see chapter 2.9.10). NK cells had to be $CD56^+$, $CD3^-$, $CD20^-$ and $CD16^+$.

Target cell incubation with IL10

Karpas422 and Ramos were sedimented (centrifugation 250xg/8min/RT), counted and resuspended in fresh cell culture medium in a density of $3x10^5$/ml (Ramos) or $5x10^5$/ml (Karpas422) for 24h. For IL10 treatment, cells were sedimented (centrifugation 250xg/ 8min/ RT), counted and 2x $5x10^6$-$1x10^7$ cells were resuspended in fresh cell culture medium in a density of $5x10^5$/ml (Ramos) or $1x10^6$/ml (Karpas422) for stimulated and unstimulated cells. 100ng IL10/ml cells was added to one of two prepared flask with cells. After 12 hours cells were analysed by flow cytometry and had to be CD20 and HLA I positive. Target cells were subsequently stained with green fluorescence DiO. $1x10^6$ cells were resuspended in 1ml PBS. 5µl DiO (3mM) was added to cells (rock, 20min, 37°C). Cells were washed twice with PBS and resuspended in cell culture medium in a density of $1x10^6$/ml.

Cytotoxicity assay

NK cells were incubated with DiO-labeled target cells in a ratio of 2:1 (50µl NK cells ($2x10^6$/ml) + 50µl target cells ($1x10^6$/ml)) at 37°C and 5% CO_2 for 4h. Rituximab and IL10 were added as indicated in results. In addition target cells were incubated

without NK cells for determination of spontaneous lysis. NK cell-mediated cytotoxicity was assessed with flow cytometry after propidium iodide staining (50µg/ml). Lysed cells were propidium iodide positive, DiO stained target cells. Specific lysis was calculated as specific lysis (%) = (lysis of sample % -spontaneous lysis %) / (100-spontaneous lysis %) x100. ADCC was calculated as ADCC (%) = (specific lysis of sample incubated with Rituximab % - specific lysis of sample incubated without Rituximab %) / (100- specific lysis of sample incubated without Rituximab %) x100.

2.10 Protein Biochemistry

2.10.1 Preparation of cell lysates

For preparation of cell lysates for Immunoblot, cells were sedimented (250xg/10min/4°C) and washed in PBS, complemented with 100mM sodium orthovanadate. If not processed immediately, pellets were frozen at -20°C.

Pellets were thawed on ice and cells were suspended in RIPA buffer (see table 2-5) for lysis and incubated for 30min on ice. This was followed by centrifugation to sediment cell debris (14.000xg/15min/4°C). The protein concentration of the supernatant was determined via Bradford assay (Bradford, 1976) using a ready to use Bradford solution and photometrical quantification with the Sunrise™ Microplate Reader and Magellan™ software.

2.10.2 SDS-PAGE

For separation of proteins SDS-PAGE was used. Proteins get negatively charged through sodium dodecyl sulfate (SDS) treatment and can be separated by size using polyacrylamide gelelectrophoresis (PAGE).

Polyacrylamide gels comprised of a separation gel containing 10% and a stacking gel with 5% Acrylamide have been prepared using the BioRad System (München, GER). After pouring the separation gel, it was covered by Isopropanol to get a smooth surface and to protect it from drying out. After polymerization of the separation gel, the isopropanol was removed and the stacking gel was poured. 10-30µg of protein samples was suspended in 4x Roti®-Load loading dye buffer, denaturized for 5 min at 95°C and loaded onto the gel. The Fullrange rainbow™ marker was loaded in

addition for later determination of protein sizes. For the first 15min, a current of 20mA was used until all probes reached the border between stacking and separation gel. Subsequently, the current was set to 40mA for separation.

The Immunoblot technique was used to transfer separated proteins onto a nitrocellulose membrane. Separation gel, Nitrocellulose membrane (Hybond™-C extra, GE Healthcare, München GER) and whatman paper were equilibrated into transfer buffer and arranged in a pile as follows: Cathode (-), 2 whatman papers, separation gel, nitrocellulose membrane, 2 whatman papers, Anode (+). Using a Tank Blot system (BioRad, München GER) the proteins were blotted (100V, max. 300mA, 300W, 1h) onto the nitrocellulose membrane.

Subsequently, equal loading was controlled by staining the proteins with Ponceau S. To remove the stain, the membrane was washed with TBS-T and blocked with 5% milk powder in TBS-T for 1h at RT. Staining with primary antibodies was done by incubation at 4°C overnight. On the next day, the membrane was washed three times for 10min in TBS-T and incubated with the respective secondary antibody for 1h at RT. After washing the membrane three times for 10min with TBS-T, it was incubated with self-made ECL (see table 2-5) for 1min at RT. Proteins were detected using the chemiluminescence camera LAS-4000 Image Reader.

2.10.3 Enzyme-linked Immunosorbent Assay (ELISA)

To estimate the amount of human IL10 in sera derived from LCLs or patients, ELISA has been used. Sera derived from LCLs were stored at -20°C, patient sera at -75°C and have been thawed on ice directly before the analysis. For the detection of IL10 the Eli-pair ELISA, specific for human IL10, with a detection limit of 5pg/ml has been used according to the manufacturer's protocol. The absorption of the samples has been detected at a wavelength of 450nm using the Sunrise™ Microplate Reader and Magellan™ software.

2.11 Molecular Biology

2.11.1 Isolation of genomic DNA

For the isolation of genomic DNA from blood samples or cell lines, the QIAamp® DNA Mini Kit was used. The procedure has been performed according to the manufacturers' protocol. To enhance the amount of isolated DNA, the amount of used samples was doubled compared to the manufactures' protocol. DNA was eluted in 200µl H_2O and the concentration was determined using the NanoDrop. DNA was stored at 4°C.

2.11.2 Allelic discrimination via Taqman assay

Allelic discrimination via Taqman assay was used for the determination of certain single nucleotide polymorphisms (SNP) of *IL10*. In addition to two locus-specific primers, two fluorescence labeled probes are included into the PCR-reaction. These probes differ with respect to the nucleotide at the position of the SNP and the fluorescent label at the 5'-end (FAM or VIC). Both probes carry a quencher at the 3'-end. If the quencher is located close to the fluorescent dye, the fluorescence signal is repressed. The probes bind to the DNA template, containing the respective SNP. During the elongation step of the PCR the Taq polymerase destroys the probe by 5'-3' exonuclease activity and the fluorescent dye is released. Thereby, the fluorescent intensity of the respective dye increases and can be measured by the instrument (ABI PRISM 7900HT). Depending on the genotype the free fluorescent dyes FAM, VIC or both (heterozygous) are accumulated.

Assay and primer details for each analysed SNP are listed in table 2-8. The reaction has been performed on a 384-well plate in a volume of 5µl. The following reaction has been used.

Applied Biosystems mix: 2.5µl Taqman Genotyping Mastermix (2x), 0.25µl Taqman SNP genotyping assay, 1.25µl H_2O, 1µl genomic DNA (10ng/µl).

Self-made Mix: 2.5µl Taqman Genotyping Mastermix (2x), 0.20µl of each primer (22.5µM) and each probe (5µM), 0.7µl H_2O, 1µl genomic DNA (10ng/µl).

The following PCR-program has been used for the reaction (ABI PRISM 7900HT):

Table 2-13 PCR program Taqman

Initial denaturation	95°C 10min	
Denaturation	95°C 15s	
Annealing/Extension	60°C 1min	40 cycles

2.11.3 SNaPshot

The SNaPshot® Multiplex System (Applied Biosystems) was used for the determination of certain *IL10* SNPs. Therefore, DNA from patients and cell lines was used to amplify three different fragments containing the SNPs of interest (IL10-12kb, -3kb or +4kb). These PCR fragments were used in a primer extension reaction with fluorescent-labeled ddNTPs. SNP-specific primers of different length with the 3'-end directly adjacent to the respective gene variation were used. The analysis was than done using the AB3130 Genetic Analyser from Applied Biosystems.

The following reactions were used for the PCR of SNP containing fragments:

Table 2-14 PCR reaction Mix for SNaPshot

2.5µl	10xPuffer (10x supplied with Taq polymerase)
0.75µl	$MgCl_2$ (50mM supplied with polymerase)
0.5µl	dNTPs (10mM each)
0.5µl	rev. Primer (10µM)
0.5µl	fwd. Primer (10µM)
0,1 µl	Taq Polymerase (Invitrogen, Karlsruhe GER)
ad. 24µl	H_2O
plus 25-50ng genomic DNA	

For the PCR fragment containing IL10-11.668G/A, IL10-11.777A/G and IL10-12.806C/T, the following PCR program was used (Thermocycler T3000):

Table 2-15 PCR program used for amplification of the *IL10*-12kb fragment

Initial Denaturation	95°C 4min	
Denaturation	94°C 45s	
Annealing	63°C 1min	
Elongation	72°C 5min	10 cycles
Denaturation	95°C 45s	
Annealing	57°C 1min	
Elongation	72°C 2min 30s	25cycles
Elongation	72°C 1h	
Pause	4°C	∞

For the PCR fragment containing IL10-3538A/T, IL10-2849G/A, IL10-2763C/A, the following PCR program was used (Thermocycler T3000):

Table 2-16 PCR program used for amplification of the *IL10*-3kb fragment

Initial Denaturation	95°C 5min	
Annealing	58°C 3min	
Elongation	72°C 3min	
Denaturation	95°C 1min	
Annealing	58°C 1min	
Elongation	72°C 2min	10 cycles
Denaturation	95°C 1min	
Annealing	56°C 1min	
Elongation	72°C 2min	30 cycles
Elongation	72°C 10min	
Pause	4°	∞

For the PCR fragment containing IL10-4259A/G and IL10+5876C/T, the following PCR program was used (Thermocycler T3000):

Table 2-17 PCR program used for amplification of the *IL10*+5kb fragment

Initial Denaturation	95°C 5min	
Annealing	65°C 3min	
Elongation	72°C 3min	
Denaturation	95°C 30s	
Annealing	65°C 1min	
Elongation	72°C 2min	40cycles
Elongation	72°C 10min	
Pause	4°C	∞

After the PCR, the PCR-fragments had to be purified. This was done according to table 2-18.

Table 2-18 Purification of PCR fragments for SNaPshot reaction

1,5µl	Shrimp Alkaline Phosphatase Reaction buffer 10x (10xRxBuf)	
3,3µl	Shrimp Alkaline Phosphatase (SAP) 1u/µl	
0,2µl	Exonuclease I (Exo I) 10u/µl	
5µl	PCR-fragment -12kb	PCR-fragment -3kb
5µl	PCR-fragment +4kb	PCR-fragment TNF
Thermocycler T3000: Digestion 1h bei 37°C, heat inactivation 15min 80°C		

Pooled primer mixes (table 2-19), using primers listed in table 2-9 and the SNaPshot reaction mix (table 2-20) were prepared, before the SNaPshot reaction (table 2-21).

Table 2-19 Pooled primer mixes

	Pooled primer Mix IL10 -12800/+4259	**Pooled primer Mix TNF/IL10**
90µl	H_2O	H_2O
2,5µl	SNaPshot IL10-12806CT (100µM)	
2µl	SNaPshot IL10-11777AG (100µM)	SNaPshot IL10 -3538 (100µM)
2µl	SNaPshot IL10+545Ex5 (100µM)	SNaPshot IL10 -2849 (100µM)
2µl	IL10 rs3024505 (100µM)	SNaPshot TNF -308 (100µM)
		SNaPshot TNF -238 (100µM)
1,5µl	SNaPshot IL10 -11668 (100µM)	SNaPshot IL10 2763 new (100µM)
100µl	total	total

Table 2-20 SNaPshot reaction mix

1,86µl	H_2O
0,64µl	SNaPShot Multiplex Ready Reaction Mix 100 RXN (Applied)
0,5µl	Pooled Primer Mix
2µl	purified PCR fragement
→ 384 well plate	

Table 2-21 PCR programs for SNaPshot reaction

Denaturation	96°C 10s	
Annealing	50°C 5s	
Elongation	60°C 30s	24cycles
Pause	4°C	∞

For the purification after SNaPshot reaction the following mix was prepared.

Table 2-22 Purification of SNaPshot reaction

0,5µl	10xRxBuf
0,5µl	SAP
1µl	total
add to each well from SNaPshot reaction Mastercycler (384 well) digestion 1h at 37°C, heat inactivation 15min 80°C	

For the analysis, 10µl Formamid, supplemented with 0.1µl GeneScan120 LIZ size standard (Applied Biosystems Part No: 4322362) have been mixed with 1µl Snapshot reaction product on a 96-well plate . This was denatured at 95°C for 10min. The SNPs are subsequently determined according to the fluorescent labeled fragments of different sizes using the AB3130 Genetic Analyser and Gene MapperID Version 3.2.

2.11.4 Fragment length analysis of IL10-7400In/Del

Fragment length analysis was used to determine, if the insertion or the deletion at IL10-7400In/Del or both were present in genomic DNA samples.

Table 2-23 Fragment length analysis of IL10-7400In/Del

Reaction Mix		PCR-program	
30ng	DNA	96°C 30s	
2,5µl	PlatinumTaq buffer (10x)	64°C 20s	
2µl	$MgCl_2$ (25mM)	72°C 15s	25 cycles
0,5µl	dNTP (10mM each)	96°C	
0,4µl	-7400forward (5µM)	60°C	
0,4µl	-7400reverse neu (5µM)	72°C	10 cycles
0,1µl (5U/µl)	PlatinumTaq	72°C	1h
ad 25µl	H2O	4°C	∞

Fragment length has subsequently been determined, by mixing 10µl Formamid with 0.15µl ROX500 (Applied Biosystems) and 1µl PCR product using the Genetic Analyser 3130 with Gene MapperID Version 3.2.

2.11.5 Sequencing

For the analysis of nucleotide sequences, fluorescent labeled ddNTPs were used (BigDye Terminator Cycle Sequencing-Kit v1.1) according to the procedure described in table 2-24.

Table 2-24 Sequencing Mix

Reaction Mix	PCR-program	
100-500ng DNA		
2µl sequencing buffer (5x)	95°C 30s	
1,5µl sequencing mix	50°C 15s	
5pmol Primer	60°C 4min	25 cycles
ad 10µl H_2O	4°C	∞

Subsequently, the reaction mix had to be purified. Therefore, the innuPREP DYEpure Kit has been used according to the manufacturers' protocol. 10µl of eluted purified PCR product of sequencing reaction have been mixed with 10µl Formamid. Sequencing analysis has been conducted using the AB3130 Genetic Analyser with Sequencing Analysis Version 5.2.

2.11.6 Isolation of RNA and Reverse Transcription

Cells for RNA Isolation were harvested via sedimentation (210xg/10min/4°C) and washed once with PBS (1000xg/4°C/ 10min). For the Isolation of RNA the RNeasy

plus Mini Kit (Qiagen) together with QIAshredder or the Nucleo Spin RNA II Kit (Machery & Nagel) were used according to the manufacturers' protocols. RNA has been eluted in 40µl RNAse free water. RNA concentrations were determined using the NanoDrop.

For the reverse transcription from RNA into cDNA, the SuperScript II Reverse transcriptase (Invitrogen) was used. Reverse transcription was performed with random hexamer primers or oligo dT primers.

2µl of random hexamer (100µM) or oligo dT (50µM) was added to each cup. 1-3µg RNA was added in 10µl H_2O. This mix was denatured for 10min on 70°C in a Thermocycler. Subsequently samples have been cooled on ice and 8µl of the Master Mix have been added to each sample. Depending on the oligonucleotide primers, a respective program was used for reverse transcription in the Thermocycler (Biometra) (table 2-25).

Table 2-25 Reverse Transcription

Master Mix	**rnd hexamer**	**oligo dT**
4µl 5x first strand buffer		
2µl DTT (0.1M)	25°C 10min	
1µl Super Script II	42°C 60min	42°C 60min
1µl dNTPs (10mM each)	65°C 10min	70°C 15min
→ 8µl per sample	4°C ∞	4°C ∞

2.11.7 quantitative Real-Time PCR (qRT-PCR)

For the quantification of transcripts, a SYBR® Green based system was used. SYBR® Green is a cyanine-dye, which intercalates with double stranded DNA. Upon binding to DNA, the dye absorbs blue light (λ_{max} = 488 nm) and emits green light (λ_{max} = 522 nm). Therefore, this system can be used to quantify the amount of double stranded PCR products. The number of PCR cycles at which an exponential increase of fluorescence can be detected (Cycle Threshold= Ct-value) correlates to the amount of DNA templates within the PCR. A self-made SYBR Green Mix (see table 2-5) was used for this purpose. The PCR has been conducted using 384-well clear optical plates. For each reaction a total volume of 10µl was used with 5.6µl SYBR Green mix and 0.3pmol/µl of each primer. An amount of cDNA has been used that corresponds to 20ng RNA. Each analysis has been conducted in triplets.

Table 2-26 qRT-PCR program

Initial Denaturation and activation of HOT FIREPol®	95°C 12min	
Denaturation Annealing/Elongation	95°C 15s 60°C 1min	40cycles
Dissoziation stage	95°C 15s 60°C 15s 95°C 15s	
Pause	4°C ∞	

To determine the relative expression of each analysed gene, the Ct-values of each triplet were normalized to the mean Ct-value of a housekeeper gene (abl or β2m see table 2-7).

$$Ct_{spez.} - Ct_{housekeeper} = \Delta Ct$$

To compare gene expression of a control sample to a modified sample the ΔΔCT was calculated.

$$\Delta Ct_{modified\ sample} - \Delta Ct_{control} = \Delta\Delta CT$$

The ΔΔCT is a value which shows whether the expression of a certain gene is higher or lower compared to the control sample. For example if *IL10* expression changes after a respective stimulation of the cells. Based on the ΔΔCt the fold change could be calculated as

$$\text{fold change} = 1/ (2^{\Delta\Delta CT})$$

If the gene of interest was not expressed in the control sample, the fold change could not be calculated and the respective normalized ΔCt-value was used.

2.11.8 PCR for ncRNA

The transcription of ncRNA has been assessed by SYBR Green PCR or conventional PCR. As template cDNA was used, which was reverse transcribed with random hexamer or oligo dT (see 2.11.6). As a control for DNA contamination cDNA reverse transcribed without reverse transcriptase has been used. As positive control for the PCR, DNA of the respective cell line was used. For SYBR Green PCR the above described protocol (see 2.11.7) was used with primers originally designed for ChIP (table 2-7).

For conventional PCR the same primers have been used but in different combinations, as indicated below the respective figures. The following reaction mix was used.

Table 2-27 Reaction mix for ncRNA detection

Master Mix	
cDNA (or DNA 50-100ng)	300ng (based on used RNA)
10xPCR buffer K (supplied with Taq)	5µl
$MgCl_2$ (50mM supplied with Taq)	1.5µl
dNTPs (10mM each)	1µl
Primer forward (10µM)	1µl
Primer reverse (10µM)	1µl
Taq Polymerase (Primetech LTD, Belarus)	0.2µl
ad 50µl H2O	

Depending on the length of the PCR product different PCR-programs have been used.

Table 2-28 PCR programs used for the detection of ncRNA via conventional PCR

	length of PCR fragments			
	100-500bp	**approx. 3kb**	**approx. 4kb**	
Initial Denaturation	95°C 5min	95°C 5min	95°C 5min	
Annealing	60°C 3min	60°C 3min	60°C 3min	
Elongation	72°C 3min	72°C 3min	72°C 3min	
Denaturation	95°C 30s	95°C 1min	95°C 1min	40 cycles
Annealing	60°C 30s	60°C 1min	60°C 1min	
Elongation	72°C 1min	72°C 3min	72°C 5min	
Elongation	72°C 10min	72°C 10min	72°C 10min	
Pause	4°C ∞	4°C ∞	4°C ∞	

2.11.9 Chromatin immunoprecipitation and Sonication test

Chromatin immunoprecipitation (ChIP) can be used to detect binding of transcription factors or specific histone modifications at defined regions of the genome. For this purpose, proteins bound to DNA are crosslinked using formaldehyde. Subsequently, the DNA is sheared by sonication. The protein-DNA complexes can be immunoprecipitated, using antibodies specifically binding modified histone modifications or transcription factors of interest. In a final step, the crosslink is reversed and the DNA fragments, which were immunoprecipitated due to their binding to respective proteins are analysed by qRT-PCR. Thereby, the binding regions of the respective proteins can be defined. Buffers used for ChIP are described in table 2-5. Used inhibitors were sodium butyrate (5mM) and Protease

inhibitor cocktail (Roche). This is indicated by $^{++}$. The procedure has been conducted using the following protocol, adjusted from the ChIP protocol from the Laboratory of Junior Professor Dr. Steven Johnsen.

For each ChIP 5-6x10^6 cells have been prepared (e.g. stimulation with PMA), depending on the question of interest. Three biological replicates were analysed in parallel. 1x10^6 cells per immunoprecipitation (IP) (5-6x10^6 per previously sample) have been crosslinked according to the best conditions for the respective cell line (for all cell line used here: 0.5% Formaldehyde in PBS for 10min at RT). Quenching of formaldehyde has been performed by adding 1ml 1.25M Glycine and incubation for 5min at room temperature. Cells were washed twice in ice-cold PBS and twice in Nelson buffer modified^{++} (12,000 g, 1 min., 4°C). The nuclear pellet was resuspended in 300µl (for 5-6x10^6 cells) SDS lysis buffer. Sonication of the samples has been performed using the Biorupter™ Next Gen for 3 x 10min (Settings: 10 sec on/off duty time at high power). Preclearing has been performed with 80-100µl Protein A-Sepharose (50% slurry in Gomes lysis buffer^{++}) for 1h at 4°C. The samples were centrifuged at 12,000xg/10min/4°C and the supernatant was used for IP. An amount of 50µl chromatin containing supernatant derived from approximately 1x10^6cells has been used per IP and the input sample. 2µg of respective antibodies were added to each sample, including an anti-IgG antibody as negative control (table 2-10) and each sample was filled up to a volume of 500µl with Gomes lysis buffer^{++}. The input DNA has been precipitated with 100µl 100% Ethanol and 1µl GlycoBlue^{TM} overnight at -20°C. Protein A-Sepharose has been blocked overnight with salmon sperm DNA and BSA. On the next day, the samples have been incubated for 1h at 4°C with 30µl Protein A-Sepharose (50% slurry in Gomes lysis buffer^{++}, washed three times after blocking). Immune complexes have been washed twice with Gomes lysis buffer, three times with Gomes wash buffer and once with 1xTE (centrifuge at 2,000xg/4°C/2min). After the last washing step, as much supernatant as possible has been removed. The input DNA has been sedimented (12,000xg/20min/4°C) and washed twice with 500µl 70%EtOH (12,000xg/5min/4°C). For DNA Isolation 100µl 10% Chelex 100 slurry has been added to the washed beads and the input DNA, vortexed briefly and heated up to 95°C for 10min. Subsequently, samples have been treated with proteinase K for 30min at 55°C. Proteinase K has been inactivated by incubating samples at 95°C for 10min. Samples have been centrifuged (12,000xg/1min/4°C). 70µl of supernatant have been transferred to a new tube,

without transferring any Chelex as this inhibits PCR-reactions. The DNA has been stored at -20 °C.

For PCR analysis all samples including the input have been diluted 1:10. A dilution series of a pooled input mix has been prepared for use as standard in the PCR. The PCR has been conducted using the SYBR Green system (see 2.11.7). For each tested primer pair (see table 2-7 and Figure 3-16) the input standard, the input and each sample has been analysed in triplicates. The amount of bound DNA was estimated as % of input.

2.11.10 Transformation of E.coli

E.coli bacteria were used for the amplification of plasmid DNA. For the transformation of plasmid DNA into E.coli, the chemically competent DH5α cells were used, which were stored at -80°C. Cells were thawed on ice for 5-10min. 4-10µl of a ligation reaction or 50ng purified plasmid DNA was added to the cells without pipetting up and down. After 30min incubation on ice a heat shock at 42°C for 42s was performed. The bacteria were kept on ice for another 10min. Subsequently, cells were suspended in 250µl SOC medium and incubated shaking for 1h at 37°C. For selection of transformed cells, the bacteria were plated on LB-agar plates containing 100µg/ml Ampicillin. These plates were incubated at 37°C overnight. On the next day, individual colonies have been transferred into 2ml of LB-medium containing Ampicillin for preparation of plasmid DNA (see 2.11.11) for sequencing analysis (see 2.11.5). Of these cultures, glycerol stocks have been established for cryo-conservation by mixing 200µl of the bacterial suspension with 200µl Glycerol (storage -80°C).

2.11.11 Isolation of Plasmid DNA

For isolation of small amounts of plasmid DNA, 2ml of bacterial culture have been incubated at 37°C shaking overnight. Isolation has been performed using the QIAGEN Plasmid Mini Kit according to the manufacturers' protocol. These have been used for sequencing analysis (2.11.5). For high amounts 110ml bacterial culture have been incubated overnight at 37°C shaking and isolation of plasmid DNA has been performed using the EndoFree Plasmid Maxi Kit according to the manufacturers' protocol. Plasmid DNA has been resolved in endotoxin free water at 4°C overnight

and concentration of DNA was measured using the NanoDrop. Plasmid DNA has been stored at 4°C.

2.11.12 qRT-PCR for *IL10* expression on LCLs /using Standard Plasmids

For the comparability of different qRT-PCRs, conducted to analyse *IL10* expression of LCLs, a standard has been developed. The PCR products of both primers used, qRT-IL10-e1-2 for *IL10* expression and β2m the housekeeper (see table 2-7) have been inserted into the pCR2.1 Topo.

Therefore, the PCRs have been conducted on DNA derived from LCL 183/2 using the Thermocycler T3000. The PCR program also used for the detection of ncRNA fragments of 100bp-500bp has been used (see table 2-28). Subsequently, the PCR products have been separated on a 1% Agarose gel. The PCR products have been cut from the Gel and purified using the QIAEX II Agarose Gel Extraction kit according to the manufacturers' protocol.

To insert the PCR products into the pCR2.1 Topo, the TOPO TA Cloning® Kit has been used according to the manufacturers' protocol. This ligation reaction has been used for transformation (see 2.11.10), followed by isolation of plasmid DNA from a 2ml culture (see 2.11.11), which has been used for sequencing (see 2.11.5).

After sequencing, one correct plasmid has been used for Maxi plasmid preparation using the EndoFree® Plasmid Maxi Kit according to the manufacturers protocol. The plasmids have been linearized by digesting them with EcoRV. 5µl buffer 3 (NEB), 5µg of the respective plasmid and 1µl EcoRV have been incubated in 50µl total Volume for 2h on 37°C.

4µl Shrimp Alkaline Phosphatase (SAP) from the SNaPshot assay has been added to both samples after controlling digestion on 1% Agarose gel. This was incubated for 1h on 37°C, followed by heat inactivation of SAP for 15min on 65°C.

For purification the QIAquick PCR purification Kit was used according to the manufacturers' protocol.

According to the number of base pairs of each plasmid, the molecular weight has been calculated. Dilutions of each plasmid of $1x10^7$ to $1x10^2$ molecules/2µl have been prepared. These have been tested in qRT-PCR analyses (see 2.11.4). The

estimated slope of the SDS 2.1 software had to be -3.32. Plasmid dilutions have been aliquoted and stored at -20°C.

2.12 Definitions and statistical Analyses/

2.12.1 Survival Analysis

For a first analysis of genotyping data of aNHL patients (for details of patients see chapter 2.1.2), the GENEPOP software was used (Version 3.4 http://genepop.curtin.edu.au/). These analyses included tests for Hardy-Weinberg equilibrium, genotypic and allelic differentiation. For the reconstitution of haplotypes, the haplotype estimation software was used (MDC, Berlin http://www.bioinf.mdc-berlin.de/projects/hap/). Later analyses were made by Dr. Mladen Tzvetkov using the Phase software (http://depts.washington.edu/uwc4c/express-licenses/assets/phase/).

Clinical characteristics between included patients and patients of the complete trials were estimated using the χ^2-test, and if required, Fisher´s exact test.

Overall survival (OS) was defined as time from first day of therapy (NHL-B1/B2) or random assignment (RICOVER-60) to death from any cause. Event-free survival (EFS) was defined as time from first day of therapy (NHL-B1/B2) or random assignment (RICOVER-60) to progressive disease under therapy, or failure to achieve complete remission, additional therapy in excess of that prescribed in the protocol, relapse or death from any cause, whatever came first. Patients without an event in EFS or OS were censored at the last day with valid information for the respective endpoint. EFS and OS were estimated according to Kaplan-Meier and compared by log-rank trend test. Multivariate analyses were performed with the use of Cox proportional hazard models to estimate hazard ratios for evolving an event.

The analyses have been conducted without adjustment for multiple comparisons. Therefore, only the most prominent aspects have been extracted. Statistical analyses were performed with R-2.6.2. by Markus Kreuz (IMISE, Leipzig).

2.12.2 LCLs

The analyses of associations between *IL10* expression or IL10 secretion of LCLs with *IL10* genotypes has been conducted assisted by Hans-Joachim Helms (Department of Medical Statistics, UMG, Göttingen).

Values estimated for *IL10* expression (see chapter 2.11.8) were not normally distributed and have therefore been ranked. This means the LCL with the lowest *IL10* expression was ranked 1 and the LCL with the highest *IL10* expression was ranked 111. Due to the fact that qRT-PCR has been conducted on different qRT-plates a two-way ANOVA has been conducted. Thereby, the influence of *IL10* gene variation and the qRT-plate as independent variables on *IL10* gene expression as the dependent variable as well as the interaction between the two independent variables has been estimated. These analyses have been conducted using the SAS software. Pair-wise comparisons have been conducted for *IL10* gene variations with significant results. A Wilcoxon-Test adjusted for Bonferroni has been done using the STATISTICA software (www.statsoft.de).

Values estimated for IL10 secretion (see chapter 2.10.4) were also not normally distributed and have been ranked prior to following analyses. Variance analyses have been conducted using Kruskal-Wallis ANOVA and STATISTICA software.

LCLs have been grouped into high and low *IL10* expressing and IL10 secreting cells according to the respective median (median expression: 0.000762 NSM IL10/NSM β2m; median secretion 737pg IL10/ml). These groups have been compared in a two-way summary table and Pearson X^2-test has been conducted using STATISTICA software.

3 Results

3.1 Characterization of Interleukin 10 gene variations and serum levels in aNHL patients

To answer the question about the prognostic relevance of *IL10* gene variations in aNHL, *IL10* gene variations were analysed in relation to OS or EFS of aNHL patients treated within three different prospective clinical trials from the DSHNHL (Deutsche Studiengruppe für hochmaligne Non-Hodgkin-Lymphome) (see Material and Methods 2.1.2). For a better understanding of this and the following chapters, the most important characteristics are summarized here.

942 patients were from the NHL-B trial. Patients within this trial have been treated every second or third week with CHOP or CHOP plus etoposide (Pfreundschuh et al., 2004a; Pfreundschuh et al., 2004b). The trial can be divided in a younger cohort, NHL-B1 (age≤60) with 477 patients and an older cohort, NHL-B2 (age>60) with 465 patients included into this study. 498 of these patients have been included into a previous study on *IL10* gene variations (Kube et al., 2008). Therefore the 942 patients are an enlargement of the previous study analysed for an extended number of *IL10* gene variations in the present study. The cohort termed “CCR-excluded” represents those 444 patients not included into the previous study. From the RICOVER-60 trial DNA of 604 patients has been available for respective analyses. This trial showed that the outcome of patients treated with Rituximab in addition to conventional CHOP therapy (R-CHOP) is superior compared to the outcome of patients treated with CHOP alone in elderly aNHL patients (age≥60) (Pfreundschuh et al., 2008). 301 patients out of the 604 patients have been treated with CHOP, while 303 have been treated with Rituximab in addition to CHOP (R-CHOP). The same effect as in RICOVER-60 was tested in younger patients within the Mab Thera International Trial (MInT) (Pfreundschuh et al., 2006). In this trial the same effect of superior survival for patients treated with Rituximab has been observed. However the general outcome in this young patient group is much better compared to the elderly patients. 178 patient DNAs from the whole MInT trial were available for our analyses. In total, DNA of 1724 patients with aNHL has been genotyped for *IL10* gene variations. The clinical characteristics of the patients, of which respective material for genotyping analyses was available (included), have been compared to those from

the complete trials (complete). The clinical characteristics of patient of each individual trial are summarized in table 3-1A and table 3-1B. Notably, the patients included into the NHL-B and the CCR-excluded cohorts are from the same trial. Therefore the clinical characteristics for the complete trial are listed only once.

Patients included into our analysed cohorts are representative for the complete trials and the different arms of NHL-B and RICOVER-60. The only exception is the CCR-excluded cohort in which the median age differs significantly from the complete trial (difference=2 years). Nevertheless this cohort was evaluated, as it was important for the validation of the effects observed in the previous study on 498 aNHL patients (Kube et al., 2008).

Genotyping has been done for 12 gene variations located in the 5' flanking region of *IL10*, with the most distal variation at -12.806bp from the transcriptional start site, one variation within the 3'-UTR (IL10$_{+4259A/G}$) and 1 variation in the proximal 3'region (IL10$_{+5876C/T}$), assisted by Frederike von Bonin and Angela Lenz. The genotyping was performed using the respective Taqman SNP genotyping assays for the gene variations IL10$_{-6752A/T}$, IL10$_{-6208G/C}$, IL10$_{-3538T/A}$, IL10$_{-1087A/G}$, IL10$_{-824C/T}$ and IL10$_{-597C/A}$ or a fragment length analysis for IL10$_{-7400In/Del}$. The gene variations IL10$_{-12806C/T}$, IL10$_{-11777A/G}$, IL10$_{-11668G/A}$, IL10$_{-2812G/A}$, IL10$_{-2726C/A}$, and IL10$_{+4259A/G}$ and IL10$_{+5876C/T}$ were analysed using SNaPshot-assay. IL10$_{-3538T/A}$ was genotyped with both methods as a cross reference. In addition to those gene variations analysed in a previous study on 498 aNHL patients (Kube et al., 2008), the gene variations IL10$_{-12806C/T}$, IL10$_{-11777A/G}$, IL10$_{-11668G/A}$, IL10$_{+4259A/G}$ and IL10$_{+5876C/T}$ have been included into the analysis due to their localization within evolutionary conserved regions and their recent functional description relevant for *IL10* expression (Jones and Flavell, 2005; Shoemaker et al., 2006), whereas IL10$_{-2812G/A,}$ IL10$_{-2726C/A}$ have been described to affect inter-individual differences in *IL10* gene expression (Gibson et al., 2001).

Table 3-1A Clinical characteristics of the NHL patient subgroup analysed for *IL10* gene variations

This table shows a comparison of the clinical characteristics of patients from the whole NHL-B trial, the young patients from the NHL-B1, the elderly patients from the NHL-B2 trial and the T-NHL patients. “Included” refers to the patients included into our analyses based on availability of respective material and “complete” refers to patients included into the original clinical trials. * IPI= International Prognostic Index LDH >N, age >60 years, ECOG >1, stage III/IV, and number of extranodal sites ≥2.

Patients characteristics	NHL-B patients included (n=942)	CCR excluded patients included (n=444)	NHL-B patients complete (n=1399)	NHL-B1 patients included (n=477)	NHL-B1 patients complete (n=710)	NHL-B2 patients included (n=465)	NHL-B2 patients complete (n=689)	T-NHL patients included (n=117)	T-NHL patients complete (n=197)
Sex male	517 (55%)	239 (54%)	789 (56%)	290 (61%)	438 (62%)	227 (49%)	351 (51%)	69 (59%)	120 (61%)
female	425 (45%)	205 (46%)	610 (44%)	187 (39%)	272 (38%)	238 (51%)	338 (49%)	48 (41%)	77 (39%)
Age Median (Min.;Max.)	60 (18;75)	58 (18;75)	60 (18;75)	49 (18;60)	48 (18;60)	67 (61;75)	67 (61;75)	58 (18;78)	61 (18;78)
IPI*									
low (IPI=0,1)	568 (60%)	288 (65%)	840 (60%)	431 (90%)	639 (90%)	137 (29%)	201 (29%)	72 (61.5%)	111 (56.4%)
intermediate low (IPI=2)	171 (18%)	73 (16%)	250 (18%)	40 (8%)	62 (9%)	131 (28%)	188 (27%)	23 (19.7%)	39 (19.8%)
intermediate high (IPI=3)	112 (12%)	46 (10%)	170 (12%)	6 (1%)	9 (1%)	106 (23%)	161 (23%)	12 (10.3%)	25 (12.7%)
high (IPI=4,5)	91 (10%)	37 (8%)	139 (10%)	0 (0%)	0 (0%)	91 (20%)	139 (20%)	10 (8.6%)	22 (11.2%)
Serum LDH > N	214 (23%)	92 (21%)	316 (23%)	0 (0%)	0 (0%)	214 (46%)	316 (46%)	22 (19%)	45 (23%)
Age Older than 60 y	465 (49%)	194 (44%)	689 (49%)	0 (0%)	0 (0%)	465 (100%)	689 (100%)	50 (43%)	99 (50%)
Performance status ECOG > 1	106 (11%)	42 (10%)	163 (12%)	24 (5%)	38 (5%)	82 (18%)	125 (18%)	13 (11%)	31 (16%)
Ann Arbor stage III,IV	376 (40%)	175 (40%)	567 (41%)	149 (31%)	217 (31%)	227 (49%)	350 (51%)	47 (40%)	85 (43%)
No of extranodal sites >1	186 (20%)	82 (19%)	276 (20%)	67 (14%)	104 (15%)	119 (26%)	172 (25%)	23 (19.7%)	36 (18.3%)
Bulky tumor (>7,5 cm)	319 (34%)	156 (35%)	467 (33%)	133 (28%)	197 (28%)	186 (40%)	270 (40%)	30 (25.7%)	51 (25.9%)
B symptoms	264 (28%)	123 (28%)	402 (29%)	98 (21%)	149 (21%)	166 (36%)	253 (37%)	45 (38.5%)	75 (38.1%)
extranodal involvement	467 (50%)	217 (49%)	698 (50%)	201 (42%)	308 (43%)	266 (57%)	390 (57%)	51 (43.6%)	88 (44.7%)

Table 3-1B Clinical characteristics of the NHL patient subgroup analysed for *IL10* gene variations

This table shows a comparison of the clinical characteristics of patients from the whole RICOVER-60 trial, the patients from the CHOP and the R-CHOP arms and patients from the MInT clinical trial. ”Included” refers to the patients included into our analyses based on availability of respective material and “complete” refers to patients included into the original clinical trials. * IPI= International Prognostic Index LDH >N, age >60 years, ECOG >1, stage III/IV, and number of extranodal sites ≥2.

Patients characteristics	RICOVER-60 patients included (n=604)	RICOVER-60 patients complete (n=1222)	CHOP patients included (n=301)	CHOP patients complete (n=612)	R-CHOP patients included (n=303)	R-CHOP patients complete (n=610)	MInT patients included (n=178)	MInT patients complete (n=291)
Sex male	320 (53%)	650 (53%)	155 (52%)	325 (53%)	165 (55%)	325 (53%)	101 (57%)	166 (57%)
female	284 (47%)	572 (47%)	146 (49%)	287 (47%)	138 (46%)	285 (47%)	77 (43%)	125 (43%)
Age Median (Min.;Max.)	68 (61;80)	68 (61;80)	68 (61;80)	68 (61;80)	68 (61;80)	68.5 (61;80)	46 (18;60)	45 (18;60)
IPI*								
low (IPI=0,1)	197(33%)	372 (30%)	88 (29%)	188 (31%)	109 (36%)	184 (30%)		
intermediate low (IPI=2)	158 (26%)	339 (28%)	87 (29%)	167 (27%)	71 (23%)	172 (28%)		
intermediate high (IPI=3)	156 (26%)	313 (26%)	84 (28%)	158 (26%)	72 (24%)	155 (25%)		
high (IPI=4,5)	93 (15%)	198 (16%)	42 (14%)	99 (16%)	51 (17%)	99 (16%)		
Serum LDH > N	288 (48%)	604 (49%)	148 (50%)	301 (49%)	140 (46%)	303 (50%)	55 (31%)	84 (29%)
Age Older than 60 y	604 (100%)	1222 (100%)	301 (100%)	612 (100%)	303 (100%)	610 (100%)	0 (0%)	0 (0%)
Performance status ECOG > 1	78 (13%)	176 (14%)	41 (14%)	87 (14%)	37 (12%)	89 (15%)		
Ann Arbor stage III,IV	303 (50%)	619 (51%)	153 (51%)	312 (51%)	150 (50%)	307 (50%)	54 (30%)	83 (29%)
No of extranodal sites >1	104 (17%)	216 (18%)	49 (16%)	107 (17%)	55 (18%)	109 (18%)	23 (13%)	38 (13%)
Bulky tumor (>7,5 cm)	241 (40%)	463 (38%)	123 (41%)	230 (38%)	118 (39%)	233 (38%)	91 (51%)	148 (51%)
B symptoms	199 (33%)	399 (33%)	102 (34%)	202 (33%)	97 (32%)	197 (32%)	57 (32%)	80 (28%)
extranodal involvement	336 (56%)	663 (54%)	167 (56%)	335 (55%)	169 (56%)	328 (54%)	77 (44%)	125 (43%)
Rituximab treatment	303(50%)	610 (50%)	0 (0%)	0 (0%)	303 (100%)	610 (100%)	89 (50%)	147 (51%)

The *IL10* gene variations are in strong LD to each other, therefore certain haplotypes are formed by these gene variations. Figure 3-1 shows the estimated haplotypes for the NHL-B and the RICOVER-60 cohort in comparison to a cohort of healthy blood donors.

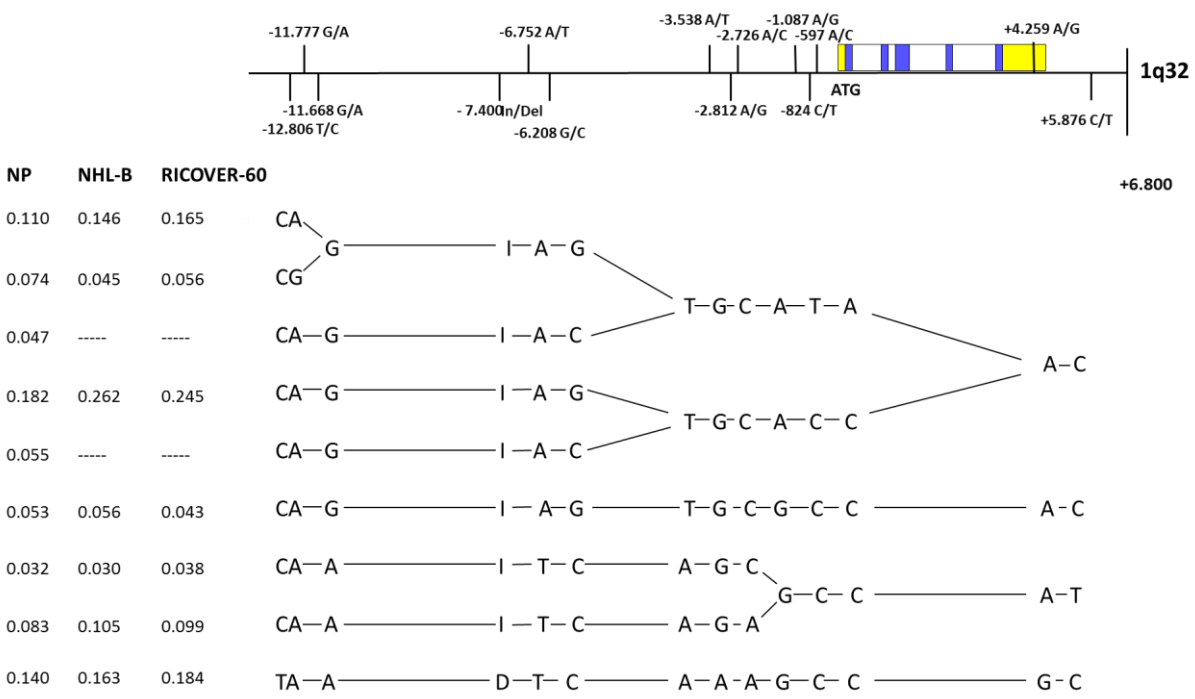

Figure 3-1 Frequency of *IL10* haplotypes

Phase software has been used to estimate haplotypes formed by the analysed *IL10* gene variations. The respective haplotypes with a frequency higher 3% are shown for healthy blood donors (normal population; NP), patients from the RICOVER-60 cohort and patients from the NHL-B cohort. Frequencies are given on the left. The human *IL10* gene locus from -12.806bp till +6800bp on chromosome 1q31/32 is shown as scheme above the haplotypes. Single nucleotide polymorphisms (SNP) and the insertion/deletion variation at -7400bp are indicated. The *IL10* gene and the position of the ATG are shown. UTR (yellow), exons (dark blue) and introns (white) are displayed.

Genotype frequencies have been estimated and are shown in table 3-2 for the complete patient cohort. All gene variations have been tested for HDW (Hardy-Weinberg). The HDW test showed no significant differences between observed and suspected numbers of genotype frequencies for the complete patient cohort. Therefore, this cohort could be used for survival analysis.

Table 3-2 *IL10* Genotype frequency and HDW of 1724 NHL patients analysed within this thesis

			Complete (n=1724)		
SNP Name	**rs-number**	**Genotype**	**number of patients**	**% of patients**	**HWE X^2**
IL10-12806C/T	rs17015865	TT	81	4,7	0,84
		CT	588	34,5	
		CC	1037	60,8	
IL10-11777A/G	rs4072227	GG	11	0,6	0,14
		AG	201	11,8	
		AA	1493	87,6	
IL10-11668G/A	rs4072226	AA	304	17,8	0,70
		AG	823	48,2	
		GG	579	33,9	
IL10-7400In/Del *	7400In/Del	DelDel	79	4,6	0,41
		InDel	606	35,3	
		InIn	1034	60,2	
IL10-6752A/T *	rs6676671	TT	265	15,4	0,94
		AT	819	47,6	
		AA	638	37,0	
IL10-6208G/C *	rs10494879	CC	299	17,4	0,66
		CG	827	48,0	
		GG	597	34,6	
IL10-3538T/A *	rs1800890	AA	265	15,4	0,86
		AT	815	47,4	
		TT	638	37,1	
IL10-2812G/A	rs6703630	AA	99	5,8	0,70
		AG	637	37,3	
		GG	974	57,0	
IL10-2726C/A	rs6693899	AA	236	13,8	0,21
		AC	766	44,8	
		CC	708	41,4	
IL10-1087A/G *	rs1800896	GG	394	22,9	0,47
		AG	844	49,0	
		AA	485	28,1	
IL10-824C/T *	rs1800871	TT	73	6,2	0,70
		CT	429	36,6	
		CC	670	57,2	
IL10-597C/A *	rs1800872	AA	101	5,9	0,81
		AC	640	37,1	
		CC	983	57,0	
IL10+4259A/G	rs3024498	GG	99	5,8	0,87
		AG	629	36,9	
		AA	977	57,3	
IL10+5876C/T	rs3024505	TT	53	3,2	0,69
		CT	473	28,6	
		CC	1129	68,2	

Survival analyses have been conducted, comparing the genotyping data to OS and EFS of the patients in univariate analyses using a log-rank test. In addition, multivariate analyses have been done using a cox-model, adjusted to the clinical parameters included into the IPI. Thereby, hazard ratios for relative risks for having an event (OS or EFS) were calculated. These analyses have been conducted from Markus Kreuz from the IMISE in Leipzig, which has the clinical data of all trials available.

The analysis of the combined patient cohort of 1724 aNHL patients revealed no significant associations between *IL10* gene variations and OS or EFS.

As the general characteristics of patients included into the three different trials differ to some extent in terms of general survival rates, age, risk groups defined by IPI, histological subtypes of NHL, general survival and treatment regiments they were analysed separately (compare clinical characteristics table 3-1A and B, histology table A-1A and A-1B as well as (Pfreundschuh et al., 2008; Pfreundschuh et al., 2004a; Pfreundschuh et al., 2004b; Pfreundschuh et al., 2006)). These analyses will be described in detail within the following chapters.

117 patients with T-NHL (see Material and Methods 2.1.2 and Table A-2) from the NHL-B and the RICOVER-60 trial have been analysed separately for associations of *IL10* gene variations and IL10 serum levels with survival rates. The results are described in detail in chapter 3.1.4.

3.1.1 Association of IL10-7400DelDel with shorter survival in aNHL patients from NHL-B could not be validated

The IL10-7400In/Del gene variation has been found to be associated with shorter OS in a representative cohort of 498 aNHL patients from the NHL-B trial, as described in the introduction (Kube et al., 2008). Therefore one of the aims of this dissertation was to test if this effect could be validated in a larger patient cohort.

A significant trend for carriers of the IL10-7400DelDel genotype towards shorter OS (p=0.032) but not EFS (p=0.088) could be observed compared to carriers of the other two genotypes in the NHL-B trial (Figure 3-2A and B). This is not surprising because this subgroup (n=942) includes the 498 aNHL patients analysed in the before mentioned previous study (Kube et al., 2008). As there was no additive effect of the minor allele IL10-7400Del, meaning that carriers of IL10-7400InDel show similar OS and EFS to carriers of IL10-7400InIn, only a comparison between homozygous carriers of this allele compared to carriers of the other two genotypes together is described here. The survival curves of a comparison of all three genotypes are shown in the Appendix (Figure A-1).

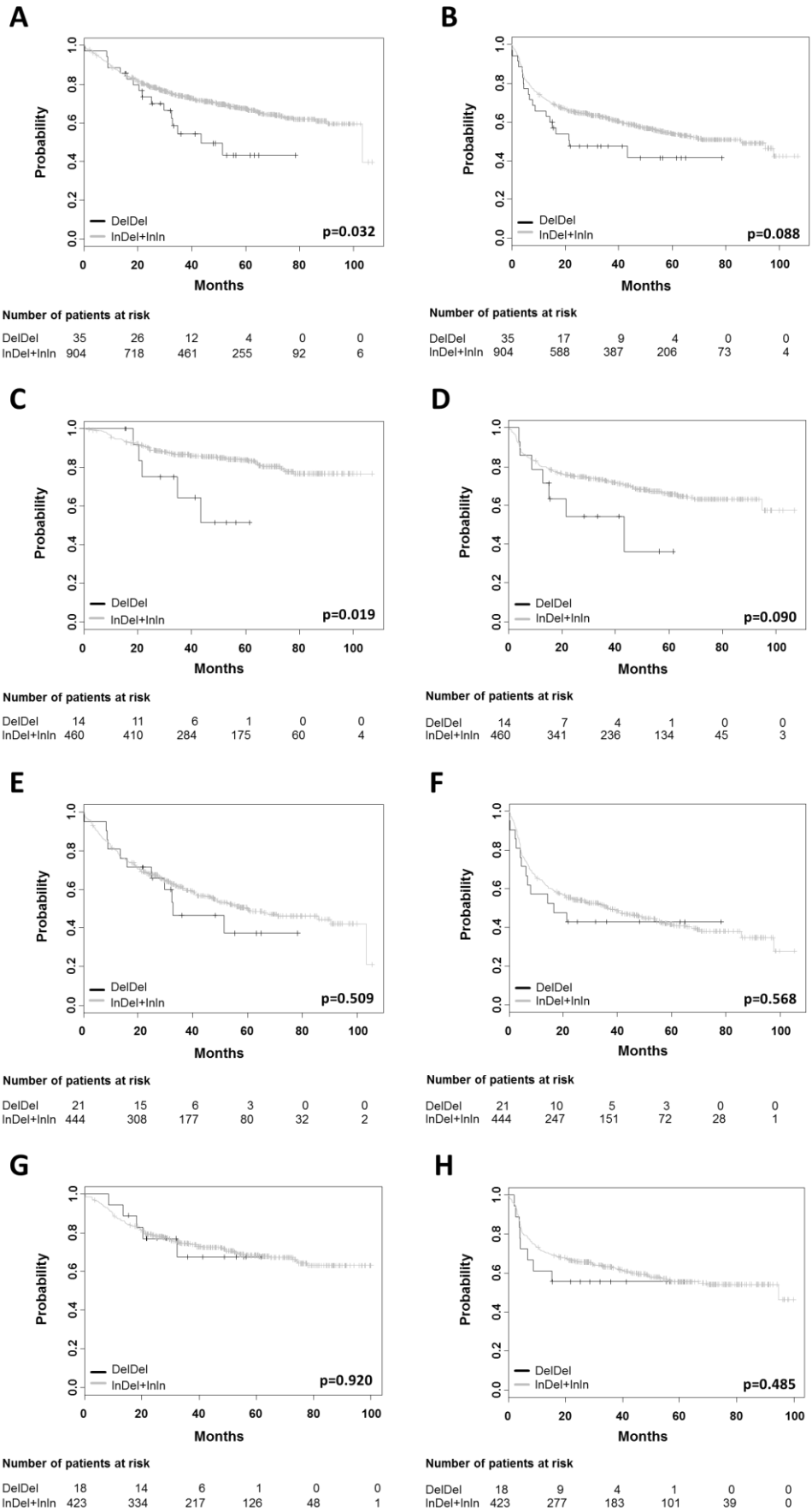

Figure 3-2 Association of IL10-7400DelDel with shorter survival rates could not be validated. Figure description on next page.

Figure 3-2 Association of IL10-740DelDel with shorter survival rates could not be validated.

Shown are the survival curves (Kaplan-Meier plots) for OS (**A,C,E,G**) and EFS (**B,D,F,H**) of aNHL patients from the NHL-B cohorts in comparison with IL10-7400In/Del genotypes (IL10-7400DelDel vs IL10-7400InIn+IL10-7400InDel). **A.** OS of patients from NHL-B. **B.** EFS of patients from NHL-B. **C.** OS of patients from NHL-B1. **D.** EFS of patients from NHL-B1. **E.** OS of patients from NHL-B2. **F.** EFS of patients from NHL-B2. **G.** OS of patients from NHL-B_CCR-excluded. **H.** EFS of patients from NHL-B_CCR-excluded. *P* refers to the log-rank test. Patients at risk represents the number of patients which still can develop an event (OS or EFS) at defined time points. Significant values have been observed for OS rates for patients from NHL-B (**A**) and NHL-B1 (**C**) studies.

Separate analyses of the NHL-B1 (patients ≤ 60 years) and B2 (patients > 60 years) cohorts revealed a difference in these two groups with respect to the IL10-7400In/Del gene variation. Consistent with the results of the NHL-B cohort a trend towards shorter OS (Figure 3-2 C and E) and EFS (Figure 3-2 D and F) was observed for both groups. Significant association between IL10-7400DelDel genotype and survival could be observed only for the younger patient cohort from the NHL-B1 study for shorter OS rates (p=0.019) but not for shorter EFS rates (p=0.090) (Figure 3-2 C and D). For the older patient cohort from the NHL-B2 study neither OS (p=0.509) nor EFS (p=0.568) rates were significantly associated with IL10-7400DelDel (Figure 3-2 E and F).

By comparing the OS and EFS rates of patients included in the CCR-excluded cohort no trends for shorter survival rates could be observed (Figure 3-2 G and H).

The respective three-year survival rates reflect the situation visualized by Kaplan-Meier survival curves in Figure 3-2 and are summarized in table 3-3.

Table 3-3 Shorter three-year survival rates for carriers of the IL10-7400DelDel genotype for OS and EFS in patients from the NHL-B cohorts

Three-year survival rates for carriers of the different genotypes of IL10-7400In/Del have been estimated for OS and EFS of patients from the four NHL-B cohorts. P refers to the log-rank test. Three-year survival rates were significantly shorter for OS for patients with IL10-7400DelDel in the NHL-B cohort and the NHL-B1 cohort. Confidence Interval (CI), Three-year survival rate (3-y rate).

cohort	Genotype IL10-7400In/Del	3-y rate OS	(95% CI)	p*	3-y rate EFS	(95% CI)	p*
NHL-B							
	InIn; InDel (n=904)	74.1	*(71.2; 77.1)*	***0.032***	61.8	*(58.7; 65.1)*	0.088
	DelDel (n=35)	54.3	(38.9; 76)		47.5	*(33.3; 67.7)*	
NHL-B1							
	InIn; InDel (n=460)	866	*(83.5; 89.9)*	***0.019***	72.8	*(68.8; 77)*	0.090
	DelDel (n=14)	64.3	(41.2; 1)		54.4	(32.9; 90.1)	
NHL-B2							
	InIn; InDel (n=444)	61.1	(56.6; 66)	0.509	50.4	(45.9; 55.4)	0.568
	DelDel (n=21)	46.6	(28.1; 77.2)		42.9	(26.2; 70.2)	
NHL-B CCR-exluded							
	InIn; InDel (n=423)	74.5	(70.4; 78.9)	0.920	63.2	(58.7; 68.1)	0.485
	DelDel (n=18)	67.4	(46.7; 97.3)		55.6	(36.8; 84)	

*log-rank test, significant p-values are italic and bold

Multivariate analyses using a Cox-Model adjusted to the IPI factors revealed an enhanced relative risk of 1.58 for shorter OS for carriers of IL10-7400DelDel (p=0.078) compared to carriers of the other two genotypes in the NHL-B cohort (see table 3-4). This relative risk was comparable to the relative risks of having a higher stage or extranodal involvement. The estimated relative risk for the carriers of IL10-7400DelDel for shorter OS in NHL-B1 was 1.92 (p=0.170). In this cohort not all IPI factors could be included into the analysis, due to the fact that higher age (>60years) and elevated LDH levels are not existing in these young patients. The estimated HR was higher than that estimated for higher stage. In the older NHL-B2 patient cohort the same trend for an enhanced relative risk for shorter OS could be observed but this was only 1.31 (p=0.390). For EFS the same, but less pronounced, effect of a higher risk for shorter survival rates associated with IL10-7400DelDel has been observed for all three cohorts (table 3-4). Notably, the confidence intervals of the estimated risks for shorter OS in the NH-B1 and NHL-B2 lie on top of each other and both include the value 1, which means that there is a possibility that the true value is 1 in both cases.

Table 3-4 Enhanced relative risk for shorter OS and EFS for carriers of IL10-7400DelDel gene variation in the NHL-B cohorts

Relative risks for shorter OS and EFS for patients with IL10-7400DelDel were estimated in multivariate analysis adjusted to the IPI factors in the NHL-B, NHL-B1, NHL-B2 and NHL-B_CCR-excluded cohorts. P refers to the Cox-model. Significant p-values are italic and bold. International Prognostic Index (IPI); overall survival (OS); event-free survival (EFS); hazard ratio for relative risk (HR); confidence interval (CI); lactate dehydrogenase (LDH); Eastern Cooperative Oncology Group (ECOG).

	Factor	HR	(95% CI)	p-value
NHL-B	**OS**			
	LDH > N	1.84	(1.38; 2.47)	***0.000042***
	age > 60 years	2.15	(1.58; 2.91)	***0.0000009***
	ECOG > 1	2.13	(1.59, 2.85)	***0.00000046***
	Stage III/ IV	1.53	(1.18; 1.97)	***0.0011***
	Extranodal involvement > 1	1.13	(0.86; 1.49)	0.380
	IL10-7400DelDel vs. InDel&InIn	1.58	(0.95; 2.62)	0.078
	EFS			
	LDH > N	1.56	(1.20; 2.03)	***0.00087***
	age > 60 years	1.47	(1.15; 1.87)	***0.0019***
	ECOG > 1	1.74	(1.33; 2.27)	***0.000059***
	Stage III/ IV	1.55	(1.25; 1.92)	***0.000058***
	Extranodal involvement > 1	1.15	(0.91; 1.46)	0.240
	IL10-7400DelDel vs. InDel&InIn	1.38	(0.87; 2.18)	0.180
NHL-B1	**OS**			
	ECOG > 1	2.68	(1.36; 5.27)	***0.0043***
	Stage III/ IV	1.28	(0.80; 2.05)	0.300
	Extranodal involvement > 1	2.23	(1.32; 3.77)	***0.0028***
	IL10-7400DelDel vs. InDel&InIn	1.92	(0.75; 4.91)	0.170
	EFS			
	ECOG > 1	1.40	(0.76; 2.60)	0.280
	Stage III/ IV	1.44	(1.03; 2.02)	***0.036***
	Extranodal involvement > 1	1.32	(0.86; 2.02)	0.210
	IL10-7400DelDel vs. InDel&InIn	1.63	(0.75; 3.54)	0.210
NHL-B2	**OS**			
	LDH > N	1.87	(1.39; 2.51)	***0.000041***
	ECOG > 1	2.11	(1.52; 2.92)	***0.0000066***
	Stage III/ IV	1.60	(1.18; 2.16)	***0.0027***
	Extranodal involvement > 1	0.92	(0.66; 1.26)	0.590
	IL10-7400DelDel vs. InDel&InIn	1.31	(0.71; 2.41)	0.390
	EFS			
	LDH > N	1.53	(1.16; 2.00)	***0.0022***
	ECOG > 1	1.87	(1.37;2.54)	***0.000066***
	Stage III/ IV	1.64	(1.24; 2.17)	***0.00051***
	Extranodal involvement > 1	1.05	(0.79; 1.41)	0.720
	IL10-7400DelDel vs. InDel&InIn	1.23	(0.68; 2.20)	0.490
NHL-B_CCR-excluded	**OS**			
	LDH > N	1.98	(1.24; 3.17)	***0.0042***
	age > 60 years	2.40	(1.51; 3.82)	***0.00023***
	ECOG > 1	2.43	(1.54; 3.83)	***0.00013***
	Stage III/ IV	1.59	(1.08; 2.32)	***0.018***
	Extranodal involvement > 1	1.39	(0.92; 2.09)	0.120
	IL10-7400DelDel vs. InDel&InIn	1.16	(0.47; 2.85)	0.750
	EFS			
	LDH > N	1.68	(1.11; 2.54)	***0.015***
	age > 60 years	1.61	(1.10;2.34)	***0.013***
	ECOG > 1	1.81	(1.18; 2.77)	***0.0064***
	Stage III/ IV	1.50	(1.09; 2.07)	***0.013***
	Extranodal involvement > 1	1.40	(0.98; 2.00)	0.062
	IL10-7400DelDel vs. InDel&InIn	1.33	(0.65; 2.72)	0.430

For the NHL-B_CCR-excluded cohort the estimated risks were 1.16 for OS (p=0.750) and 1.33 for EFS (p=0.430). Both values are below the estimated risks of any of the IPI factors.

Taken together, a tendency towards shorter survival rates associated with IL10-7400DelDel could be observed in the NHL-B, the NHL-B1 and the NHL-B2 cohorts, whereby this was most pronounced in the young NHL-B1 cohort. No trends for IL10-7400DelDel to be associated with shorter or longer survival could be observed in the NHL-B_CCR-excluded cohort. Therefore, the negative predictive effect of IL10-7400DelDel, observed in the previously published NHL-B cohort of 498 patients, could not be validated in the enlarged patient cohort.

In contrast to NHL-B, in the Ricover-60 cohort the IL10-7400DelDel genotype was associated with a better survival of the patients (Figure 3-4 A-F). This will be described in more detail in chapter 3.1.2.

No statement can be done about this gene variation and survival of patients within the MInT cohort. The number of homozygous carriers of IL10-7400DelDel was too low for survival analysis.

No other *IL10* gene variation showed significant associations with survival in the NHL-B, the NHL-B1, NHL-B2 or NHL-B_CCR-excluded cohort. Significant values for the log-rank test have been observed frequently. The respective gene variations were in LD with the IL10-7400In/Del as, for example, the IL10-6752A/T in NHL-B or the IL10-2812G/A in NHL-B1. Therefore significant associations are thought to be caused by IL10-7400In/Del, as the trend for shorter survival were associated with those variants observed only together with IL10-7400Del in one haplotype (compare to figure 3-1).

Taken together, the negative predictive effect of IL10-7400DelDel could not be validated in a larger patient cohort, neither in univariate nor in multivariate analyses of IL10-7400In/Del compared to survival rates of aNHL patients.

3.1.2 Investigation of prognostic relevance of *IL10* gene variations and IL10 serum levels in the RICOVER-60 trial

3.1.2.1 IL10-11.668AA is associated with better treatment outcome in patients from the RICOVER-60 and the R-CHOP cohort

Univariate analyses of associations between *IL10* gene variations and OS or EFS in the RICOVER-60 cohort revealed several significant associations. The same was true for those patients treated with R-CHOP. None of these associations was significant for the patients treated without Rituximab, even though the observed trends were consistent with those observed in the other two cohorts.

After comparing the estimated haplotypes (Figure 3-1) to the results of the univariate analyses one could conclude that the IL10-11.668G/A could be the gene variation that is causing the observed effects. The A-allele is part of most of the haplotypes with significantly associated alleles. Therefore, this gene variation is described here in more detail.

As for the IL10-7400In/Del there was no additive effect of the minor allele IL10-11.668A, meaning that carriers of IL10-11.668AG show similar OS and EFS to carriers of IL10-11.668GG, only a comparison between homozygous carriers of this allele compared to carriers of the other two genotypes together is described here. The survival curves of a comparison of all three genotypes are shown in the Appendix (Figure A-2).

The IL10-11.668AA genotype was significantly associated with longer OS and highly significantly associated with longer EFS in the whole RICOVER-60 cohort (OS: p=0.039; EFS: p=0.010; Figure 3-3 A and B) as well as in the R-CHOP cohort (OS: p=0.041; EFS: p=0.007; Figure 3-3 C and D). The same trend for longer survival rates associated with IL10-11.668AA could be observed in the CHOP cohort. Albeit these differences were not significant within this cohort and the survival curves especially for OS but also for EFS overlap within the first month (OS: p=0.340 and EFS: p=0.240) (Figure 3-3 E and F). Respective three-year survival rates have been estimated (see table 3-5). A trend for longer survival has been observed for carriers of the IL10-11.668AA genotype in all three cohorts.

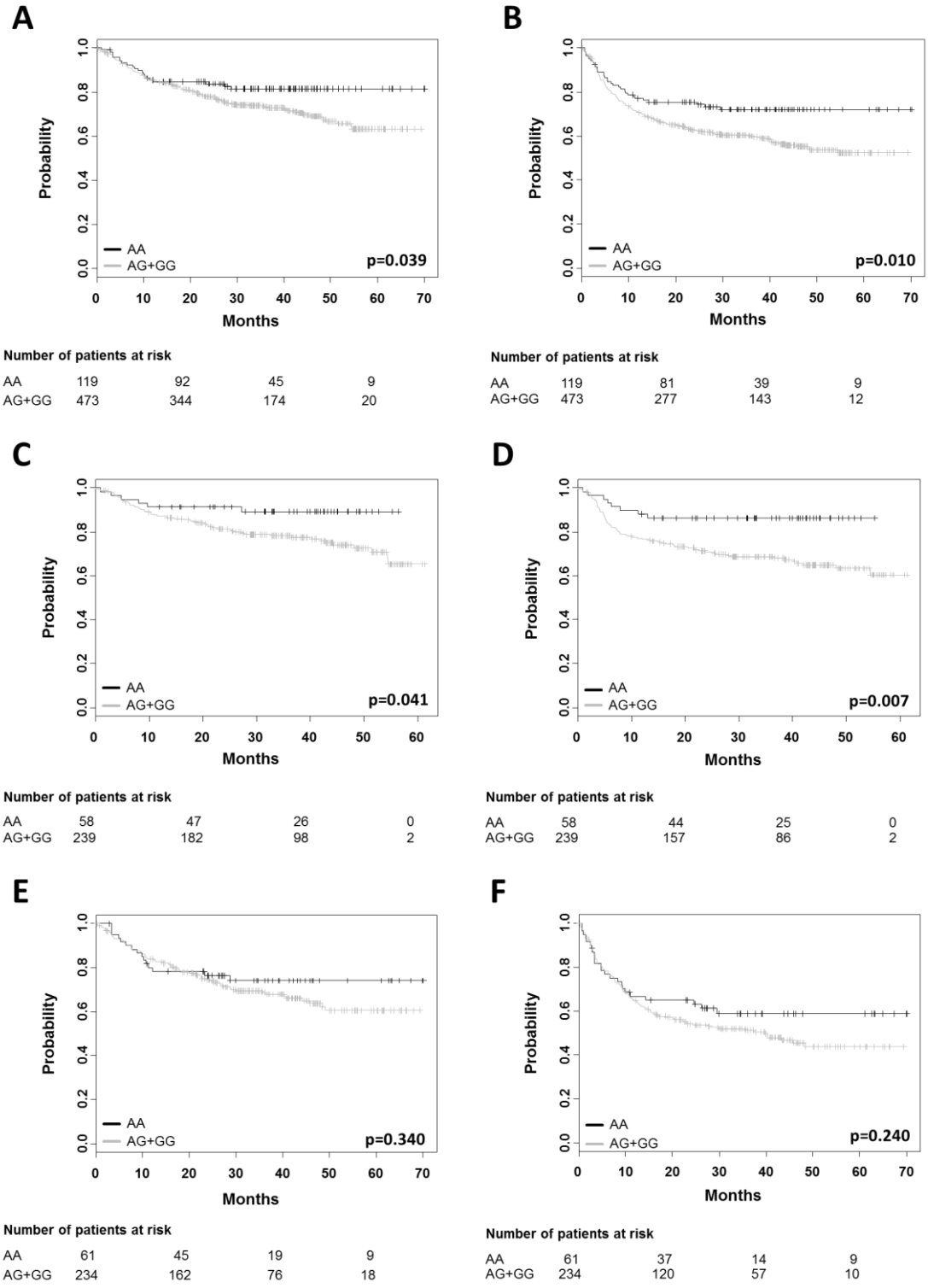

Figure 3-3 The IL10-11.668AA genotype is associated with longer survival rates for OS and EFS in patients from the RICOVER-60 cohort and in patients within the R-CHOP cohort.

Shown are the survival curves (Kaplan-Meier plots) for OS (**A,C,E**) and EFS (**B,D,F**) of aNHL patients from the RICOVER-60 cohorts in comparison with IL10-11.668G/A genotypes. **A.** OS of patients from RICOVER-60. **B.** EFS of patients from RICOVER-60. **C.** OS of patients from R-CHOP arm of RICOVER-60. **D.** EFS of patients from R-CHOP arm of RICOVER-60. **E.** OS of patients from CHOP arm of RICOVER-60. **F.** EFS of patients from CHOP arm of RICOVER-60. *P* refers to the log-rank test. Patients at risk represents the number of patients which still can develop an event (OS or EFS) at defined time points. Significant values have been observed for OS and EFS rates for patients from RICOVER-60 cohort (A,B) and for patients from the R-CHOP arm (C,D).

Table 3-5 Longer three-year survival rates for carriers of the IL10-11.668AA genotype for OS and EFS in patients from the RICOVER-60 cohorts

Three-year survival rates for carriers of the different genotypes of IL10-11.668G/A have been estimated for OS and EFS of patients from the three RICOVER-60 cohorts. P refers to the log-rank test. Three-year survival rates were significantly longer for patients with IL10-11.668AA in the RICOVER-60 cohort and the R-CHOP cohort. Confidence Interval (CI), Three-year survival rate (3-y rate).

cohort	Genotype IL10-11.668G/A	3-y rate OS	(95% CI)	p*-value	3-y rate EFS	(95% CI)	p*-value
RICOVER-60							
	GG; GA (n=473)	73.6	(69.5; 77.9)	***0.039***	60.1	(55.7; 64.8)	***0.010***
	AA (n=119)	81.5	(74.6; 89)		72.2	(64.4; 80.9)	
R-CHOP							
	GG; GA (n=239)	78.2	(73; 83.8)	***0.041***	68.7	(62.9; 75)	***0.007***
	AA (n=58)	89.2	(81.3; 97.8)		86.2	(77.7; 95.5)	
CHOP							
	GG; GA (n=234)	68.7	(62.6; 75.3)	0.340	51.3	(45; 58.4)	0.240
	AA (n=61)	74.1	(63.6; 86.4)		58.9	(47.4; 73.2)	

*log-rank test, significant p-values are italic and bold

Multivariate analyses adjusted to the IPI factors revealed a reduced relative risk for shorter OS and EFS for carriers of IL10-11.668AA compared to the other two genotypes in all three cohorts from the RIVOVER-60 trial (see table 3-6). In the RICOVER-60 cohort the estimated relative risk was significantly lower for OS (HR=0.6; p=0.030) and EFS (HR=0.60; p=0.007) for carriers of IL10-11.668AA. The estimated relative risk in the R-CHOP cohort was also significantly lower for OS (HR=0.39; p=0.030) and EFS (HR=0.35; p=0.005). In the CHOP arm the same trend for a reduced relative risk could be observed but this was not significant for OS (HR=0.78; p=0.400) or EFS (HR=0.79; p=0.300). Notably, the confidence intervals of the estimated relative risks for IL10-11.668AA for the R-CHOP cohort and the CHOP cohort overlap to some extent, whereby the confidence interval of the R-CHOP cohort does not include the value 1.

Table 3-6 Reduced relative risk for shorter OS and EFS for carriers of IL10-11.668AA

Relative risks for shorter OS and EFS for patients with IL10-11.668AA genotype have been estimated in comparison to carriers of IL10-11.668GG or IL10-11.668AG in multivariate analysis adjusted to the IPI factors. P refers to the Cox-model. Significant p-values are italic and bold. Reduced relative risks have been estimated for all three cohorts, RICOVER-60, R-CHOP and CHOP for OS and EFS. Abbreviations see table 3-4.

	Factor	HR	(95% CI)	p-value
RICOVER-60	**OS**			
	LDH > N	2.31	(1.61; 3.32)	***0.0000064***
	ECOG > 1	1.65	(1.11; 2.46)	***0.0130***
	Stage III/ IV	1.52	(1.04; 2.23)	***0.0320***
	Extranodal involvement > 1	1.32	(0.88; 1.98)	0.180
	IL10-11.668AA vs. GG&AG	0.60	(0.38; 0.95)	***0.030***
	EFS			
	LDH > N	1.57	(1.18: 2.08)	***0.002***
	ECOG > 1	1.70	(1.21; 2.40)	***0.0026***
	Stage III/ IV	1.76	(1.29; 2.40)	***0.00039***
	Extranodal involvement > 1	1.23	(0.88; 1.72)	0.230
	IL10-11.668AA vs. GG&AG	0.60	(0.41; 0.87)	***0.0068***
R-CHOP	**OS**			
	LDH > N	2.61	(1.46; 4.67)	***0.0013***
	ECOG > 1	1.52	(0.81; 2.83)	0.190
	Stage III/ IV	1.60	(0.86; 2.99)	0.140
	Extranodal involvement > 1	1.14	(0.62; 2.10)	0.670
	IL10-11.668AA vs. GG&AG	0.39	(0.17; 0.91)	***0.030***
	EFS			
	LDH > N	1.95	(1.21; 3.15)	***0.0064***
	ECOG > 1	1.61	(0.93; 2.78)	0.090
	Stage III/ IV	1.96	(1.15; 3.35)	***0.014***
	Extranodal involvement > 1	1.20	(0.72; 2.00)	0.490
	IL10-11.668AA vs. GG&AG	0.35	(0.17; 0.72)	***0.0047***
CHOP	**OS**			
	LDH > N	2.19	(1.37; 3.48)	***0.00099***
	ECOG > 1	1.71	(1.02; 2.89)	***0.043***
	Stage III/ IV	1.49	(0.92; 2.41)	0.110
	Extranodal involvement > 1	1.63	(0.94; 2.83)	0.080
	IL10-11.668AA vs. GG&AG	0.78	(0.45; 1.38)	0.400
	EFS			
	LDH > N	1.37	(0.96; 1.95)	0.080
	ECOG > 1	1.81	(1.16; 2.81)	0.0088
	Stage III/ IV	1.64	(1.12; 2.40)	***0.011***
	Extranodal involvement > 1	1.40	(0.90; 2.19)	0.140
	IL10-11.668AA vs. GG&AG	0.79	(0.51; 1.23)	0.300

Because of the prognostic relevance of the IL10-11.668G/A in the RICOVER-60 cohort this gene variation was considered attentively again in the combined cohort as well as the NHL-B cohorts. Neither positive nor negative associations with survival could be observed in any of the cohorts.

Similar results as for IL10-11.668G/A could be observed in survival analysis of the RICOVER-60 cohort for other IL10 genotypes, namely the IL10-7400In/Del (Figure 3-4) as well as IL10-2812G/A. In both cases the homozygous carriers of the minor alleles IL10-7400DelDel and IL10-2812AA showed a superior OS and EFS compared to carriers of the other two genotypes of the respective gene variation. For IL10-7400In/Del this was not significant for RICOVER-60 (OS: p = 0.074 and EFS: p = 0.237; Figure 3-4 A and B) but for OS in the R-CHOP cohort (OS: p = 0.047 and EFS: p = 0.054, Figure 3-4 C and D). For IL10-2812G/A the significance was higher in the R-CHOP cohort (OS: p = 0.032 and EFS: p = 0.030) compared to the RICOVER-60 cohort (OS: p = 0.048 and EFS: p = 0.256). In the CHOP arm an insignificant trend for a better outcome associated with IL10-7400DelDel was observed for OS (p=0.499; Figure 3-4 E) but not EFS (p=0.976; Figure 3-4 F). The same trends were observed for carriers of IL10-2812AA in the CHOP arm (OS: p=0.385; EFS: p=0.909). Survival curves showing a comparison of all three genotypes for IL10-7400In/Del are shown in the Appendix (Figure A-3). Again there was no additive effect and therefore, only a comparison of survival rates of homozygous carriers of the minor allele with those of carriers of the other two genotypes together is described here.

The respective Three-year survival rates are given in table 3-7.

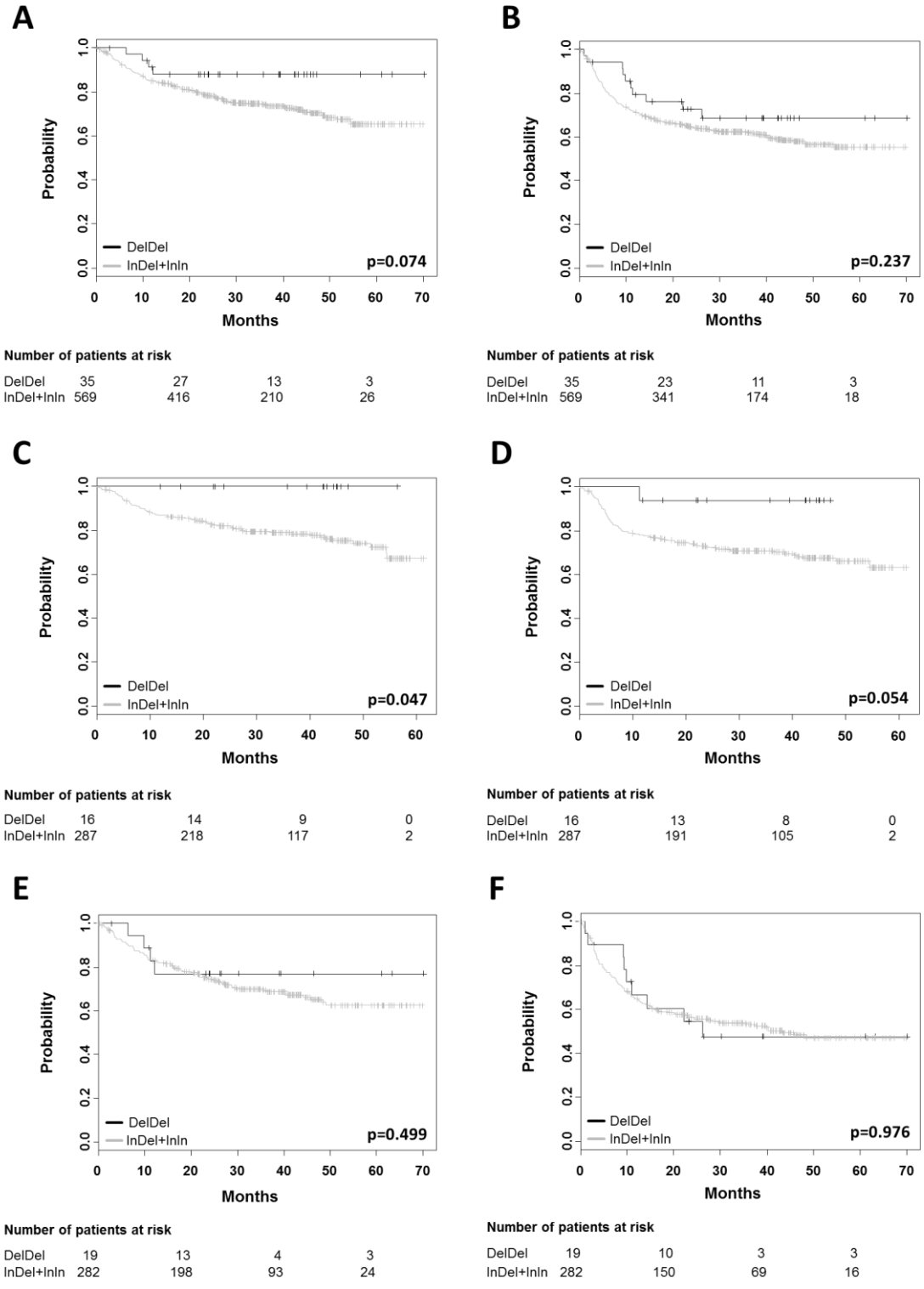

Figure 3-4 The IL10-7400DelDel genotype is associated with longer survival rates for OS and EFS in patients from the RICOVER-60 cohort and patients from the R-CHOP cohort.

Shown are the survival curves (Kaplan-Meier plots) for OS (**A,C,E**) and EFS (**B,D,F**) of aNHL patients from the RICOVER-60 cohorts in comparison with IL10-7400In/Del genotypes. **A.** OS of patients from RICOVER-60. **B.** EFS of patients from RICOVER-60. **C.** OS of patients from R-CHOP arm of RICOVER-60. **D.** EFS of patients from R-CHOP arm of RICOVER-60. **E.** OS of patients from CHOP arm of RICOVER-60. **F.** EFS of patients from CHOP arm of RICOVER-60. *P* refers to the log-rank test. Patients at risk represents the number of patients which still can develop an event (OS or EFS) at defined time points. A Significant association has been observed for OS rates for patients from the R-CHOP arm (C).

Table 3-7 Longer three-year survival rates for carriers of the IL10-7400DelDel genotype for OS and EFS in patients from the RICOVER-60 cohorts

Three-year survival rates for carriers of the different genotypes of IL10-7400In/Del have been estimated for OS and EFS of patients from the three RICOVER-60 cohorts. P refers to the log-rank test. Three-year survival rates were significantly longer for patients with IL10-7400DelDel in the R-CHOP cohort. Confidence Interval (CI), Three-year survival rate (3-y rate).

cohort	Genotype IL10-7400In/Del	3-y rate OS	(95% CI)	p*-value	3-y rate EFS	(95% CI)	p*-value
RICOVER-60							
	InIn; InDel (n=569)	74.2	(70.6; 78.1)	0.074	62	(58.1; 66.3)	0.237
	DelDel (n=35)	87.9	(77.5; 99.8)		68.7	(54.1; 87.2)	
R-CHOP							
	InIn; InDel (n=282)	79	(74.2; 84)	***0.047***	70.8	(65.6; 76.4)	0.054
	DelDel (n=19)	1			93.8	(82.6; 100)	
CHOP							
	InIn; InDel (n=287)	69.3	(63.9; 75.3)	0.499	53.1	(47.4; 59.5)	0.976
	DelDel (n=16)	77	(59.6; 99.6)		47.7	(28.8; 79)	

*log-rank test, significant p-values are italic and bold

Consistent with the univariate analyses, multivariate analyses adjusted to the IPI factors revealed a reduced relative risk for OS or EFS (Table 3-8). In the RICOVER-60 cohort this relative risk was estimated to be 0.36 (p=0.042) for OS and 0.60 (p=0.120) for EFS. This positive effect was even more pronounced for patients within the R-CHOP cohort. The relative risk for OS could in fact not be calculated because the number of events was too low. For EFS it was estimated to be 0.15 (p=0.056). In the CHOP cohort, where the relative risk for shorter OS was 0.67 (p=0.440) and 0.94 (p=0.870) for EFS, the effect was less pronounced. However, the respective confidence intervals of the R-CHOP and the CHOP cohort still overlap to some extent and therefore, the positive prognostic effect of IL10-7400DelDel cannot be ascribed to Rituximab.

Taken together, aNHL patients carrying the IL10-11.668AA genotype show a significantly better treatment outcome compared to carriers of the other two genotypes in the RICOVER-60 cohort and in the R-CHOP cohort, whereby the same trend is seen in patients within the CHOP cohort.

A follow up study of the RICOVER-60 trial has been conducted in which all patients received Rituximab. Genotyping for the most important *IL10* gene variations has been completed and the data is currently under evaluation in the IMISE in Leipzig.

Table 3-8 Reduced relative risk for shorter OS and EFS for carriers of IL10-7400DelDel

Relative risks for shorter OS and EFS for patients with IL10-7400DelDel genotype have been estimated in comparison to carriers of IL10-7400InIn or IL10-7400In/Del in multivariate analysis adjusted to the IPI factors. P refers to the Cox-model. Significant p-values are italic and bold. Reduced relative risks have been estimated for all three cohorts, RICOVER-60, R-CHOP and CHOP for OS and EFS. Abbreviations see table 3-4.

	Factor	HR	(95% CI)	p-value
RICOVER-60	**OS**			
	LDH > N	2.46	(1.71; 3.53)	0.0000011
	ECOG > 1	1.54	(1.04; 2.28)	0.031
	Stage III/ IV	1.48	(1.01; 2.16)	0.043
	Extranodal involvement > 1	1.46	(0.98; 2.17)	0.063
	IL10-7400DelDel vs. InDel&InIn	0.36	(0.13; 0.97)	0.042
	EFS			
	LDH > N	1.68	(1.26; 2.22)	0.00035
	ECOG > 1	1.57	(1.12; 2.20)	0.0095
	Stage III/ IV	1.72	(1.26; 2.34)	0.00063
	Extranodal involvement > 1	1.31	(0.94; 1.83)	0.110
	IL10-7400DelDel vs. InDel&InIn	0.60	(0.32; 1.14)	0.120
R-CHOP	**EFS**			
	LDH > N	2.12	(1.31; 3.41)	0.0022
	ECOG > 1	1.39	(0.81; 2.41)	0.240
	Stage III/ IV	1.79	(1.05; 3.04)	0.032
	Extranodal involvement > 1	1.34	(0.81; 2.23)	0.260
	IL10-7400DelDel vs. InDel&InIn	0.15	(0.02; 1.05)	0.056
CHOP	**OS**			
	LDH > N	2.28	(1.43; 3.62)	0.00052
	ECOG > 1	1.68	(1.01; 2.79)	0.045
	Stage III/ IV	1.50	(0.92; 2.43)	0.100
	Extranodal involvement > 1	1.75	(1.02; 2.99)	0.041
	IL10-7400DelDel vs. InDel&InIn	0.67	(0.24; 1.84)	0.440
	EFS			
	LDH > N	1.46	(1.03; 2.08)	0.034
	ECOG > 1	1.75	(1.14; 2.71)	0.011
	Stage III/ IV	1.65	(1.13; 2.42)	0.010
	Extranodal involvement > 1	1.46	(0.94; 2.27)	0.089
	IL10-7400DelDel vs. InDel&InIn	0.94	(0.48; 1.87)	0.870

3.1.2.2 High IL10 serum levels are associated with worse treatment outcome in the RICOVER-60 trial

To estimate the effect of elevated IL10 serum levels on the outcome of aNHL patients IL10 levels have been determined by ELISA in serum samples of 523 patients from the RICOVER-60 trial. Thereof 252 patients were treated with CHOP and 271patients were treated with R-CHOP.

According to the detection limit of 5pg/ml of the ELISA, patients were defined as high or low IL10 producers. In Figure 3-5 the respective Kaplan-Meier survival curves are shown. The relative risk for shorter OS and EFS rates for the patient group with high IL10 secretion levels was estimated using a univariate Cox-model. In addition a multivariate Cox-model adjusted for the IPI factors has been used to calculate relative risks. Statistical analyses were conducted by Markus Kreuz (IMISE).

Patients with IL10 secretion levels ≥5pg/ml were characterized by significantly shorter OS and EFS in all analysed subgroups from the RICOVER-60 cohort (Figure 3-5). Consistently the respective three-year survival rates of those patients with detectable and therefore elevated IL10 serum levels were shorter compared to those patients without detectable amounts of IL10 in their serum (Table 3-9).

Table 3-9 Shortened 3-year survival rates for OS and EFS of patients from the RICOVER-60 trial with elevated IL10 serum levels

Three-year survival rates have been estimated for OS and EFS of patients from the RICOVER-60 cohorts. According to the detection limit of 5pg/ml of the ELISA, patients were defined as high or low IL10 producers. Three-year survival rates were significantly shorter for patients with IL10 serum levels ≥5pg/ml for OS and EFS in all three cohorts. Confidence Interval (CI), Three-year survival rate (3-y rate).

	IL10 serum level	3-y rate OS	(95% CI)	p-value*	3-y rate EFS	(95% CI)	p-value*
RICOVER-60							
	<5pg/ml	78.9	(74.5; 83.5)	***0.0000089***	67.3	*(62.4; 72.6)*	***0.00028***
	≥5pg/ml	61	(53.7; 69.3)		50.3	(43.1; 58.8)	
R-CHOP							
	<5pg/ml	83.5	(78.2;.89.3)	***0.0011***	76.7	(70.8; 83.1)	***0.0091***
	≥5pg/ml	68.7	(59; 79.9)		59.9	(49.9; 71.9)	
CHOP							
	<5pg/ml	73.5	(66.7; 81.1)	***0.0036***	56.7	(49.2; 65.2)	***0.015***
	≥5pg/ml	53.3	(43.1; 66)		41.1	(31.6; 53.5)	

*univariate Cox-model, significant p-values are italic and bold

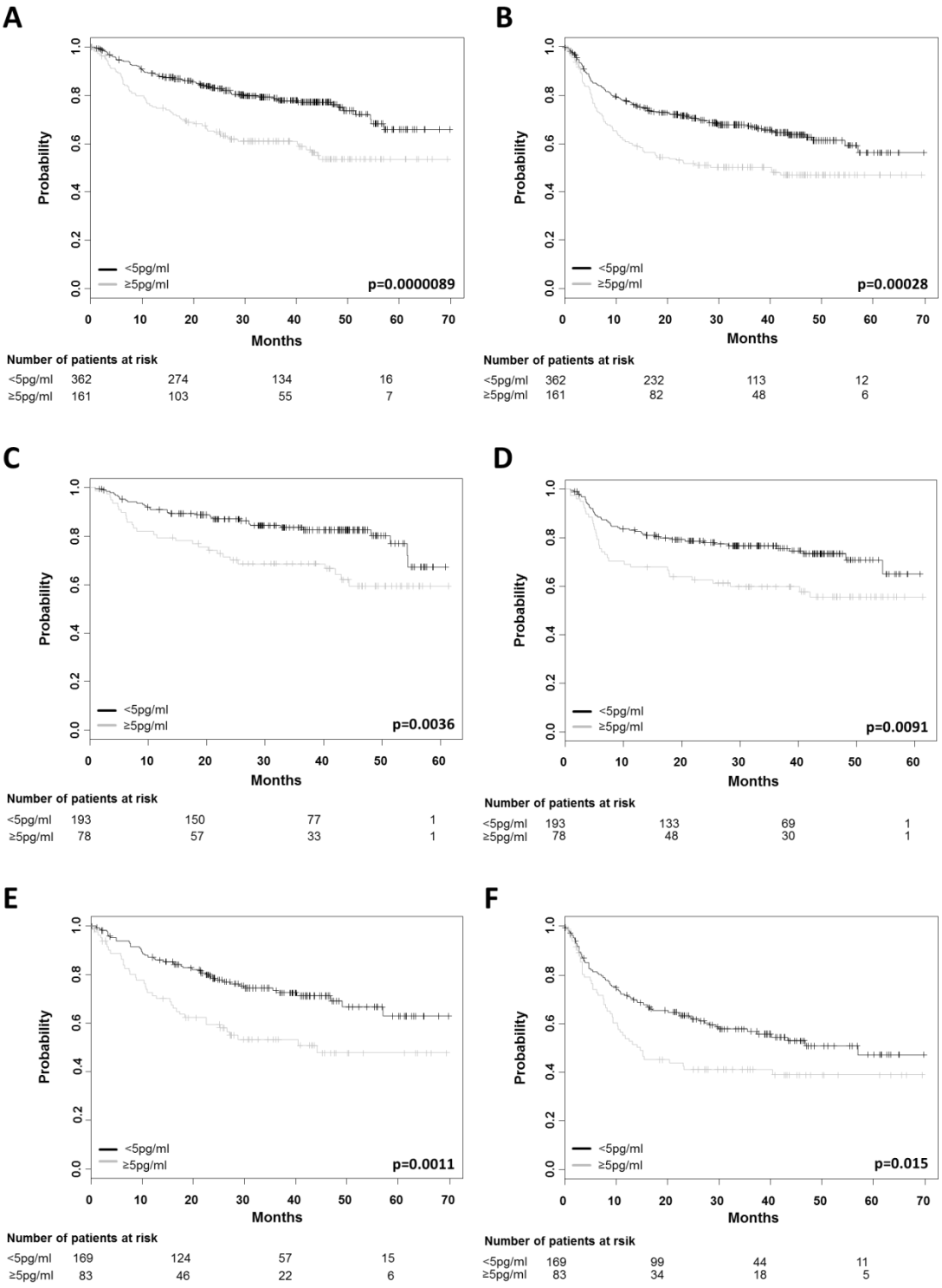

Figure 3-5 Elevated IL10 serum levels are associated with shorter survival in patients from the RICOVER-60 trial.

Shown are the survival curves (Kaplan-Meier plots) for OS (**A,C,E**) and EFS (**B,D,F**) of aNHL patients from the RICOVER-60 cohorts in comparison with IL10 serum levels. According to the detection limit of 5pg/ml of the ELISA, patients were defined as high or low IL10 producers. **A.** OS of patients from RICOVER-60. **B.** EFS of patients from RICOVER-60. **C**. OS of patients from R-CHOP arm of RICOVER-60. **D.** EFS of patients from R-CHOP arm of RICOVER-60. **E.** OS of patients from CHOP arm of RICOVER-60. **F.** EFS of patients from CHOP arm of RICOVER-60. Patients at risk represents the number of patients which still can develop an event (OS or EFS) at defined time points. P refers to the univariate Cox-model. Significant association has been observed for patients with IL10 serum levels ≥5pg/ml for OS and EFS in all three cohorts.

Multivariate analyses adjusted to the IPI factors revealed that the estimated relative risks of IL10 serum levels ≥5pg/ml are comparable to clinical factors included into the IPI in all the RICOVER-60 subgroups (Table 3-10). The estimated relative risks are comparable in all three cohorts and higher for OS than EFS.

In the RICOVER-60 cohort the relative risk for shorter OS for patients with elevated IL10 serum levels was estimated to be 1.72 (p=0.0014), while it was 1.40 (p=0.020) for shorter EFS. In both cases it was higher than the estimated risk for extranodal involvement or higher ECOG. Notably, in both cases the confidence interval did not include the 1, which means that that the probability that the real relative risk is higher than 1 is given.

In the R-CHOP cohort the estimated relative risk for shorter OS was 1.72 (p=0.036) and 1.47 (p=0.092) for EFS. For OS this was higher than the estimated relative risk for all other IPI factors excluding enhanced LDH levels. The value 1 was not within the confidence interval. For EFS it was higher than the risks estimated for extranodal involvement and higher ECOG.

In the CHOP cohort a relative risk for shorter OS of 1.71 (p=0.018) and of 1.33 for EFS (p=0.130) was calculated. This estimated relative risk was higher compared to the risks calculated for higher ECOG or higher stage in case of OS but not EFS.

Taken together it could be shown that high IL10 production negatively influences treatment outcome in the RICOVER-60 cohort. The addition of Rituximab to CHOP therapy does not overcome adverse prognostic features reported here and elsewhere for elevated IL10 levels.

Table 3-10 Enhanced relative risks for patients from the RICOVER-60 cohorts with elevated IL10 serum levels

Relative risks for shorter OS and EFS for patients with elevated IL10 serum levels (≥5pg/ml) have been estimated in multivariate analysis adjusted to the IPI factors in the RICOVER-60, R-CHOP and CHOP cohorts. Enhanced relative risks have been estimated for all three cohorts for OS and EFS. P refers to the Cox-model. Significant p-values are italic and bold. Abbreviations see table 3-4.

	Factor	HR	(95% CI)	p-value
RICOVER-60	**OS**			
	LDH > N	2.12	(1.46; 3.07)	***0.00007***
	ECOG > 1	1.37	(0.90; 2.09)	0.140
	Stage III/ IV	1.55	(1.04; 2.3)	***0.030***
	Extranodal involvement > 1	1.47	(0.98; 2.21)	0.061
	IL10≥5pg/ml	1.72	(1.23; 2.39)	***0.0014***
	EFS			
	LDH > N	1.52	(1.12; 2.05)	***0.0068***
	ECOG > 1	1.38	(0.95; 2.00)	0.092
	Stage III/ IV	1.89	(1.35; 2.64)	***0.00019***
	Extranodal involvement > 1	1.30	(0.92; 1.84)	0.140
	IL10≥5pg/ml	1.40	(1.06; 1.87)	***0.020***
R-CHOP	**OS**			
	LDH > N	2.2	(1.22; 3.94)	***0.008***
	ECOG > 1	1.39	(0.74; 2.61)	0.310
	Stage III/ IV	1.60	(0.84; 3.05)	0.160
	Extranodal involvement > 1	1.25	(0.68; 2.29)	0.470
	IL10≥5pg/ml	1.72	(1.04; 2.86)	***0.036***
	EFS			
	LDH > N	1.78	(1.08; 2.94)	***0.023***
	ECOG > 1	1.27	(0.71; 2.26))	0.420
	Stage III/ IV	1.75	(0.99; 3.07)	0.053
	Extranodal involvement > 1	1.33	(0.79; 2.27))	0.290
	IL10≥5pg/ml	1.47	(0.94; 2.31)	0.092
CHOP	**OS**			
	LDH > N	2.13	(1.31; 3.47)	***0.002***
	ECOG > 1	1.37	(0.77; 2.42)	0.280
	Stage III/ IV	1.48	(0.89; 2.46)	0130
	Extranodal involvement > 1	2.02	(1.16; 3.53)	***0.013***
	IL10≥5pg/ml	1.71	(1.10; 2.66)	***0.018***
	EFS			
	LDH > N	1.40	(0.95; 2.05)	0.088
	ECOG > 1	1.59	(0.96; 2.62)	0.070
	Stage III/ IV	1.93	(1.27; 2.94)	***0.002***
	Extranodal involvement > 1	1.53	(0.96; 2.46)	0.076
	IL10≥5pg/ml	1.33	(0.92; 1.94)	0.130

3.1.3 No associations of *IL10* gene variations with survival of patients within the small MInT cohort with superior outcome

The number of patients (n=178) in the MInT cohort was comparably small. 89 patients were in the CHOP and 89 patients in the R-CHOP arm of this cohort. For gene variations with a low frequency of the minor allele, like IL10-7400In/Del or IL10+5876C/T, survival analysis could not be conducted for homozygous carriers of these alleles.

The only significant results were obtained for IL10-824C/T and IL10-597C/A. These gene variations are in such strong LD, that the same patients are in each genotype group. The minor allele was associated with significantly shorter OS rates (p=0.011). No effect of these gene variations was observed for EFS. However, the same effect is not seen in any other cohort to this extend. Therefore and due to the very low number of homozygous carriers of the minor alleles (n=11) this effect should not be over interpreted.

The MInT trial was similar to the RICOVER-60 trial in terms of tested treatment strategies. These two trials differ regarding the age of recruited patients. The three-year-survival rates for OS were 93% for the R-CHOP arm compared to 84% in the CHOP cohort (Pfreundschuh et al., 2006). This means that the general outcome is much better in this trial compared to the RICOVER-60 trial (Pfreundschuh et al., 2008) and overall differences are pretty small.

Due to the small of patients in this cohort and the general very good treatment outcome, the two treatment arms could not be analysed separately.

3.1.4 *IL10* gene variations and serum levels do not have significant prognostic relevance for treatment outcome in T-NHL patients

Associations of 13 *IL10* gene variations and IL10 serum levels with OS and EFS have been analysed to determine if they are of prognostic relevance for treatment outcome of T-NHL. We analysed the gene variations IL10-12806C/T, IL10-11777A/G, IL10-11668G/A, IL10-7400In/Del, IL10-6752A/T, IL10-6208G/C, IL10-3538T/A, IL10-2812G/A, IL10-2726C/A, IL10-1087A/G, IL10-597C/A and IL10+4259A/G but not IL10-824C/T and IL10+5876C/T. IL10-824C/T is in strong LD with IL10-597C/A. IL10+5876C/T has been

included into our analyses at a later time point of our studies. In addition IL10$_{+5876C/T}$ is very rare, therefore its value information in a cohort of only 117 T-NHL patients would be rather poor. Genotyping for *IL10* gene variations has been done mainly by Frederike von Bonin and determination of respective IL10 serum levels via ELISA has been done by Dr. rer. nat. Nils Schoof as part of his dissertation. The impact of this dissertation was the completion of the genotyping data for *IL10* gene variations and mainly the evaluation and interpretation of the results obtained from Markus Kreuz from the IMISE in Leipzig.

In addition to *IL10* gene variations and serum levels the cytokine receptor genes coding for IL4 receptor (IL4R), tumor necrosis factor alpha receptor I (TNFRI) and TNFRII as well as the respective circulating levels of soluble receptors have been examined in the same patient cohort. This work has been done by Dr. rer. nat. Nils Schoof and Dr. med. Irene Stoller as part of their dissertations, assisted by Frederike von Bonin.

A manuscript with the title “Circulating levels of TNF- receptor II are prognostic for patients with peripheral T cell Non-Hodgkin lymphoma” resulted from this work and is attached to this dissertation.

The most important finding of the study was a strong association of circulating levels of sTNFRII with OS and EFS. T-NHL patients with serum levels of TNFRII >2.16ng/ml had significantly shorter OS (p=0.003) and EFS (p=0.0007).

The impact of this dissertation was the evaluation of all available data supplied by Markus Kreuz and writing of the above mentioned manuscript. During the evaluation process, analyses of associations between the respective circulating serum levels of soluble receptors and survival have been requested.

3.1.4.1 Associations of *IL10* gene variations with OS or EFS of T-NHL patients

Univariate analyses of OS and EFS in correlation with *IL10* gene variations revealed shorter survival rates for the IL10$_{-7400DelDel}$ (Figure 3-6 A and B). The respective three-year survival rates for patients characterized by IL10$_{-7400DelDel}$ were calculated to be shorter compared to the three-year survival rates of carriers of IL10$_{-7400InIn}$ or IL10$_{-7400InDel}$ (Table 3-11).

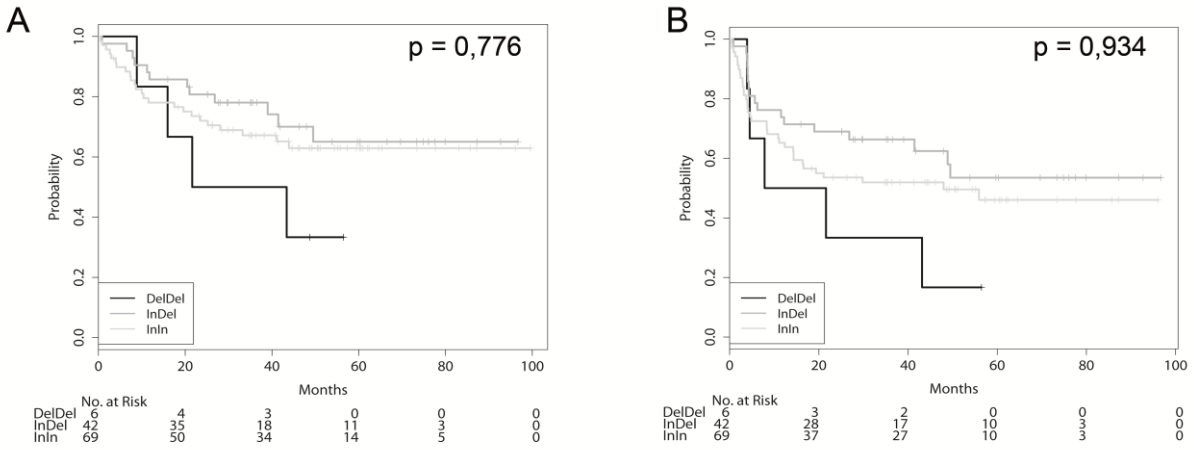

Figure 3-6 IL10-7400DelDel is insignificantly associated with shorter OS and EFS in patients suffering from T-NHL.

Shown are the survival curves (Kaplan-Meier plots) for OS (A) and EFS (B) of T-NHL patients in comparison with IL10-7400In/Del genotypes. P refers to the log-rank trend test. Patients at risk represents the number of patients which still can develop an event (OS or EFS) at defined time points. Figure is taken from the Manuscript "Circulating levels of TNF- receptor II are prognostic for patients with peripheral T cell Non-Hodgkin lymphoma" by Heemann et al.

This tendency was comparable to the observations described within the large cohort of 942 aNHL patients in the NHL-B. However, the observed differences were not significant for T-NHL patients. Table 3-11 shows the results obtained via comparison of carriers of all three genotypes and of homozygous carriers of the minor allele with carriers of the other two genotypes together.

Table 3-11 Shorter three-year survival rates for carriers of the IL10-7400DelDel genotype for OS and EFS in patients with T-NHL

Three-year survival rates for carriers of the different genotypes of IL10-7400In/Del have been estimated for OS and EFS of patients from the T-NHL cohort. P refers to the log-rank test. Three-year survival rates were shorter for patients with IL10-7400DelDel. Confidence Interval (CI), Three-year survival rate (3-y rate). The table is taken and modified from the manuscript "Circulating levels of TNF- receptor II are prognostic for patients with peripheral T cell Non-Hodgkin lymphoma" by Heemann et al.

Genotype	3-y rate OS	p*	3-y rate EFS	p*	Genotype	3-y rate OS	p*	3-y rate EFS	p*
IL10-7400In/Del									
InIn (n=69)	67.2	0.776	51.9	0.934	InIn; InDel	71.2	0.153	57.3	0.139
InDel (n=42)	78.1		66.3		DelDel	50		33.3	
DelDel (n= 6)	50.0		33.3						
*log-rank trend test, significant p-values are italic and bold									

A respective multivariate Cox model for every *IL10* gene variation adjusted for the IPI factors was estimated. This multivariate analysis showed a 2.2 (OS) or 1.9 (EFS) times increased relative risk for carriers of IL10-7400DelDel, which is close to that of having elevated LDH, higher ECOG-status or age, but was not significant in our study due to the low number of patients carrying this gene variation (Table 3-12).

Table 3-12 Enhanced relative risk for shorter OS and EFS for carriers of IL10-7400DelDel gene variation in the T-NHL cohort

Relative risks for shorter OS and EFS for patients with IL10-7400DelDel genotype have been estimated in multivariate analysis adjusted to the IPI factors in the T-NHL cohort. P refers to the Cox-model. Significant p-values are italic and bold. Abbreviations are given in table 3-4. The table was taken and modified from the Manuscript "Circulating levels of TNF- receptor II are prognostic for patients with peripheral T cell Non-Hodgkin lymphoma" by Heemann et al.

	Factor	RR	(95% CI)	p-value
IL10 -7400In/Del	**OS**			
	LDH > N	2.25	(0.95; 5.34)	0.065
	age > 60 years	2.41	(1.07; 5.38)	***0.033***
	ECOG > 1	2.73	(1.03; 7.20)	***0.043***
	Stage III/ IV	0.75	(0.35; 1.61)	0.467
	Extranodal involvement > 1	4.64	(2.13;10.08)	***<0.001***
	DelDel vs InDel&InIn	2.21	(0.74; 6.65)	0.157
	EFS			
	LDH > N	1.63	(0.75; 3.51)	0.215
	age > 60 years	1.73	(0.92; 3.28)	0.091
	ECOG > 1	2.16	(0.46; 5.15)	0.083
	Stage III/ IV	0.74	(0.40; 1.38)	0.349
	Extranodal involvement > 1	2.89	(1.51; 5.51)	***0.001***
	DelDel vs InDel&InIn	1.90	(0.72; 4.97)	0.193

In a previous study of Lee and colleagues a protective effect of the ATA haplotype (formed by IL10-1087A, -824T, -597A) has been described (Lee et al., 2007). Therefore, this effect was evaluated in our T-NHL cohort focusing on IL10-824C/T representing the ATA haplotype best (Figure 3-1). Patients characterized by the presence of at least one T-allele (IL10-824TT, IL10-824CT) were compared to homozygous carriers for the C-allele (IL10-824CC). Thereby shorter survival rates for OS (p=0.178) and EFS (p=0.359) could be observed for patients carrying at least one T-allele. However, this was not significant. A further detailed analysis revealed that the four T-NHL patients with IL10-824TT showed a very short OS and EFS within the first 30 month of follow up. Furthermore, no comparable trends for shorter cumulative OS or EFS were detected for any of the other *IL10* gene variations analysed.

3.1.4.2 Associations of circulating serum levels of IL10 with survival of T-NHL patients

As circulating levels of certain cytokines are parameters that could, to some extent reflect the actual host-lymphoma interaction and thereby influence the prognosis of lymphoma patients, the circulating levels of IL10 were determined by ELISA using pretreatment sera of T-NHL patients whenever possible. The ELISA was done by Dr. Nils Schoof. Statistical analysis was done by Markus Kreuz (IMISE). The evaluation of the statistical results was part of this dissertation.

To define high and low producers, the threshold for IL10 was set on 5 pg/ml, according to the detection limit. OS and EFS rates of T-NHL patients were compared to high and low serum levels in univariate analyses.

During the first 40 months patients with IL10 serum levels ≥5 pg/ml seemed to relapse more often (have more events for OS or EFS) compared with those patients having <5 pg/ml IL10 in their serum. However, at the end of the follow up both groups show the same OS and EFS. Due to the low number of patients the curves become instable at this point. The overall analysis revealed no statistical significant differences according to the IL10 serum levels (OS: p=0.54; EFS p=0.36) (Figure 3-7 A and B).

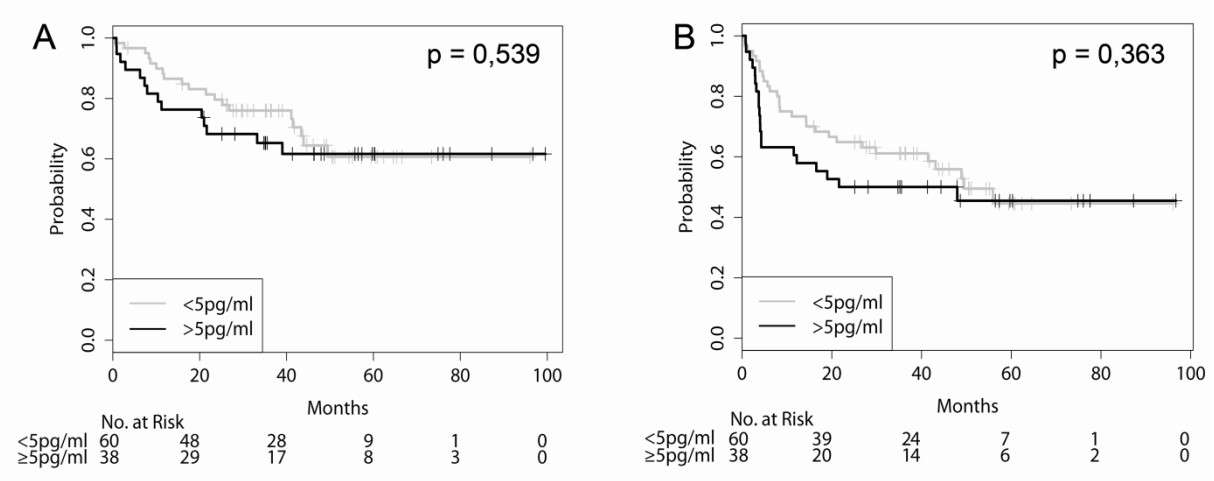

Figure 3-7 Overall and Event free survival of patients suffering from T-NHL in relation to IL10 serum levels.

The survival curves (Kaplan-Meier plots) show a comparison of the OS (**A**) and EFS (**B**) of T-NHL patients with IL10 serum levels. Patients with serum levels >5pg/ml are considered as high and patients <5pg/ml as low producers. *P* refers to the log-rank test. Patients at risk represents the number of patients which still can develop an event (OS or EFS) at defined time points (here 10 month interval monitored). The figure was taken and modified from the Manuscript “Circulating levels of TNF-receptor II are prognostic for patients with peripheral T cell Non-Hodgkin lymphoma” by Heemann et al.

3.2 Investigation of interindividual differences of IL10 production capacity in comparison to *IL10* gene variations in LCLs

Interindividual differences in IL10 production capacity have been attributed to genetic variations in the *IL10* promoter (Gibson et al., 2001; Mormann et al., 2004; Rieth et al., 2004). In one of these studies the IL10-7400DelDel genotype has been found to be associated with high levels of IL10 secretion in LPS stimulated peripheral blood mononuclear cells (PBMCs) (Rieth et al., 2004). The same trend has been observed for lymphoblastoid cell lines (LCLs). These are immortalized B lymphocytes, established via infection with the EBV strain B95/8 (for detailed information see Material and Methods 2.9.2). Due to the fact that the IL10-7400DelDel genotype is rather rare only 4 homozygous LCL were included into that study.

Therefore, this dissertation aimed to enlarge the overall number of LCLs measured for IL10 secretion, thereby enhancing the number of LCLs with the IL10-7400DelDel genotype and to analyse additional *IL10* gene variations compared to the study of Rieth et al.(Rieth et al., 2004).

All IL10 gene variations included into the survival analysis have also been included into this analysis. The gene variations IL10-12806C/T, IL10-11777A/G, IL10-11668G/A, IL10+4259A/G, IL10+5876C/T, IL10-2812G/A and IL10-2726C/A have been included due to the same reasons as they have been included into the survival analysis of aNHL patients, their localization within evolutionary conserved regions and their functional description relevant for *IL10* expression (Gibson et al., 2001; Jones and Flavell, 2005; Shoemaker et al., 2006).

Approximately 130 LCLs established in the context of previous studies from Prof. Dr. Kube have been cultured, these include the 80 LCLs published within the study of Rieth et al (Rieth et al., 2004). Not all these cell lines could be successfully recultured. Therefore, attempts were done to establish new LCLs from B cells, whereof only 6 were successfully immortalized. In addition to this, 8 LCLs were derived from the HapMap project. These have to be evaluated with care due to the fact that all available HapMap LCLs with IL10-7400DelDel genotype (n=4) have been included into this study, which is no random selection and not correct in terms of population genetics. However, the IL10-7400DelDel genotype was of particular interest for this thesis and only two cell lines of the remaining LCLs had this genotype.

Table 3-13 Genotype frequencies and HDW of analysed LCLs

Genotype frequencies and results of the HDW exact test are shown for all analysed LCLs (n=111) in comparison to the LCLs excluding all HapMap (HM) LCLs (n=103), which have been chosen without random selection. In case of n≠111 or n≠103 respective genotyping analysis was not successful.

			All LCLs (n=111)			LCLs without HM (n=103)		
SNP Name	**rs-number**	**Genotype**	**number of LCLs**	**% of LCLs**	**HWE exact**	**number of LCLs**	**% of LCLs**	**HWE exact**
IL10-12806C/T	rs17015865	TT	9	8.1	0.320	5	4.9	1.000
		CT	38	34.2		35	34.0	
		CC	64	57.7		63	61.2	
		total	111			103		
IL10-11777A/G	rs4072227	GG	0	0.0	1.000	0	0.0	1.000
		AG	16	14.4		16	15.5	
		AA	95	85.6		87	84.5	
		total	111			103		
IL10-11668G/A	rs4072226	AA	28	25.2	0.057	23	22.3	0.162
		AG	45	40.5		43	41.7	
		GG	38	34.2		37	35.9	
		total	111			103		
IL10-7400In/Del	7400In/Del	DelDel	7	6.4	0.608	3	3.0	0.758
		InDel	38	34.9		35	34.7	
		InIn	64	58.7		63	62.4	
		total	109			101		
IL10-6752A/T	rs6676671	TT	21	19.6	0.226	17	17.2	0.295
		AT	45	42.1		42	42.4	
		AA	41	38.3		40	40.4	
		total	107			99		
IL10-6208G/C	rs10494879	CC	27	24.8	0.059	22	21.8	0.154
		CG	44	40.4		42	41.6	
		GG	38	34.9		37	36.6	
		total	109			101		
IL10-3538T/A	rs1800890	AA	23	20.7	0.118	19	18.4	0.157
		AT	45	40.5		42	40.8	
		TT	43	38.7		42	40.8	
		total	111			103		
IL10-2812G/A	rs6703630	AA	12	10.9	0.148	7	6.9	0.600
		AG	38	34.5		36	35.3	
		GG	60	54.5		59	57.8	
		total	110			102		
IL10-2726C/A	rs6693899	AA	15	13.5	0.677	12	11.7	0.828
		AC	48	43.2		45	43.7	
		CC	48	43.2		46	44.7	
		total	111			103		
IL10-1087A/G	rs1800896	GG	31	28.7	0.056	27	27.0	0.164
		AG	44	40.7		43	43.0	
		AA	33	30.6		30	30.0	
		total	108			100		
IL10-824C/T	rs1800871	TT	6	5.5	1.000	6	5.9	1.000
		CT	40	36.7		40	39.6	
		CC	63	57.8		55	54.5	
		total	109			101		
IL10-597C/A	rs1800872	AA	6	5.5	1.000	6	5.9	1.000
		AC	40	36.7		40	39.6	
		CC	63	57.8		55	54.5	
		total	109			101		
IL10+4259A/G	rs3024498	GG	12	11.0	***0.048***	7	6.9	0.399
		AG	34	31.2		33	32.7	
		AA	63	57.8		61	60.4	
		total	109			101		
IL10+5876C/T	rs3024505	TT	2	1.8	0.517	2	2.0	0.511
		CT	34	31.2		33	32.7	
		CC	73	67.0		66	65.3	
		total	109			101		

Italic bold p-values are significant

In the end, 111 LCLs have been successfully cultured. Pellets for DNA and RNA (qRT-PCR) preparation as well as supernatants for ELISA (n=107) have been harvested. DNA has been used for genotyping analysis using Taqman SNP genotyping assays, and the SNaPshot-assay or a fragment length analysis for IL10-7400In/Del (for details see Material and Methods 2.11.3 and table 2-9). Genotype frequencies and results of the HDW are shown in table 3-13. Only the gene variation IL10+4259G/A was not in HDW. This was caused by the HapMap LCLs, because it was no longer observed in the group, excluding all these cell lines. However, for statistical analysis the complete group of LCLs was used, because in a preliminary analysis (data not shown) only IL10-7400In/Del showed significant associations.

Once sufficient LCLs have been cultured, qRT-PCR and ELISA were conducted (for details see Material and Methods 2.10.3 and 2.11.12). As not all samples could be measured on the same qRT-PCR plate, linearized plasmids containing PCR products of the respective primers used for the qRT-PCR (IL10e1-2 and β2m) have been used as standards in order to obtain comparable results for all plates.

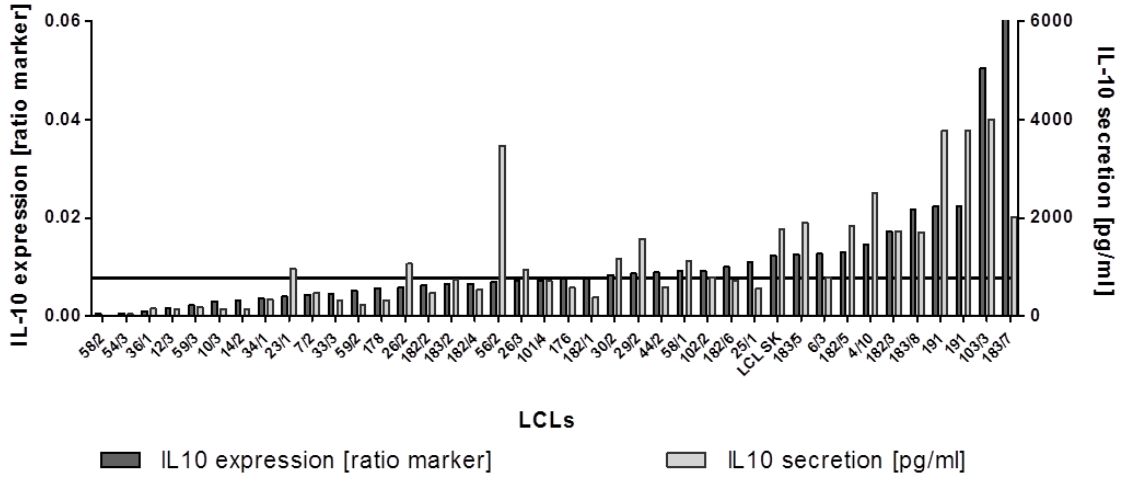

Figure 3-8 *IL10* expression and secretion of LCLs are comparable.

LCLs were cultured in a density of $5*10^5$/ml. Pellets for RNA preparation and supernatants were harvested after 24h. *IL10* expression was measured using qRT-PCR. Linearized plasmids containing PCR products of the respective primers used for the qRT-PCR (IL10e1-2 and β2m) have been used as standards. Results are shown as ratio marker of number of corresponding standard molecules (NSM) IL10/ NSM β2m on the left y-axis. For details see chapter 2.11.8. Supernatants of LCLs were used to define IL10 secretion by ELISA and the results are shown in pg/ml on the right y-axis. (for details see chapter 2.10.4 and 2.11.8) On the x-axis LCL numbers are shown ordered from the cell with the lowest *IL10* expression to the highest. The median of *IL10* expression and IL10 secretion are marked with overlapping lines. The results of 40 representative LCLs out of 111 LCLs are shown.

The results of qRT-PCR and ELISA measurements are plotted in one graph exemplary for 40 LCLs in figure 3-8. Besides some exceptions both measurements seem to be comparable.

All statistical analyses have been conducted supported by Hans Joachim Helms from the department of medical statistics.

3.2.1 *IL10* expression of LCLs in comparison to *IL10* gene variations

RNA of 111 LCLs has been harvested after 24h cultivation and cDNA has been reverse transcribed from these samples for qRT-PCR analysis of *IL10* expression of the respective LCLs.

Due to the relative large amount of collected RNA samples, three 384-well plates were used for the qRT-PCR analysis. Therefore, each qRT-plate must be thought of as an independent experiment. To enhance comparability of the three measurements, plasmids, containing the respective PCR-Products of *IL10* and the housekeeper β2m primers, have been used in different concentrations as a standard. This standard was included onto each qRT-PCR analysis (see Material and Methods 2.11.12). In addition to this, a two-way analysis of variance (ANOVA) has been conducted, examining the impact of the two variables *IL10* gene variation and qRT-PCR plate (independent variables) on *IL10* expression, in order to exclude that observed associations between *IL10* expression level and the respective *IL10* gene variation were caused by the fact that the samples were measured on different qRT-PCR plates. Because the results of the qRT-PCR were not normally distributed, all measured values have been ranked before analysis of variance.

The qRT-PCR plates had no influence on the results as there were no significant associations observed between *IL10* gene variations and the qRT-PCR plates. No interactions between these two variables were found, meaning that none of the gene variations differed significantly between plate one, two and three. Significant results were obtained for two *IL10* gene variations, IL10$_{-7400In/Del}$ and IL10$_{+5876C/T}$ (Table 3-14).

Table 3-14 Associations of *IL10* gene expression of LCLs with the gene variations IL10-7400In/Del and IL10+5876C/T

111 LCLs were cultivated in a density of $5x10^5$/ml and pellets for RNA preparation were harvested after 24h. After reverse transcription into cDNA, *IL10* expression has been measured using qRT-PCR analysis (for details see Chapter 2.11.12). Shown are the results of a two-way ANOVA, examining associations between *IL10* expression levels with *IL10* gene variations.

SNP Name	rs-number	IL10 gene variation (p-value*)
IL10-12806C/T	rs17015865	0.2885
IL10-11777A/G	rs4072227	0.0791
IL10-11668G/A	rs4072226	0.9344
IL10-7400In/Del	7400In/Del	***0.0308***
IL10-6752A/T	rs6676671	0.5710
IL10-6208G/C	rs10494879	0.9946
IL10-3538T/A	rs1800890	0.7635
IL10-2812G/A	rs6703630	0.1698
IL10-2726C/A	rs6693899	0.4067
IL10-1087A/G	rs1800896	0.3430
IL10-824C/T	rs1800871	0.1362
IL10-597C/A	rs1800872	0.1362
IL10+4259A/G	rs3024498	0.1597
IL10+5876C/T	rs3024505	***0.0454***

* two way AVOVA variance analysis, Italic bold p-values are significant

In a last step *IL10* gene variations showing significant associations with *IL10* expression (IL10-7400In/Del and IL10+5876C/T) have been examined in a pair comparison using the Wilcoxon Test. For the comparisons of the IL10-7400In/Del genotypes no significant differences could be observed (Figure 3-9 A). The median of *IL10* expression is lowest in the group with IL10-7400DelDel but the interquartile range of this group is quite big. The number of LCLs with this genotype is rather small (n=8). Therefore, the real median *IL10* expression of the IL10-7400DelDel group could be much higher than in the group of LCLs included into this study.

The only significant result was obtained for the comparison of IL10+5876CC with IL10+5876CT (p=0.020) but not for the comparison of IL10+5876CC and IL10+5876TT (Figure 3-9 B). The median *IL10* expression of the IL10+5876TT group is higher than the median of the other two genotypes. However the interquartile ranges of the other two genotypes overlap with the one of the IL10+5876TT group. In addition to this, the number of LCLs carrying the IL10+5876TT genotype is only 2 and therefore the observation should not be over interpreted.

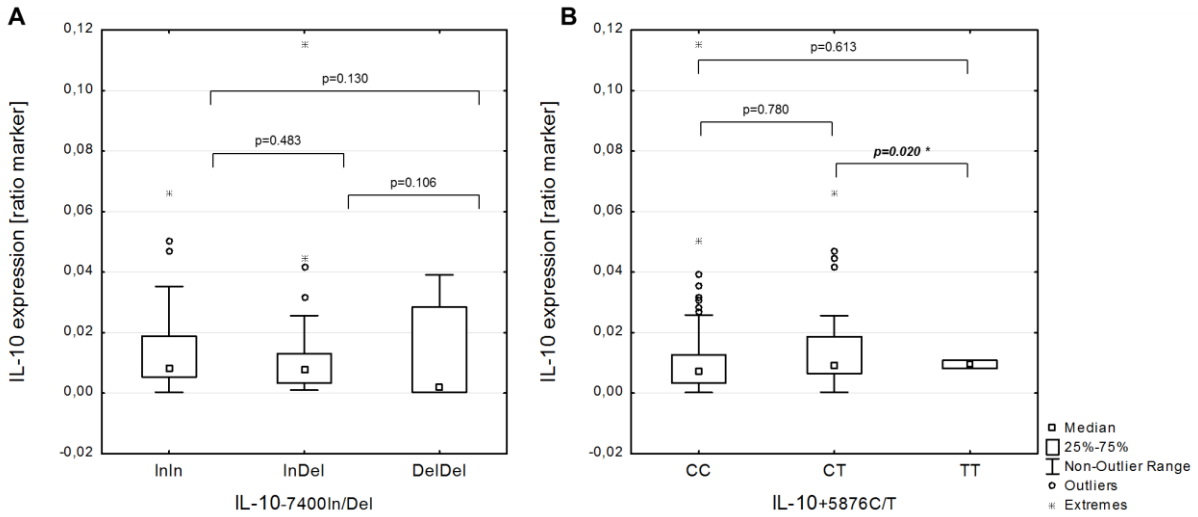

Figure 3-9 The difference between *IL10* expression level of LCLs with different *IL10* genotypes was significant only for the LCLs with IL10$_{+5876CT}$ compared to LCLs with IL10$_{+5876TT}$.

IL10 expression of LCLs was measured using qRT-PCR (see figure 3-8). Shown are the median and the interquartile ranges of *IL10* expression for each possible genotype of the gene variations IL10$_{-7400In/Del}$ and IL10$_{+5876C/T}$. *IL10* expression results are shown as ratio marker of NSM IL10/ NSM β2m. P refers to the Wilcoxon test adjusted for Bonferroni used for pair wise comparison of *IL10* expression of LCLs with different genotypes. Significant p-value is shown in italic and bold.

Subsequently, a second kind of statistical analysis has been conducted. According to the median *IL10* expression (0.000762 NSM IL10/NSM β2m) LCLs were divided into two groups; *IL10* high expressing LCLs (*IL10* expression ≥ median) and *IL10* low expressing LCLs (*IL10* expression < median). In table A-3 in the appendix the frequencies of all genotypes are compared between *IL10* high and low expressing LCLs. A Pearson X^2 test was used to examine whether significant differences can be observed between the two groups associated with any genotype of the analysed *IL10* gene variations. No significant associations were found. The smallest p-value was again observed for IL10$_{+5876C/T}$, were the minor genotype IL10$_{+5876TT}$ was only found in 2 LCLs with high *IL10* expression.

In summary, no associations between *IL10* expression and *IL10* gene variations could be observed for the analysed LCLs.

3.2.2 IL10 secretion of LCLs in comparison to *IL10* gene variations

IL10 secretion of 107 LCLs has been measured using an ELISA assay for the detection of human IL10 (see Material and Methods 2.10.3). In accordance to the qRT-PCR results, the values measured for IL10 secretion were not normally distributed. Therefore, all measured values have been ranked first. After this they were used for a Kruskal-Wallis ANOVA. As shown in table 3-15 none of the analysed *IL10* gene variations showed significant associations with IL10 secretion level.

In figure 3-10 this comparison is shown in a box-plot for IL10$_{-7400In/Del}$ and IL10$_{+5876C/T}$. These graphs look similar to those obtained for *IL10* expression. For IL10$_{-7400In/Del}$ the median IL10 secretion is lowest in the group of IL10$_{-7400DelDel}$ but the interquartile range of this group includes all values in the interquartile ranges of the other two genotypes.

The plot of IL10$_{+5876C/T}$ shows again the highest median for the group of IL10$_{+5876TT}$. This group includes only two LCLs and the interquartile ranges of the other two groups include values much higher than the median of the IL10$_{+5876TT}$ group. Therefore, no statement on the influence of the IL10$_{+5876C/T}$ gene variation on IL10 secretion can be made.

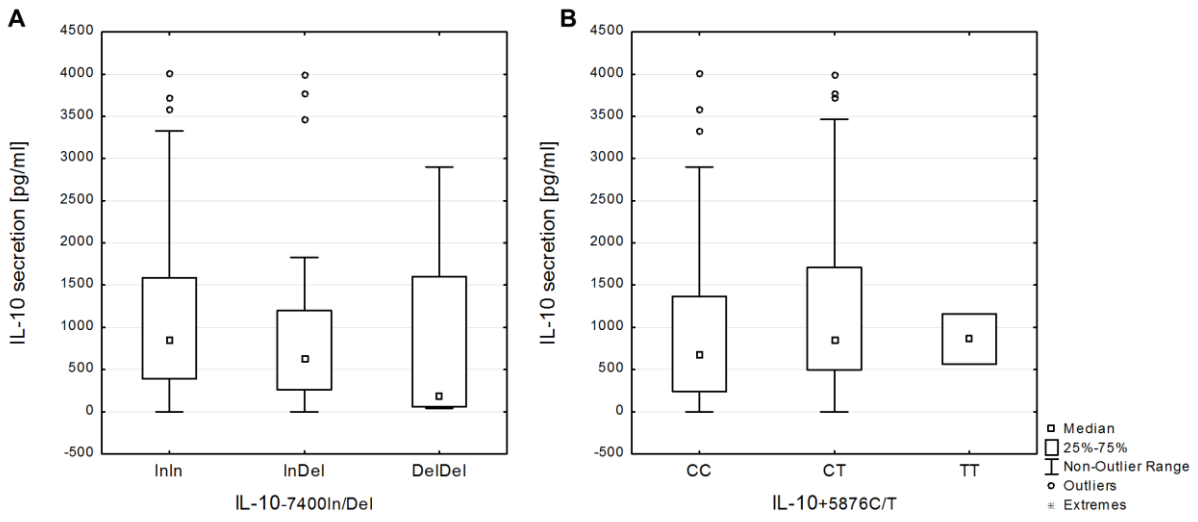

Figure 3-10 No differences between IL10 secretion levels of LCLs with different *IL10* genotypes

IL10 secretion of 107 LCLs was measured using ELISA (for details figure 3-8). Shown are the median and the interquartile ranges of IL10 secretion for each possible genotype of the gene variations IL10$_{-7400In/Del}$ and IL10$_{+5876C/T}$. IL10 secretion is shown in pg/ml cell culture supernatant.

Table 3-15 No associations between IL10 secretion levels and *IL10* genotypes in LCLs

107 LCLs were cultivated in a density of $5x10^5$/ml and supernatants for determination of IL10 secretion via ELISA were harvested after 24h (see 2.10.3). Measured values have been ranked first. Shown are the sum of ranks and mean rank values of LCLs with different *IL10* genotypes. Associations between IL10 secretion levels with *IL10* gene variations have been examined using a Kruskal-Wallis ANOVA. In case of n≠107 respective genotyping analysis was not successful.

SNP Name	rs-number	Genotype	number of LCLs	Sum of Ranks	Mean Rank	p-value*
IL10-12806C/T	rs17015865	TT	8	347.0	56.38	0.494
		CT	37	1935.5	52.31	
		CC	62	3495.5	43.38	
		total	107			
IL10-11777A/G	rs4072227	GG	0	0.0	0	0.955
		AG	16	857.5	53.59	
		AA	91	4920.5	54.07	
		total	107			
IL10-11668G/A	rs4072226	AA	26	1417.5	54.52	0.209
		AG	44	2123.0	48.25	
		GG	37	2237.5	60.47	
		total	107			
IL10-7400In/Del	7400In/Del	DelDel	7	295.0	42.14	0.256
		InDel	36	1742.5	48.40	
		InIn	62	3527.5	56.90	
		total	105			
IL10-6752A/T	rs6676671	TT	20	1103.5	55.18	0.231
		AT	44	2033.0	46.20	
		AA	39	2219.5	56.91	
		total	103			
IL10-6208G/C	rs10494879	CC	26	1398.5	53.79	0.494
		CG	43	2109.0	49.05	
		GG	36	2057.5	57.15	
		total	105			
IL10-3538T/A	rs1800890	AA	22	1265.5	57.52	0.330
		AT	44	2141.0	48.66	
		TT	41	2371.5	57.84	
		total	107			
IL10-2812G/A	rs6703630	AA	12	510.0	42.50	0.265
		AG	36	1837.5	51.04	
		GG	58	3323.5	57.30	
		total	106			
IL10-2726C/A	rs6693899	AA	14	835.5	59.68	0.156
		AC	47	2231.0	47.47	
		CC	46	2711.5	58.95	
		total	107			
IL10-1087A/G	rs1800896	GG	32	1598.5	49.95	0.250
		AG	44	2197.0	49.93	
		AA	29	1769.5	61.02	
		total	105			
IL10-824C/T	rs1800871	TT	6	378.0	63.00	0.310
		CT	38	2180.5	57.38	
		CC	61	3006.5	49.29	
		total	105			
IL10-597C/A	rs1800872	AA	6	378.0	63.00	0.310
		AC	38	2180.5	57.38	
		CC	61	3006.5	49.29	
		total	105			
IL10+4259A/G	rs3024498	GG	12	501.0	41.75	0.344
		AG	32	1667.5	52.11	
		AA	61	3396.5	55.68	
		total	105			
IL10+5876C/T	rs3024505	TT	2	113.0	56.50	0.265
		CT	33	1980.5	60.02	
		CC	70	3471.5	49.59	
		total	105			

*Kruskal-Wallis ANOVA

In addition to the variance analysis the associations of IL10 secretion and *IL10* gene variations have been analysed after grouping the LCLs according to the median IL10 secretion (737pg IL10/ml) into high (IL10 secretion ≥ median) and low (IL10 secretion < median) IL10 secreting LCLs, as it was done for *IL10* expression in the previous chapter. This analysis did not reveal any significant associations between IL10 secretion and *IL10* genotypes (table A-4). The two LCLs with IL10$^{+5876TT}$ are even assigned to the two different groups.

The analysis shown in table A-4 in the Appendix has been done with all LCLs cultivated including the HapMap LCLs. However a second analysis has been done with a group of LCLs excluding the HapMap LCLs (data not shown). No significant associations could be detected.

In conclusion, no associations between IL10 secretion and *IL10* gene variations could be observed for the analysed LCLs, neither for the ANOVA nor for the grouped analysis.

3.2.3 LMP1 expression in comparison to IL10 production capacities of LCLs

IL10 production of LCLs is induced by EBV immortalization of B cells. Therefore, the interindividual production capacities could as well be caused by differing levels of EBV associated proteins like LMP1. This was tested in 15 LCLs with high IL10 production and 15 LCLs with low IL10 production via immunoblot of LMP1 (for details see Material and Methods 2.10.2).

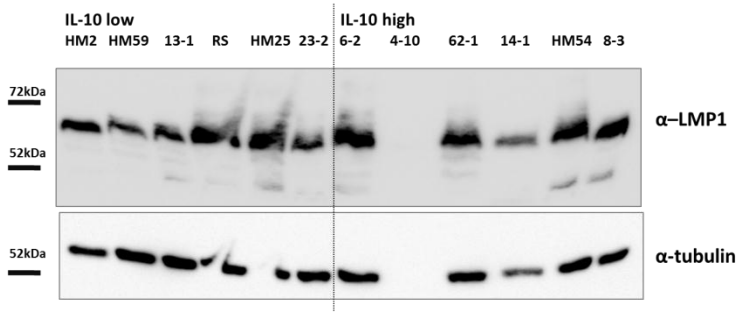

Figure 3-11 LMP1 IL10 production of LCLs is not dependent on LMP1 protein level.

LCLs were cultured in a density of 5x10^5/ml. Pellets for protein preparation have been harvested after 24h. The protein level of LMP1 was visualized by immunoblot. The results shown are representative for three independent experiments with different LCLs.

As seen in figure 3-11 the LMP1 level did not differ between LCLs with high or low IL10 production. Therefore, one can conclude that the interindividual differences in IL10 production of LCLs are not due to differences in LMP1 protein levels.

3.3 Regulation of *IL10* gene expression in B cells

IL10 is expressed by a diverse set of immune cells, monocytes and macrophages, certain T cell subpopulations and also by B cells. Several studies investigated mechanisms that contribute to *IL10* gene regulation in macrophages and T cells. These studies have been mainly conducted in mouse cell lines. Therefore, one of the aims of this dissertation was to investigate molecular mechanisms, contributing to *IL10* gene regulation in human B cells.

3.3.1 B cell model systems used to analyse mechanisms of *IL10* gene regulation

In order to identify a model system that can be used for the analysis of mechanisms involved in regulation of *IL10* gene expression, different cell lines have been tested for their capacity to induce *IL10* gene expression. The aim was to find a cell line without constitutive but high inducible *IL10* expression to be able to see clear changes in chromatin modifications and other processes involved in *IL10* gene regulation. Two different B cell models systems have been identified. The L428 Hodgkin-Lymphoma cell line stimulated with phorbol-12-myristate-13-acetate (PMA) (Figure 3-12) and the Ramos Burkitt's lymphoma cell line stimulated with CD40-ligand (CD40L) (Figure 3-13). In addition to this three B cell lines with constitutive *IL10* gene expression have been identified (Figure 3-14).

The L428 cell line was stimulated with PMA as previously described (Vockerodt 2001) for different incubation times (see also Material and Methods 2.9.3). Unstimulated cells have been harvested at two different time points to exclude an influence of cell culture effects on *IL10* expression. *IL10* expression levels have been determined using qRT-PCR (Figure 3-12). The highest expression of *IL10* has been observed after 30h and was still visible after 48h of stimulation. Because the aim was to analyse mechanisms that lead to the induction of *IL10* gene expression, like histone modifications, L428 cells were stimulated for 12h or 24h in the following

experiments. After these incubation times a clearly detectable *IL10* expression was induced in L428 but the highest level and therefore the plateau of *IL10* expression was not reached.

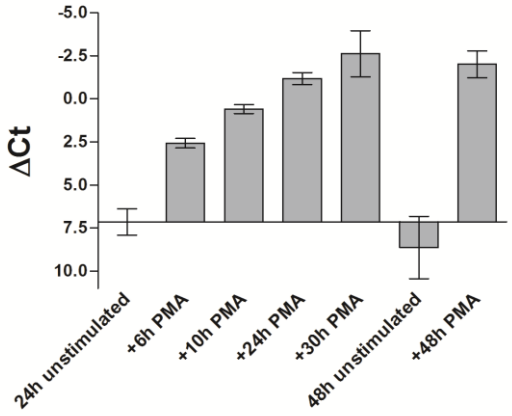

Figure 3-12 *IL10* expression can be induced in L428 Hodgkin cell line using PMA.

The L428 Hodgkin cell line has been stimulated with 20ng/ml PMA or left untreated. All samples have been centrifuged after the first hour of stimulation and pellets have been resuspended in fresh medium (for detailed information see Material and Methods 2.9.3). Cells have been harvested for RNA preparation after the indicated time points. *IL10* expression was analysed using qRT-PCR. As the *IL10* expression is below detectable levels in unstimulated samples no fold change could be calculated. Therefore, results are presented as ΔCt values relative to abl as housekeeper.

To stimulate Ramos with CD40L, baby hamster kidney (BHK) cells, stably transfected with a CD40L expression plasmid (BHK-CD40L), were used (see also Material and Methods 2.9.4). BHK and BHK-CD40L cells were seeded 24h pre-stimulation.

Ramos cells were added to the BHK and BHK-CD40L cells and harvested at different time points (Figure 3-13). As a control Ramos cells were cultivated without any BHK cells (unstimulated). *IL10* expression was determined using qRT-PCR. *IL10* expression could be detected already 3h after stimulation with CD40L. The highest induction of *IL10* expression was detected after 24h of stimulation and was reduced again after 32h. No detectable *IL10* expression was visible with unstimulated or BHK stimulated cells.

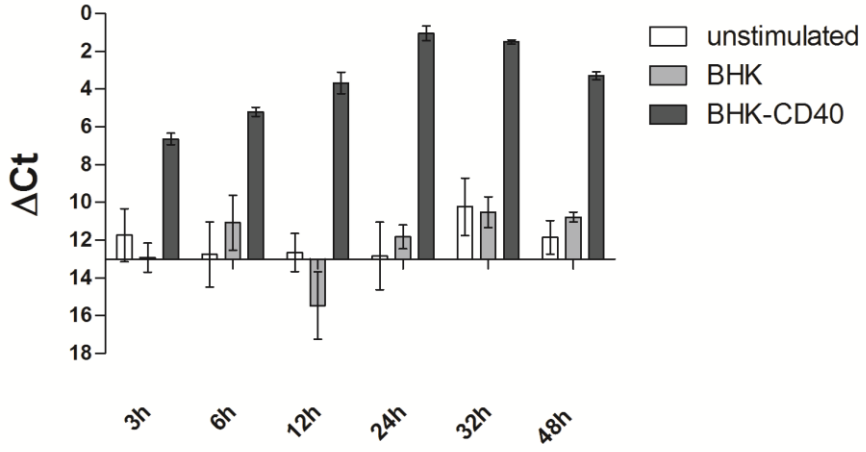

Figure 3-13 *IL10* expression can be induced in Ramos Burkitt cell line after CD40 crosslink.

The Ramos cell line has been co-cultivated with BHK or BHK-CD40L or left untreated (for detailed information see Material and Methods 2.9.3). Cells have been harvested for RNA preparation after the indicated time points. *IL10* expression was analysed using qRT-PCR. As *IL10* expression levels are below detectable levels in unstimulated samples no fold change could be calculated. Therefore, results are presented as ΔCt values relative to abl as housekeeper.

In addition to this, several B cell lines were tested for their constitutive expression of *IL10* using qRT-PCR (Figure 3-14). Thereby, the cell lines MC116, Balm3 and BJAB have been identified as being positive for *IL10* expression. All the other tested B cell lines (Ramos, Bl2, Karpas422, SuDHL4, OCI Ly3 and OCI Ly6) did not express detectable levels of *IL10*.

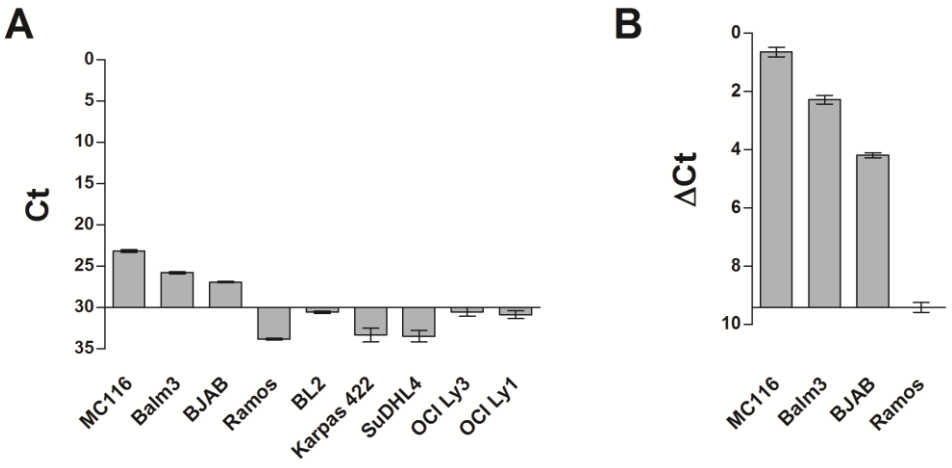

Figure 3-14 The cell lines MC116, Balm3 and BJAB express *IL10* constitutively.

Different B cell lines (MC116, Balm3, BJAB, Ramos, Bl2, Karpas422, SuDHL4 OCI Ly3 and OCI Ly1) have been tested via qRT-PCR for *IL10* gene expression. **A.** For most of the cell line the Ct-value was above 30 and the respective dissociation curves did not have the right Tm of the *IL10* primers used, meaning that these cell lines do not express detectable levels of *IL10*. **B.** The cell lines MC116, Balm3 and BJAB do express *IL10* visualized here using the ΔCt value relative to the housekeeper abl.

Two model systems with inducible *IL10* expression, L428 stimulated with PMA and Ramos stimulated with CD40L as well as 3 cell lines with constitutive *IL10* expression, MC116, Balm3 and BJAB have been identified.

3.3.2 Characterization of pathways involved in PMA-induced *IL10* expression

PMA-induced *IL10* expression in L428 has been further characterized using inhibitors against components of certain signaling pathways, protein kinase C (PKC), phosphoinositide 3-kinase (PI3K) and extracellular-regulated kinase (ERK).

PMA is a homolog of Diacylglycerol (DAG). Signaling through the B cell receptor leads to activation of phospholipase C-γ2 (PLC-γ2) which hydrolyses phosphatidyl inositol-bisphosphate (PIP_2) into the second messengers Inositol trisphosphate (IP_3) and DAG. While IP_3 stimulates calcium release from intra- and extracellular sources, DAG mobilizes and activates PKC. DAG also regulates RasGRP, a nucleotide exchange factor that activates Ras kinase via exchange of GDP for GTP to activate the MAP kinase cascade. This finally leads to the activation of ERK1/2. Ras can also activate PI3K.

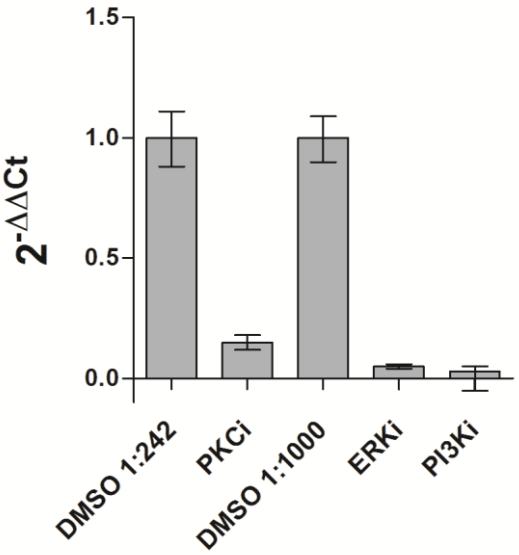

Figure 3-15 Pathways involved in PMA-induced *IL10* expression in L428

L428 cells were preincubated with specific pathway inhibitors (for detailed information see Material and Methods 2.9.5). Subsequently, the cells have been stimulated for 12h with 20ng/ml PMA according to the procedure described in chapter 2.9.3 and 3.3.1. *IL-10* expression was determined using qRT-PCR.
Results are presented as $2^{-\Delta\Delta Ct}$ relative to the housekeeper gene abl. The *IL-10* expression of respective DMSO (solvent control) treated cells was set to 1.

L428 cells were preincubated with specific inhibitors of PKC, PI3K and ERK (for details see Material and Methods 2.9.5). DMSO in respective concentrations was used as a solvent control. After 3h, cells were stimulated with PMA and treated again with inhibitors or DMSO after the washing step with fresh medium. After 24h of PMA stimulation pellets were harvested and *IL10* expression was determined using qRT-PCR (Figure 3-15). The *IL10* expression of respective DMSO treated cells was set to

1. Treatment with all three inhibitors led to a reduction of *IL10* expression. Therefore, all three signaling components, PKC, PI3K and ERK, seem to be involved in PMA-induced *IL10* expression in L428 cell line.

3.3.3 Far distal enhancer regions revealed by ChIP

After adjustment of the ChIP protocol to suspension cells, ChIP was used for the analysis of the chromatin modifications acetylated histone 3 (acH3), tri-methylated lysine 4 of histone 3 (H3K4me3) and mono-methylated lysine 4 on histone 3 (H3K4me1). The antibody used for acH3, detects H3 acetylated at Lysine 9 and 14, a modification generally observed at actively transcribed genes, often together with H3K4me3 (Koch et al., 2007; Peterson and Laniel, 2004). H3K4me3 is a modification characteristic for transcription start sites (TSS) and H3K4me1 is found at enhancer regions (Heintzman et al., 2007). PMA stimulation induces strong expression of *IL10* in L428 cells, which do not express *IL10* without any stimulus (Figure-3-12). Therefore, this model was used to analyse changes of chromatin modifications associated with the induction of *IL10* expression. L428 cells were stimulated for 24h with PMA or left untreated (see Material and Methods 2.9.3). Three biological triplicates were prepared (3x stimulated and 3x unstimulated). ChIP has been performed according to the procedure described in Material and Methods 2.11.9. After crosslinking of proteins to the DNA via formaldehyde treatment, the chromatin has been sheared into fragments of 200bp-750bp. The sheared chromatin has been used for IP with specific antibodies (see table 2-10) and DNA has been purified. For the identification of regions, where the respective chromatin modifications are localized, qRT-PCR was used (see Material and Methods 2.11.7). Oligonucleotide primers were designed spanning the *IL10* gene variations of interest, the TSS or certain CNS (Figure 3-16 and table 2-7).

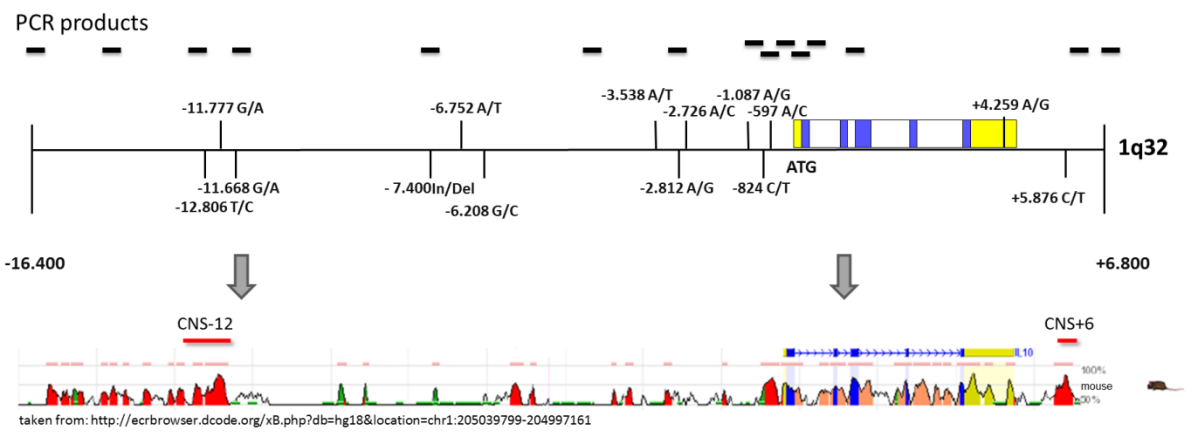

Figure 3-16 Positions of oligonucleotide primers used for ChIP

Shown are the positions of PCR products of the designed oligonucleotide primers used for the evaluation of ChIP via qRT-PCR relative to the *IL10* gene locus and CNS. All primer pairs amplify products between 75 and 130bp of length and are optimized for amplification at 60°C. The human *IL10* gene locus from -16.400bp till +6800bp is shown as scheme. All gene variations of interest are indicated. The *IL10* gene is shown starting with ATG. UTR (yellow), exons (dark blue) and introns (white) are indicated. A comparison of the human *IL10* gene locus (x-axis) and the mouse *IL10* gene locus (y-axis) is aligned to the scheme to visualize CNS. This comparison has been calculated using the browser for evolutionary conserved regions (ECR) (http://ecrbrowser.dcode.org). Sequences of similarity are marked by the height of the curves. A vertical axis cut-off of 50% to 100% identity is utilized to visualize only the significant alignments. Annotated genes are depicted as a horizontal line above the graph. ECRs (pink rectangles on top of the plot), coding exons (blue), intronic regions (salmon-pink), transposons and simple repeats (green) and intergenic regions (red) are indicated. In addition the positions of CNS-12 and CNS+6 are indicated with red horizontal lines.

One representative experiment is shown in figure 3-17. AcH3 is mainly observed after PMA stimulation around the TSS, in the beginning of the *IL10* coding region and at the proximal parts of the 5'-region (to 1000bp upstream of the TSS). A slight increase of acH3 could also be observed at the region around CNS-12.

As expected, H3K4me3 could be detected at regions around the TSS of the *IL10* gene from 1000bp upstream till the beginning of the *IL10* coding region after PMA stimulation. H3K4me3 could not be detected around CNS-12 or regions further upstream, therefore no other TSS is located within this region.

At the TSS, the more proximal parts of the 5'-region and the 3'region of *IL10* gene locus, H3K4me1 could be detected. While this was inducible by PMA stimulation in the 5'region and 3' of the *IL10* coding region at +6.800bp, it was detected with or without PMA stimulation in the coding region as well as in the 3'region of *IL10* at +6000bp, where CNS+6 is located.

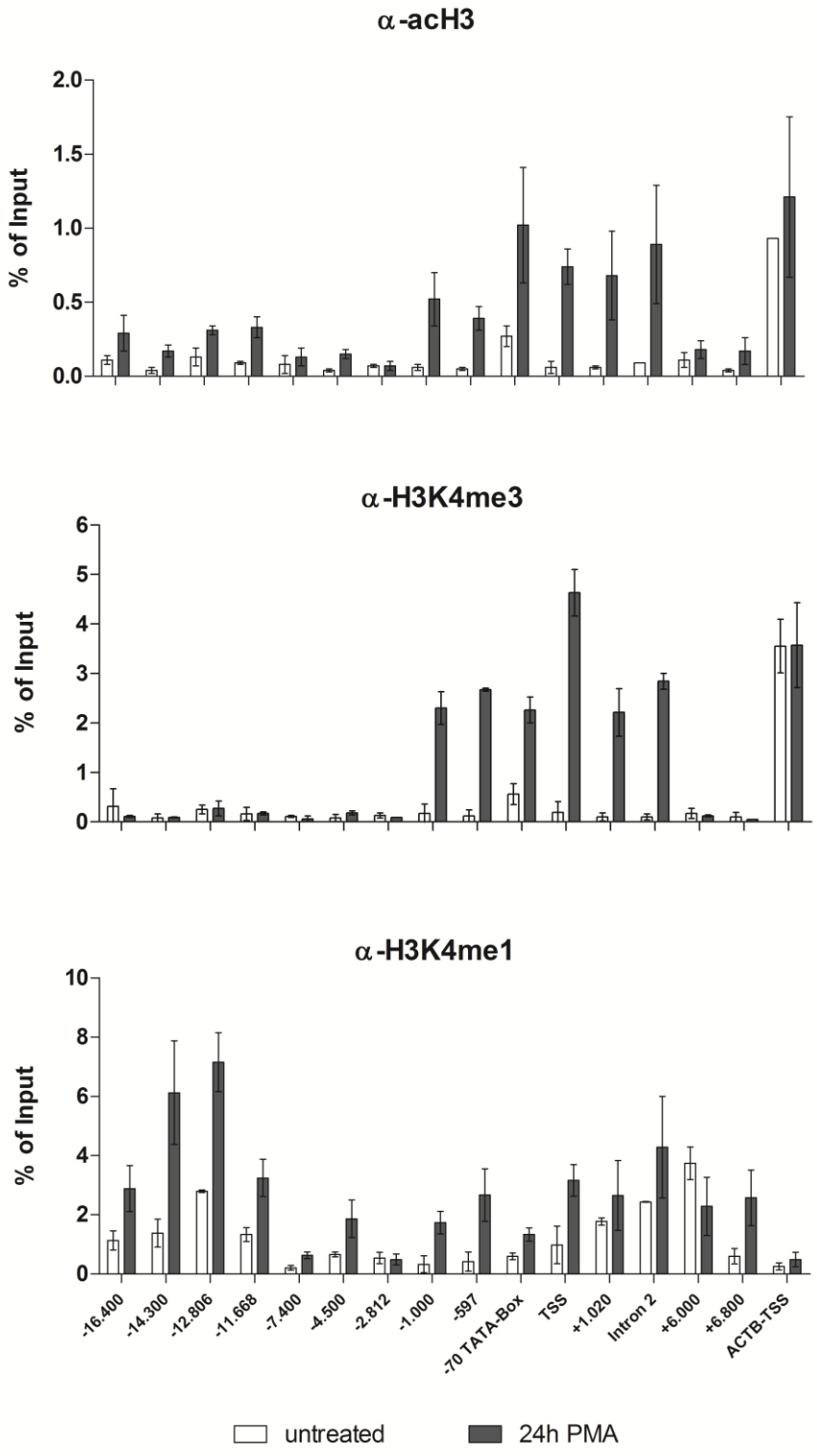

Figure 3-17 ChIP of histone modifications in PMA stimulated L428

ChIP has been performed using the L428 Hodgkin cell line stimulated with PMA for 24h (see chapter 2.11.10 for details). Shown are results for acH3, a general mark for active transcription; H3K4me3, a mark generally found at transcription start sites and H3K4me1, a histone modification associated with enhancer activity. qRT-PCR has been done using primers amplifying different regions of the *IL10* gene locus and one primer for the TSS of ACTB as a control. The standard deviation results from three biological replicates within the shown experiment. One representative result of 4 independent experiments is shown.

The region around CNS-12 shows relatively high inducible H3K4me1 and therefore enhancer activity after induction of *IL10* expression. Already before PMA stimulation, a basic enhancer activity is visualized via localization of H3K4me1 to this region.

The histone modifications acH3 and H3K4me3 but not H3K4me1 have been observed at the housekeeping gene ACTB-TSS. This was not dependent on PMA stimulation.

As a negative control, an anti-IgG antibody has been used for the IP (data not shown). Detected binding of IgG in qRT-PCR was not higher than 0.05% and mostly lower or the dissociation curves did not have the right melting temperature, meaning the right PCR-product was not amplified and therefore not detected by the instrument.

The same experiment was done after 12h of PMA stimulation to examine whether a different histone modification pattern would be observed to an earlier time point. The results did not differ between 12h and 24h of PMA stimulation (Data not shown).

The most important finding of the ChIP experiments was the identification of far distal enhancer regions, by localization of H3K4me1 to CNS-12 and regions further upstream.

3.3.4 Chromatin modifications in two cell lines with constitutive *IL10* expression

To address the question whether histone modifications differ between B cells with induced and cell lines with constitutive *IL10* expression, the same histone modifications analysed in the L428 cell line were examined in the cell lines BJAB and MC116 (Figure 3-18). Three biological triplicates have been prepared for both cell lines. ChIP has been performed as described in the previous chapter (see 3.3.3).

Again qRT-PCR was used to identify regions, where respective chromatin modifications were localized. Oligonucleotide primers spanning the *IL10* gene variations of interest, the TSS or certain CNS have been used. One representative experiment is shown in figure 3-18.

The region of the *IL10* gene locus where acH3 has been detected starts at -1000bp, peaks within the beginning of the *IL10* coding region and is reduced at the end of this region. This observation can be seen in both examined cell lines and is basically in line with the localization of acH3 found in PMA stimulated L428. Notably, in BJAB there is also acH3 at the CNS+6 (+6000bp), which was not detected in L428 or MC116. In the more proximal regions of the *IL10* gene locus, low levels of acH3 where visible.

As expected, H3K4me3 is only visible around the TSS and in the beginning of the coding region of *IL10*. No differences between the two cell lines could be observed.

However, strong differences could be detected with respect to H3K4me1, the histone modification associated with enhancer activity. This modification is represented to a generally higher extend in the BJAB cell line. In BJAB this histone modification can be observed around CNS-12, the distal part of the *IL10* promoter (-1000 and -597) and in the coding region of *IL10*. The most important regions emphasized here, where this modification could be localized, are the region around -4500bp and the CNS+6 (+6000bp). Particularly in comparison to the L428, these two regions attract attention. Notably, the region around -4500 contains a putative NF-κB binding site and the CNS+6 contains a putative AP1 binding site. The peak in H3K4me1 at -11.668bp was not observed in the following ChIP experiment, whereby the peaks at -4500 and +6kb were reproducible. In the MC116 cell line the highest signal for H3K4me1 could be observed at the distal *IL10* promoter and again at CNS+6 but not at -4500bp.

All three histone modifications were also assessed at the ACTB-TSS. In this case the detected levels were always stronger in the BJAB cell line, too.

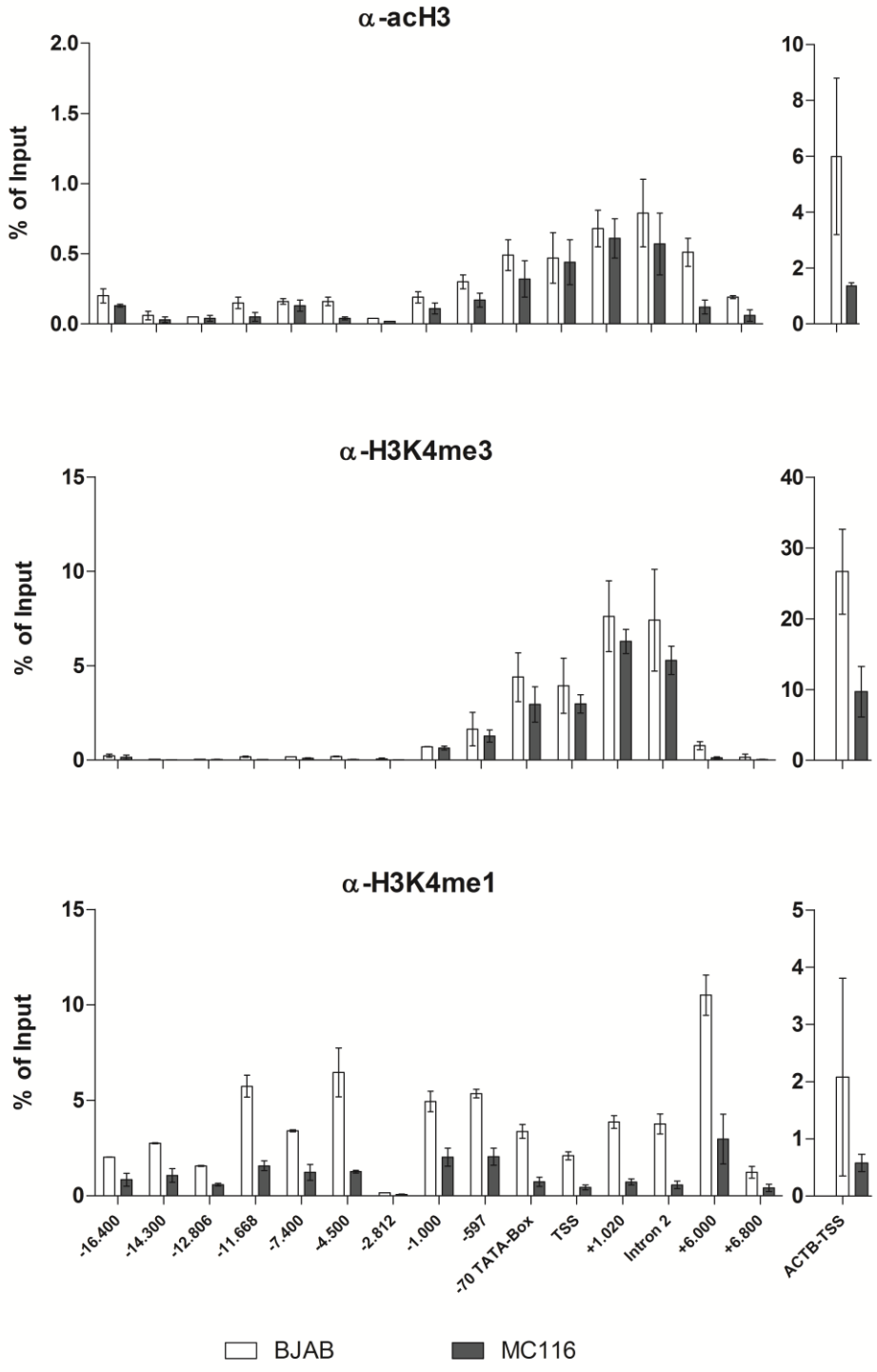

Figure 3-18 ChIP of histone modifications in BJAB and MC116 with constitutive *IL10* expression

ChIP has been performed using the unstimulated BJAB and MC116 cell lines. Cells were seeded in a density of $5x10^5$/ml and harvested after 24h. $1x10^6$ cells were used per IP. Shown are results for acH3, a general mark for active transcription; H3K4me3, a mark generally found at transcription start sites and H3K4me1, a histone modification associated with enhancer activity. qRT-PCR has been done using primers amplifying different regions of the *IL10* gene locus and one primer for the TSS of ACTB as a control. As the results for ACTB-TSS differ strongly, they were plotted on a separate graph. The standard deviation results from three biological replicates within the shown experiment. One representative result of 2 independent experiments is shown. Compare to figure 3-17.

Taken together, this experiment showed that histone modification patterns in B cell lines with constitutive *IL10* expression show similarities but also differ to some extent. Some molecular mechanisms involved in the *IL10* regulation in these cell lines seem to be common, while other are different between the cell lines. In BJAB cells a region around a putative NF-κB binding site, shown to be important in macrophages and the CNS+6, containing a putative AP1 binding site, showed strong enhancer activity. In MC116 only the CNS+6 showed this strong enhancer activity. Most importantly, enhancer activity could be detected at distal regions around CNS-12 in all three examined cell lines.

3.3.5 Transcription of ncRNA from *IL10* gene locus in B cells

In mature Th2 cells it has been shown that ncRNA (non-coding RNA) is transcribed from certain CNS. Therefore, the transcription of RNA from regions outside the coding region of the *IL10* gene has been assessed in the B cell model systems introduced in chapter 3.3.1. For details of the procedure used to analyse ncRNA see Materials and Methods 2.11.8.

At first, it has been determined whether ncRNA is transcribed from CNS-12 in L428 stimulated with PMA (Figure 3-19). The L428 cell line has been stimulated for different time points with PMA as described in chapter 3.3.1. The same RNA samples as in Figure 3-12 have been used for conventional PCR for the determination of ncRNA transcribed from CNS-12 (Figure 3-19 A). RNA has been reverse transcribed with or without Reverse transcriptase (RT) as a negative control. DNA from L428 has been used as a positive control for the respective PCR, using primers originally designed for ChIP. PCR products were obtained for samples using DNA of L428 and cDNA from PMA stimulated samples reverse transcribed with RT, while no PCR products were obtained for unstimulated samples and cDNA reverse transcribed without RT. Therefore, RNA is transcribed from non-coding regions of the *IL10* gene locus in L428 cells after PMA stimulation. This RNA will be referred ncRNA.

Next, it was assessed whether this transcription of ncRNA is dependent on the duration of PMA stimulation like it has been observed for *IL10* transcription (Figure 3-12). For this purpose, qRT-PCR analysis of transcription of CNS-12 has been done

using the same RNA as for Figure 3-12 reverse transcribed with or without RT. As seen in figure 3-19 B, in contrast to *IL10* transcription the transcription level of ncRNA was the same for all analysed incubation times and not enhanced after longer stimulation with PMA. In samples reverse transcribed without RT the dissociation curves were similar to water samples, representative for primer dimers. Therefore, no ΔCt could be calculated.

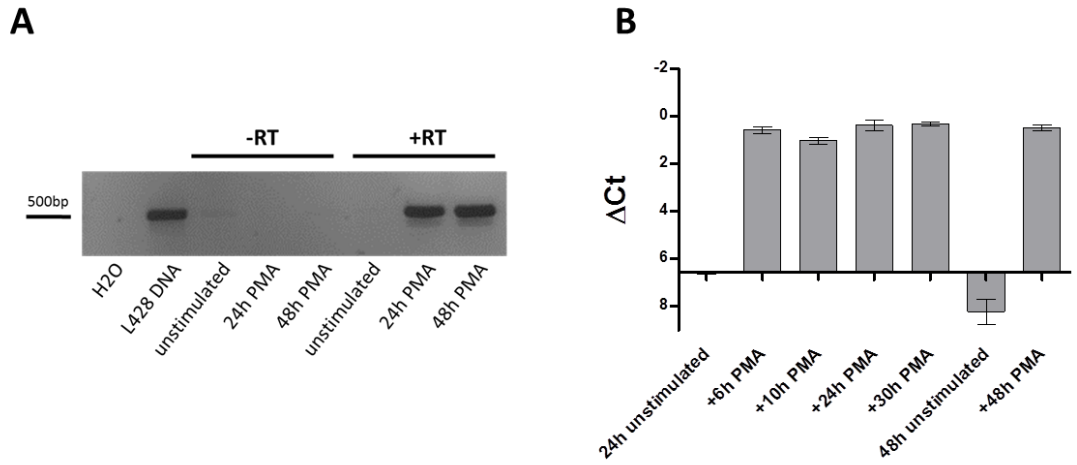

Figure 3-19 Transcription of ncRNA from *IL10* gene locus after PMA stimulation in L428

The L428 Hodgkin cell line has been stimulated with 20ng/ml PMA or left untreated (see Methods 2.9.3). Cells have been harvested for RNA preparation after the indicated time points. RNA has been reverse transcribed into cDNA with and, as a negative control, without Reverse Transcriptase (RT). **A.** Transcription of ncRNA from the *IL10* gene locus has been detected via conventional PCR using oligonucleotide primers for the CNS-12 (ChIP_IL10_CNS-12fwd and ChIP_IL10-11668rev; product = 497bp). PCR products were separated on 1% agarose gel. PCR products were obtained for L428 DNA (positive control) and cDNA of PMA stimulated L428 reverse transcribed with RT. **B**. Transcription of CNS-12 was analysed using qRT-PCR (ChIP_IL10_CNS-12). Shown are only the results for +RT, because no PCR products were obtained from -RT samples. Transcription of CNS-12 is below detectable levels in unstimulated samples and no fold change could be calculated. Therefore, results are presented as ΔCt values relative to abl as housekeeper. The level of ncRNA does not increase after longer stimulation with PMA.

To further characterize the ncRNA expressed in L428 cells, its transcription was determined at different regions of the *IL10* gene locus in comparison to the *IL10* transcription using qRT-PCR (see 2.11.8). For this purpose primers were used, originally designed for ChIP, spanning several *IL10* gene variations and CNS-12 (Figure 3-20 and table 2-7). As seen in figure 3-20, ncRNA was expressed from all examined regions in a level comparable to *IL10* transcription.

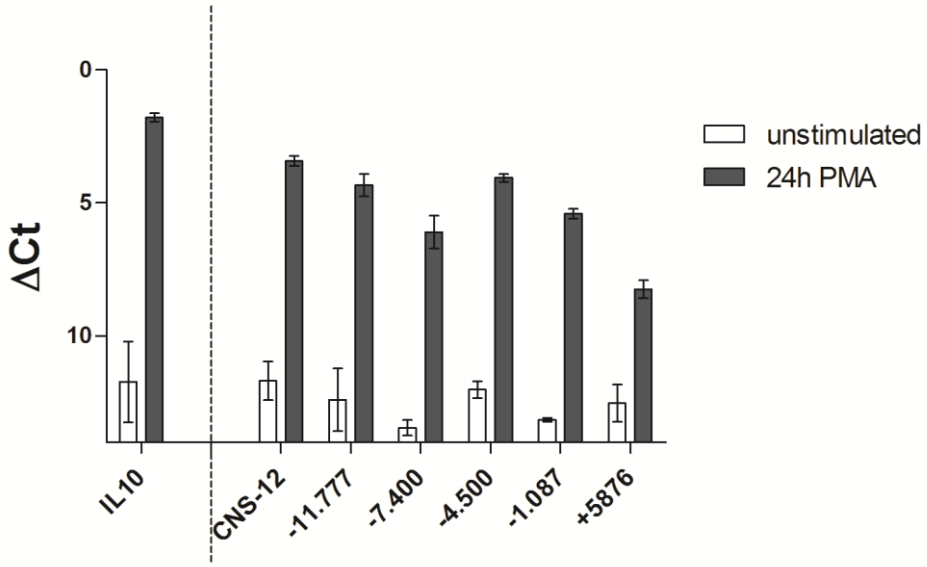

Figure 3-20 Several regions of the *IL10* gene locus are transcribed into ncRNA (qRT-PCR)

The L428 Hodgkin cell line has been stimulated with 20ng/ml PMA or left untreated for 24h and respective RNA has been reverse transcribed into cDNA (for details see figure 3-19). Transcription of *IL10* (IL10) as well as transcription of ncRNA from different regions of the *IL10* gene locus was analysed using qRT-PCR. As the transcription levels are below detectable levels in unstimulated samples, no fold change could be calculated. Results are presented as ΔCt values relative to abl as housekeeper. From the cDNA reverse transcribed without RT no detectable PCR products resulted.

Subsequently, conventional PCRs have been made using different primer combinations spanning the *IL10* gene locus according to the examples shown in figure 3-19 A (Figure 3-21). PCR products have been obtained for DNA samples used as positive controls for the PCR (compare to lane 5, Figure 3-21) and also in all examined cases for PMA stimulated L428 RNA samples, reverse transcribed with RT (compare to lane 4, Figure 3-21). In one case a PCR product was also obtained for unstimulated RNA samples reverse transcribed with RT (compare to lane 3 in Figure 3-21 A). However, this band is very weak compared to the stimulated sample. In one case a second PCR product was obtained for RNA reverse transcribed with RT (compare to lane 3 and 4 in Figure 3-21 F-asterisk). This PCR product does not show the expected size and is therefore an unspecific amplification product. No PCR product was obtained for RNA reverse transcribed without RT. In conclusion ncRNA is transcribed from all examined regions within the *IL10* gene locus.

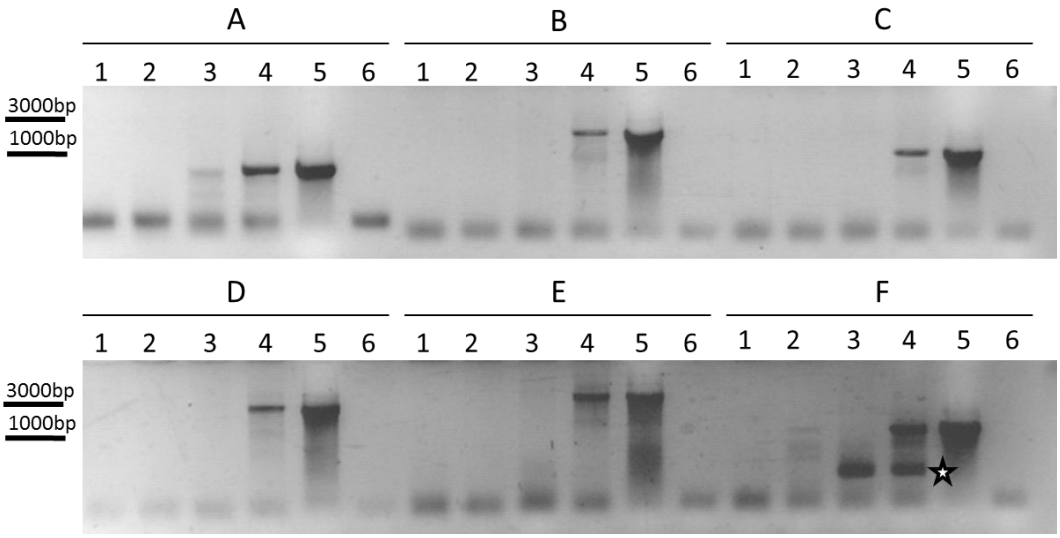

Figure 3-21 Several regions of the *IL10* gene locus are transcribed into ncRNA (PCR)

The L428 Hodgkin cell line has been stimulated with 20ng/ml PMA or left untreated for 24h and respective RNA has been reverse transcribed into cDNA (for details see figure 3-19). Transcription of ncRNA from the *IL10* locus has been detected via conventional PCR using oligonucleotide primers for several regions of the 5'- and 3'-region of *IL10* and PCR products were separated on 1% agarose gel. Primer pairs (see table 2-7) used were **A.** hIL10-9133_fwd and hIL10-8583_rev; **B.** ChIP_IL10-16.400_fwd and ChIP_IL10-14.700_rev; **C.** hIL10-8583_fwd and ChIP_IL10-7400_rev; **D.** ChIP_IL10-7400_fwd and ChIP_IL10-4500_rev; **E.** ChIP_IL10-3538_fwd and ChIP_IL10-1087_rev; **F.** ChIP_IL10-AP1 (+6000)_fwd and ChIP_IL10+6800_rev. Used templates were **1**. L428 cDNA unstimulated –RT; **2**. L428 cDNA +24h PMA –RT; **3.** L428 cDNA unstimulated +RT; **4** L428 cDNA +24h PMA +RT; **5.** L428 DNA (positive control) and **6**. H_2O. PCR products were obtained for L428 DNA (positive control) and cDNA of PMA stimulated L428 reverse transcribed with RT. Asterisks= wrong size/unspecific amplification product.

Transcription of ncRNA was observed in all regions shown schematically in Figure 3-22. Transcription of ncRNA has been detected from all examined regions analysed. This means gaps in this scheme represent regions that have not been examined until the time of handing in this thesis, and not regions where transcription of ncRNA has not been detected.

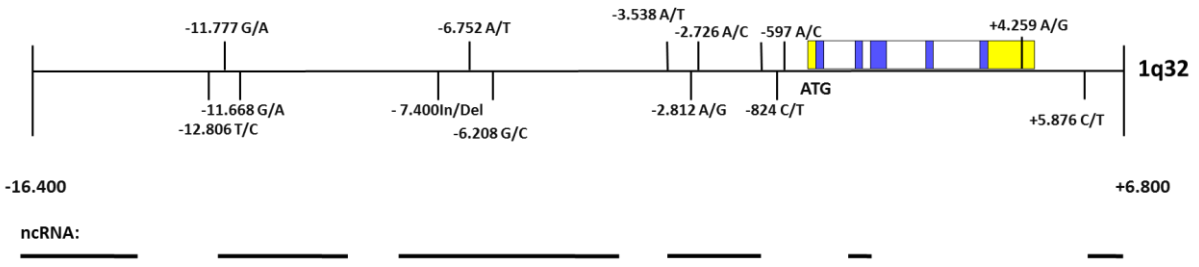

Figure 3-22 Regions of *IL10* gene locus shown to be transcribed into ncRNA

A scheme of the *IL10* gene locus spanning from -16.400bp to +6.800bp (counted from TSS) on chromosome 1q32 is shown. All analysed *IL10* gene variations examined within this dissertation are indicated. The *IL10* coding region comprised of 5'- and 3'-UTR (yellow), Introns (white) and exons (blue) is shown. The ATG is displayed. Black lines below the scheme represent regions were transcription of ncRNA has been detected.

Transcription of ncRNA has also been assessed in the other model systems introduced in chapter 3.3.1. RNA of Ramos cells stimulated with BHK-CD40L, MC116, BJAB and Balm3 has been reverse transcribed with or without RT. Transcription of ncRNA has been assessed using conventional PCR according to the procedure shown for L428 in figure 3-19.

The result for Ramos stimulated with BHK cells is shown in Figure 3-23. Bands are visible only in the lanes with the PCR products obtained from amplification of DNA (positive control) and of Ramos cells stimulated with CD40 crosslink, reverse transcribed with RT. Therefore, ncRNA is also transcribed in Ramos after CD40 crosslink for 24h.

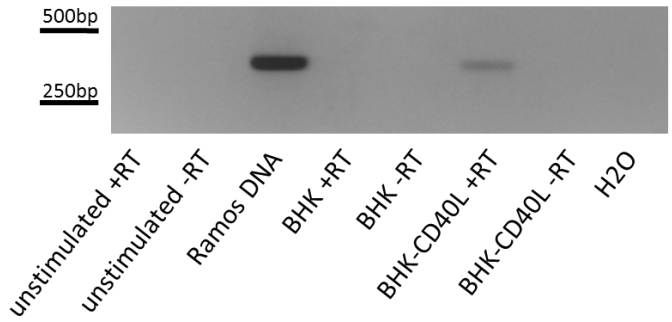

Figure 3-23 Transcription of ncRNA in Ramos cells stimulated with CD40 crosslink

The Ramos Burkitt's lymphoma cell line has been co-cultivated with BHK or BHK-CD40L or left untreated (for detailed information see Methods 2.9.4). Cells have been harvested for RNA preparation after 24h. RNA has been reverse transcribed into cDNA with (+RT) and, as a negative control, without RT (-RT). Transcription of ncRNA from the *IL10* gene locus has been detected via conventional PCR using oligonucleotide primers for the CNS-12 (ChIP_IL10_CNS-12_fwd and ChIP_IL10-11777_rev; product = 387bp). PCR products were separated on 1% agarose gel. 1kb ladder has been used. PCR products were obtained for Ramos DNA (positive control) and cDNA of Ramos after CD40 crosslink reverse transcribed with RT.

BJAB, MC116 and Balm3 cell lines have been analysed using the same procedure as for Ramos. RNA of MC116, BJAB and Balm3 has been reverse transcribed with or without RT. Transcription of ncRNA has been assessed using conventional PCR. The results are shown in figure 3-24. PCR products were obtained only for the DNA samples and the cDNA reverse transcribed with RT (+RT) but not for those cDNA samples reverse transcribed without RT (-RT). The only exception was a faint band for Balm3 cDNA reverse transcribed without RT. This might be due to a vast amount of RNA in the samples used for the PCR, which might results in primer binding on

RNA. Contamination with DNA can also not be excluded. As the PCR products obtained for the sample after reverse transcription with RT is much stronger, one can conclude that ncRNA is transcribed in Balm3. Notably, the transcription of ncRNA in BJAB is very weak. However it is still detectable.

Therefore, these experiments showed that in all three cell lines with constitutive *IL10* gene expression also ncRNA is transcribed from the *IL10* gene locus.

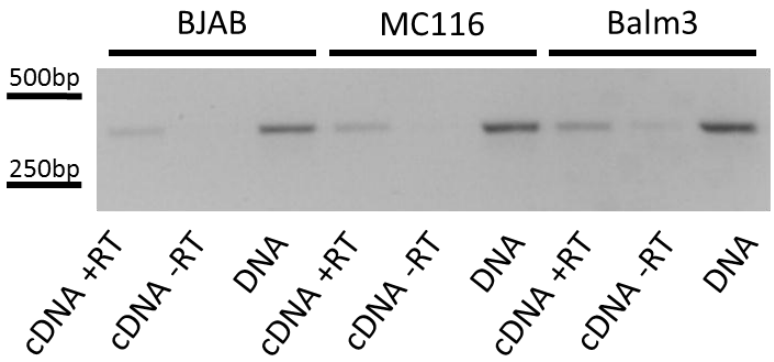

Figure 3-24 Transcription of ncRNA in cell lines with constitutive *IL10* expression

The BJAB, MC116 and Balm3 cell lines have been cultivated in a density of $5x10^5$/ml. Cells have been harvested for RNA preparation after 24h. RNA has been reverse transcribed into cDNA with (+RT) and, as a negative control, without RT (Reverse Transcriptase) (-RT). Transcription of ncRNA from the *IL10* gene locus has been detected via conventional PCR using oligonucleotide primers for the CNS-12 (ChIP_IL10_CNS-12fwd and ChIP_IL10-11777_rev; product = 387bp). PCR products were separated on 1% agarose gel. 1kb ladder has been used. PCR products were obtained for all samples amplified from DNA (positive control) and cDNA of cell lines reverse transcribed with RT. A faint band has been detected for Balm3 after reverse transcription without RT.

Taken together all B cell model systems and cell lines, introduced in chapter 3.3.1 with inducible or constitutive *IL10* gene expression, do also transcribe ncRNA from the *IL10* gene locus under the same conditions needed for *IL10* transcription.

3.3.6 Transcription levels of *IL10* and ncRNA in LCLs are not comparable

The transcription of ncRNA has also been assessed in LCLs using qRT-PCR. LCLs were cultured in a density of $5x10^5$/ml for 24h. Subsequently, pellets for RNA preparation were harvested. RNA was reverse transcribed into cDNA (+RT only) and this was used to evaluate *IL10* transcription as well as transcription of ncRNA via qRT-PCR. In figure 3-25 this is shown exemplary for 14 LCLs. Transcription of

ncRNA was detected in all LCLs examined. A comparison between *IL10* expression and the transcription level of ncRNA from CNS-12 did not reveal any correlations.

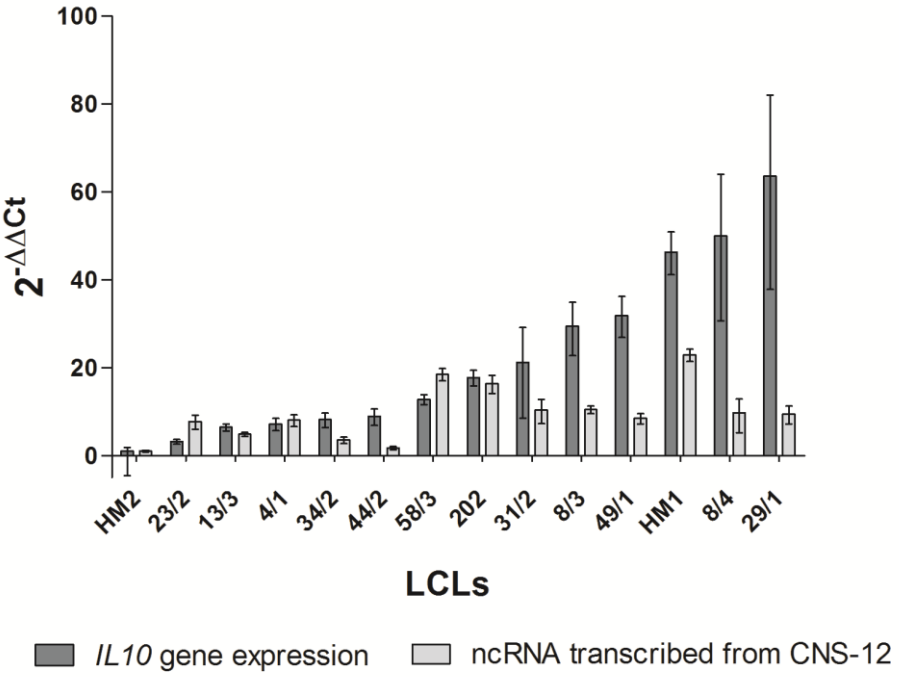

Figure 3-25 Transcription levels of *IL10* and ncRNA transcribed from the *IL10* gene locus are not comparable in LCLs.

LCLs were cultured in a density of 5*10^5/ml. Pellets for RNA preparation were harvested after 24h (see figure 3-8). Transcription of *IL10* and ncRNA from CNS-12 were measured using qRT-PCR. Results are presented as $2^{-\Delta\Delta CT}$ values (fold change) relative to β2m housekeeper. The LCL with the lowest *IL10* gene expression level (HM2) was set to 1. On the x-axis LCL numbers are shown ordered from the cell with the lowest *IL10* expression level to the highest.

Taken together EBV immortalization leads to transcription of ncRNA from the *IL10* gene locus in LCLs but the levels of *IL10* transcription do not correlate with transcription levels of ncRNA from the *IL10* gene locus. This means that neither *IL10* gene expression levels depend on transcription of ncRNA nor the other way around. Therefore, ncRNA is not the factor that regulates interindividual differences in IL10 production capacity in LCLs.

3.4 Investigation of the influence of IL10 on CDC or ADCC of B cells

In chapter 3.1.2 it was described that several *IL10* gene variations have been identified that are associated with disease outcome of NHL patients treated with Rituximab in addition to conventional CHOP therapy. Rituximab is thought to mediate its effects via complement dependent cytotoxicity (CDC) or antibody dependent

cellular cytotoxicity (ADCC). Therefore, it has been examined whether exogenous IL10 or levels of endogenous *IL10* expression influence these mechanisms after Rituximab treatment of different B cell lines.

3.4.1 IL10 does not influence complement dependent cytotoxicity after Rituximab treatment

The effect of endogenous IL10 on CDC has been examined. At first, different B cell lines were tested for their responsiveness to IL10 stimulation. Therefore, the B cell lines have been stimulated with recombinant human IL10 and the responsiveness to this stimulus has been visualized via immunoblot of phosphorylated STAT3 (data not shown). The cell lines Balm3, Ramos and Karpas422 responded to IL10 stimulation with phosphorylation of STAT3. In OCI Ly3 constitutive activation of STAT3 was detected. These four cell lines were therefore used for the following experiments.

Viability and proliferation of these cell lines have been examined, following treatment with different concentrations of Rituximab, representing the induction of CDC. The lower the viability and the proliferation of the cells, the higher was the induced CDC. CDC needs complement factors, which are usually destroyed via heat decomplementation of the serum used for cell culture medium. For this experiment human serum was used either heat decomplemented as a negative control or left untreated to retain complement factors. Before the treatment with Rituximab and complement, the cell lines were treated with IL10 for 3h. However, in none of the examined cell lines an influence of IL10 treatment could be observed (Figure 3-26). The cell line Balm3 was lysed after treatment with complement and 10µg/ml Rituximab, without a difference between those cells that have been pretreated with IL10 and those without this treatment. Already the addition of complement seemed to reduce proliferation of the cells. Ramos cells reacted similar to Balm3. But for Ramos the addition of 0.1µ/ml Rituximab already reduced the proliferation considerably. In contrast to Balm3 and Ramos, Karpas422 and OCI Ly3 do not show a reduction of viability or proliferation upon Rituximab treatment. For OCI Ly3 a reduction of proliferation was observed after the addition of complement as it was seen for Balm3. For both cell lines an enhanced viability could be seen after the addition of complement. However, this effect has not been observed in other experiments and is therefore not representative.

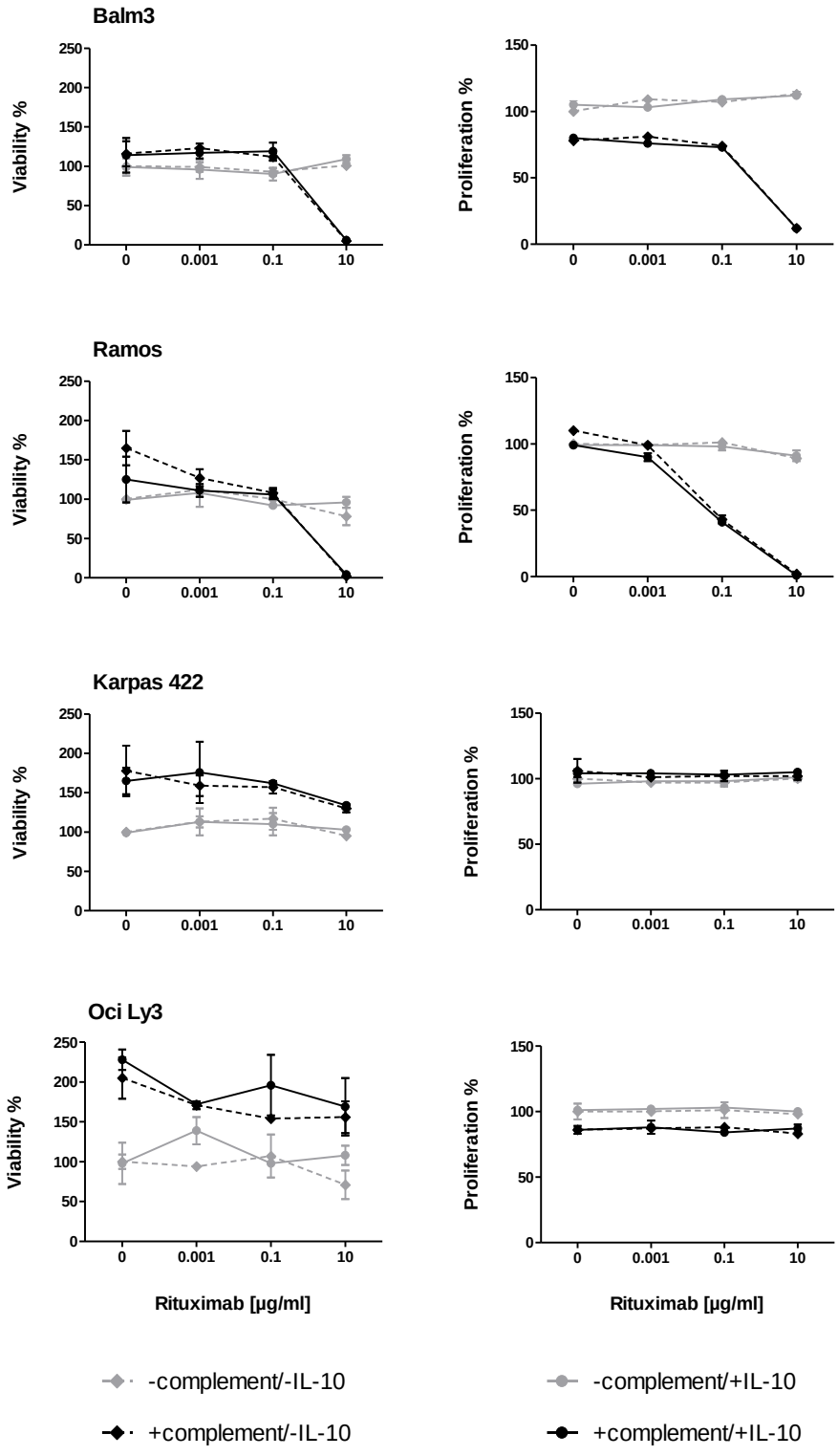

Figure 3-26 No Influence of exogenous IL10 on complement dependent cytotoxicity after Rituximab treatment

Viability (left) and proliferation (right) of Balm3, Ramos, Karpas 422 and OCI Ly3 cell lines were measured after Rituximab treatment for 24h as a read-out for CDC. Cells were cultured either with decomplemented human serum (-complement) or with undecomplemented human serum (+complement) with (+IL10) or without (-IL10) preincubation with IL10 for 3h. Viability and proliferation of cells cultured without Rituximab and without complement are set to 100%. Rituximab was used in three different concentrations (0.001µg/ml, 0.1µg/ml and 10µg/ml).

Next, the effect of endogenous *IL10* expression levels has been assessed. As seen in Figure 3-14, only the B cell lines MC116, Balm3 and BJAB express *IL10* in detectable amounts. These cell lines have been analysed in comparison to cell lines without *IL10* expression. All cell lines have been treated with different concentrations of Rituximab, with or without complement. Viability and proliferation have been measured as a read out for CDC. For some cell lines, namely MC116 and Ramos, lysis of the cells could be seen visually after treatment with 10µg/ml Rituximab on the 94-well plates used for the assays. As seen in Figure 3-27 for proliferation and Figure 3-28 for viability no influence of *IL10* transcription could be observed for CDC. The addition of complement already leads to a reduction of proliferation in all examined cell lines. All three cell lines with *IL10* expression showed a reduction of viability (Figure 3-28) after Rituximab treatment and a reduction of proliferation was observed for MC116 and Balm3 (Figure 3-27). For those cell lines without endogenous *IL10* expression different results from complete lysis in Ramos and SuDHL4, represented by reduction in proliferation and viability, to no effect at all as seen for Karpas422 and OCI Ly3 have been observed. If endogenous *IL10* expression would influence CDC, it would have been expected that cells from the one group would show stronger reaction on Rituximab treatment than cells from the other group. This has not been observed. Therefore, one can conclude that endogenous *IL10* expression does not influence Rituximab-mediated CDC.

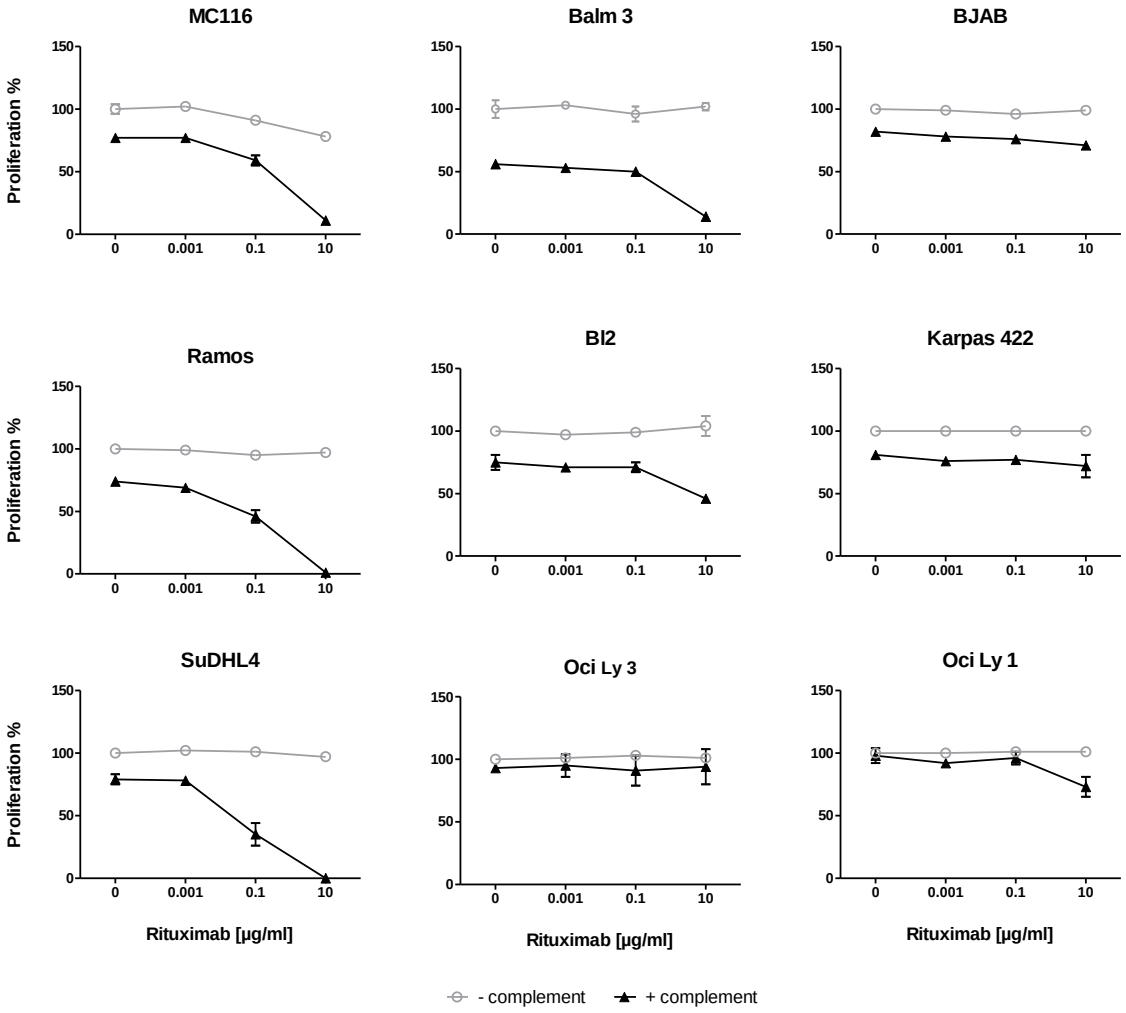

Figure 3-27 Endogenous IL10 does not influence complement dependent cytotoxicity after Rituximab treatment, visualized by proliferation of cell lines.

Proliferation of cell lines with *IL10* expression (MC116, Balm3, BJAB; upper lane) and cell lines without *IL10* expression (Ramos, Bl2, Karpas422, SuDHL4 OCI Ly3 and OCI Ly1) was measured after Rituximab treatment for 24h as a read-out for CDC. Cells were cultured either with decomplemented human serum (-complement) or with undecomplemented human serum (+complement). Rituximab was used in three different concentrations (0.001µg/ml, 0.1µg/ml and 10µg/ml). Proliferation of cells cultured without Rituximab and without complement was set to 100%. The cell lines are ordered according to *IL10* expression level. MC116 is the cell line with the highest *IL10* expression level.

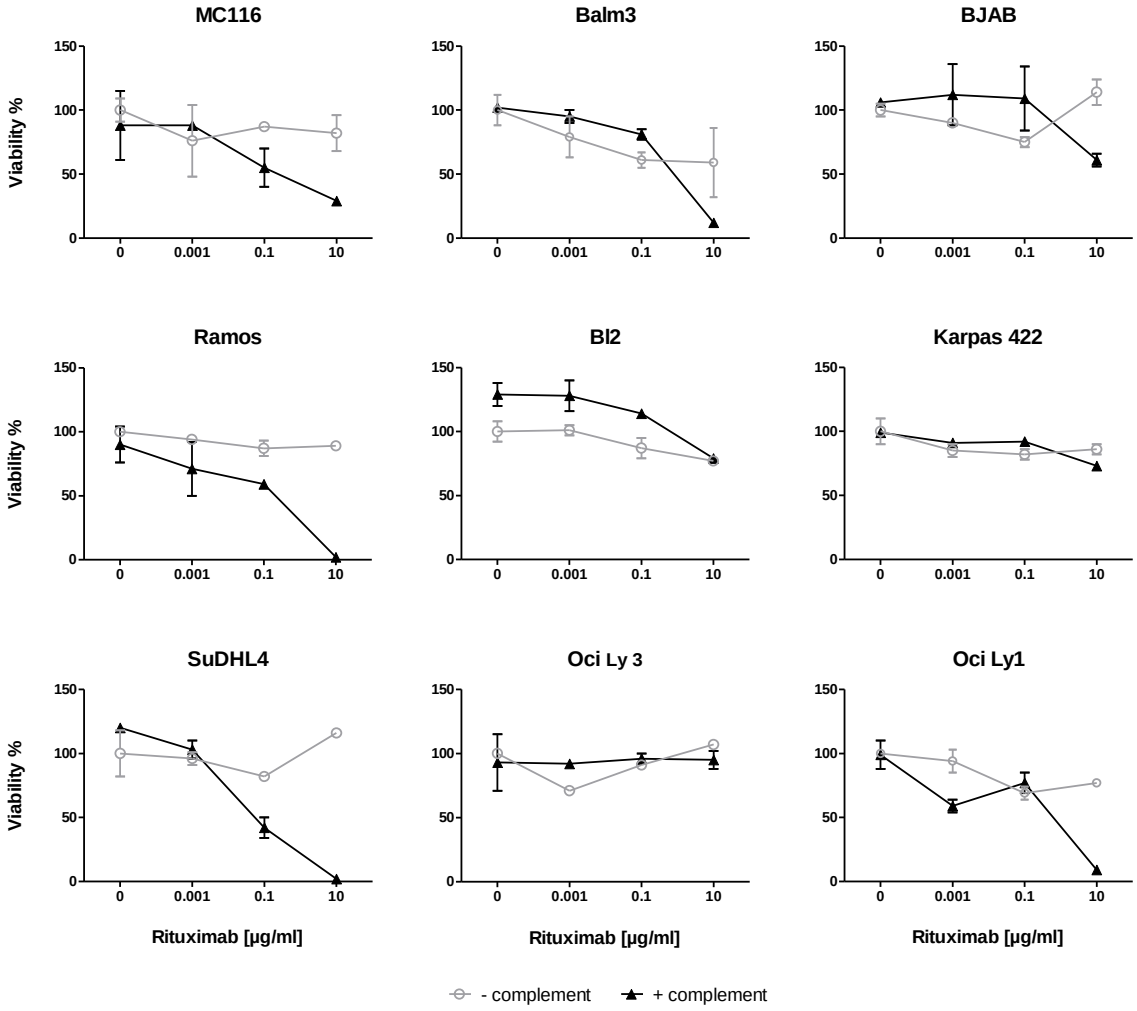

Figure 3-28 Endogenous IL10 does not influence complement dependent cytotoxicity after Rituximab treatment, visualized by viability of cell lines.

Viability of cell lines with *IL10* expression (MC116, Balm3, BJAB; upper lane) and cell lines without *IL10* expression (Ramos, Bl2, Karpas422, SuDHL4 OCI Ly3 and OCI Ly1) was measured after Rituximab treatment for 24h as a read-out for CDC. Cells were cultured either with decomplemented human serum (-complement) or with undecomplemented human serum (+complement). Rituximab was used in three different concentrations (0.001µg/ml, 0.1µg/ml and 10µg/ml). Proliferation of cells cultured without Rituximab and without complement was set to 100%. The cell lines are ordered according to *IL10* expression level. MC116 is the cell line with the highest *IL10* expression level.

Taken together, it has been shown that neither exogenous IL10 nor *IL10* expression levels influence Rituximab-mediated CDC.

3.4.2 Rituximab-mediated ADCC of target cells is inhibited by IL10

The effect of IL10 on Rituximab-mediated ADCC of target cells has been examined using Ramos and Karpas422 cell lines. NK cells were (for details see chapter 2.9.11). 12h prior to the ADCC assay Ramos and Karpas422 were stimulated with recombinant IL10 (see 2.9.6) or left untreated. On the next morning, FACS analysis of NK cells and target cells has been performed. NK cells had to be $CD56^+$, $CD16^+$, $CD3^-$ and $CD20^-$. Target cells had to be $CD20^+$. The expression of HLA class I was also assessed and target cells were positive. The expression of HLA class I did not change significantly after IL10 treatment.

Subsequently, target cells were stained with 3,3′-Dioctadecyloxacarbocyanine perchlorate (DiO) and incubated for 4h with or without NK cells, with or without IL10 and different concentrations of Rituximab. To determine specific lysis of the target cells FACS analysis has been performed after addition of propidium iodide (PI) to stain dead cells. Specific lysis has been calculated as the percentage of all PI positive cells of all DiO positive cells. ADCC has been calculated as the amount of cells, which have been lysed due to Rituximab treatment compared to the amount of target cells lysed already without Rituximab. The ADCC assay was performed by Christina Kiecke.

No Rituximab-mediated lysis of target cells could be observed without the addition of NK cells for Karpas422 or Ramos (Figure 3-29 A and B). The addition of IL10 alone did not lead to any lysis. Karpas422 cells as well as Ramos cells have been lysed by NK cells less effectively after pretreatment with IL10. In accordance to this, ADCC was lower in cells treated with IL10 in addition to Rituximab (Figure 3-29 C). This was most pronounced in Ramos treated with 0.1µg/ml Rituximab. A Student’s t-test was used to calculate significance.

Therefore, IL10 induces changes probably of surface expression of certain proteins on target cells, which lead to a reduction of target cell killing via ADCC.

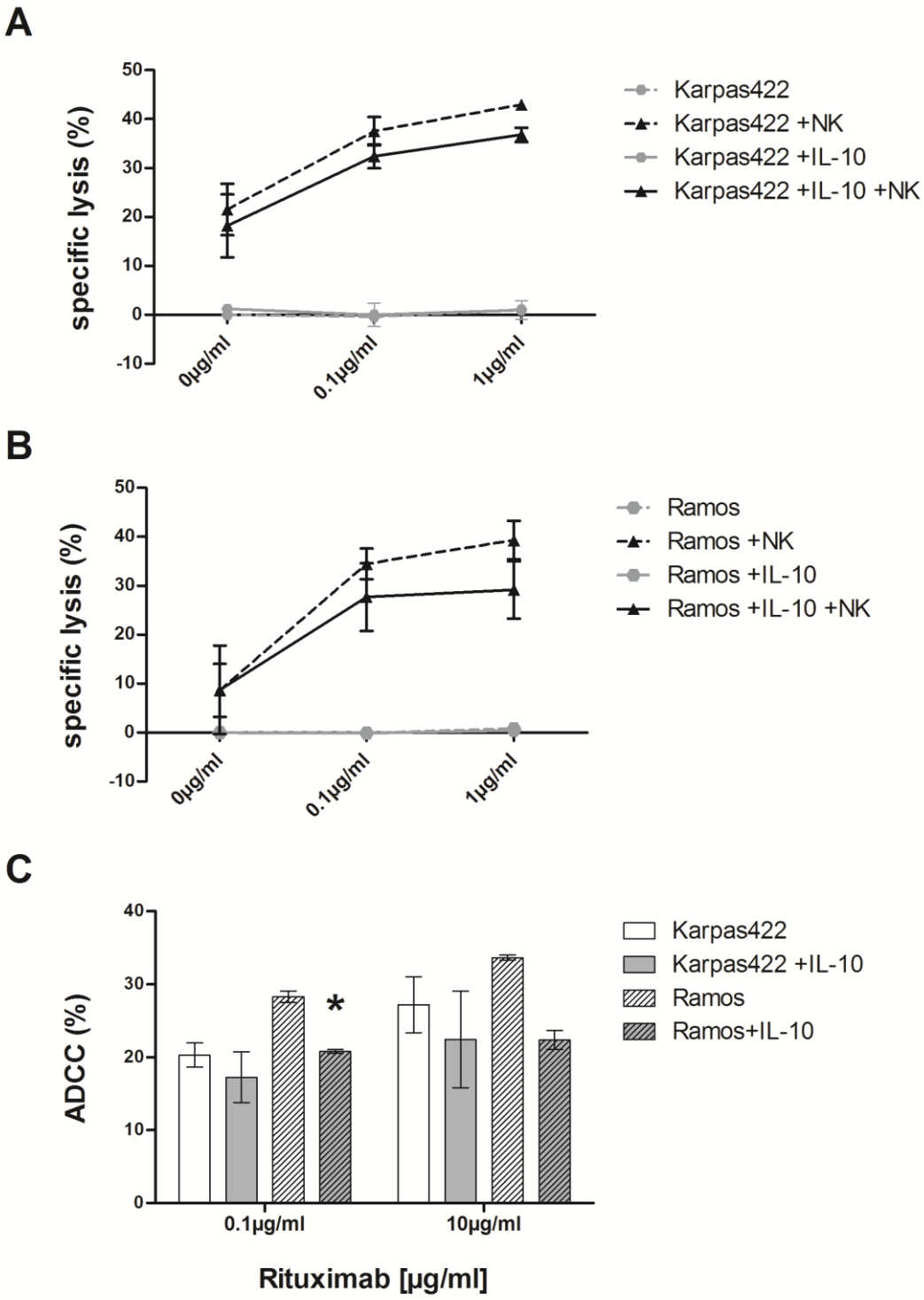

Figure 3-29 Rituximab-mediated ADCC of target cells is inhibited after IL10 treatment.

NK cells have been purified according to the method described in 2.9.11 Karpas422 and Ramos cells have been treated with 100ng IL10/ ml cells. 12h later these cells have been labeled with DiO, followed by 4h incubation with different concentrations of Rituximab, with or without NK cells, with or without IL10. Specific lysis of the target cells Karpas422 (**A**) and Ramos (**B**) has subsequently been determined as the percentage of PI positive cells of all DiO-labeled cells using FACS analysis. ADCC has been calculated as the amount of cells, which have been lysed due to Rituximab treatment compared to the amount of target cells lysed without Rituximab. Significance of ADCC has been determined using Student's t-test. The mean of two independent experiments is shown.

4 Discussion

This thesis aimed at the elucidation of the role of *IL10* gene variations and elevated IL10 serum levels for the treatment outcome of aNHL. The prognostic relevance of an increased number of *IL10* gene variations in independent cohorts of aNHL patients was investigated. Furthermore, the influence of so called regulatory gene variations within the *IL10* gene locus on interindividual IL10 production was examined in LCLs.

Despite the fact that approximately 90% of aNHL originate from B cells and IL10 acts as a potent growth factor for these cells, most studies on *IL10* gene regulation were implemented in T cells and macrophages. Hence, molecular mechanisms contributing to *IL10* gene regulation in B cells, including histone modifications, were assessed in this thesis.

4.1 Characterization of elevated IL10 serum levels and *IL10* gene variations with respect to the clinical outcome of aNHL patients treated with or without Rituximab

Within this thesis associations of high IL10 levels with the treatment outcome of aNHL patients treated with or without Rituximab have been assessed in a comparably large cohort of 523 patients. High serum levels of IL10 have been shown to be significantly associated with worse treatment outcome (Figure 3-5). No conspicuous differences could be observed between patients treated with Rituximab or CHOP alone. Therefore, at least within the RICOVER-60 trial the addition of Rituximab does not overcome adverse prognostic features reported here for high IL10 serum levels.

In line with this, also T-NHL patients with high IL10serum levels showed a trend towards shorter survival (Figure 3-7). However, due to the low number of patients at the end of the observation time, the survival curves become instable and the results should therefore not be over interpreted.

Our observations that high pretreatment serum levels of IL10 are associated with worse treatment outcome are in line with several previous studies (Blay et al., 1993; Lech-Maranda et al., 2010; Lech-Maranda et al., 2006). Two of these studies were conducted on DLBCL patients by Lech-Maranda and colleagues (Lech-Maranda et al., 2010; Lech-Maranda et al., 2006). Patients included into these trials have been

treated with anthracyclin-based regimens. The standard therapy today is CHOP therapy in combination with Rituximab. Rituximab mediates downregulation of the anti-apoptotic protein Bcl-2 via downregulation of autocrine IL10 production, which leads to chemosensitization of the B cell lymphoma cells (Alas et al., 2001). Therefore, the authors stated that Rituximab treatment may abolish the adverse effects of elevated IL10 serum levels on treatment outcome. Furthermore, they concluded that studies evaluating the effect of high IL10 serum levels on treatment outcome of patients treated with Rituximab would be important (Lech-Maranda et al., 2010; Lech-Maranda et al., 2006).

Until very recently, no studies have been published assessing whether high serum levels of IL10 would also be a negative predictive factor in patient cohorts treated with Rituximab. During the writing process of this thesis, one study was published, in which this question was assessed in 70 patients with DLBCL (Gupta et al., 2012). Supporting our findings, also this study found high IL10 serum levels to be associated with a worse treatment outcome, shown by shorter EFS periods.

In contrast to the here reported findings, other studies reported no correlation of high IL10 serum levels and treatment outcome (Cortes et al., 1995; Ozdemir et al., 2004; Stasi et al., 1994). These studies have been conducted in relatively small cohorts. Moreover, these patient cohorts differ to ours with respect to general treatment outcome. In the study of Ozdemir and colleagues for example 71% of the patients experienced a complete remission and 21% a partial remission. This was a much better outcome compared to patients from the trails used in this thesis. Stasi and colleagues reported that high IL10 levels together with high sIL2R levels are indeed of prognostic relevance. No study reported a superior treatment outcome for patients with high IL10 levels.

Taken together, the results indicate that high serum levels of IL10 are most likely an adverse prognostic factor in aNHL patients and that these adverse prognostic features are not overcome by Rituximab treatment.

So far a potential role of IL10 during the manifestation and progression of lymphomas is still debated (Lin and Karin, 2007; Mocellin et al., 2005). IL10 can act as a growth factor for normal and transformed B cells, leading to an enhanced proliferation of the lymphoma cells and exerts strong immunosuppressive activity, which allows

malignant cells to escape from an active immune response (Mocellin et al., 2005; Voorzanger et al., 1996). But also the opposite has been reported (Lin and Karin, 2007; Mocellin et al., 2005). The immunosuppressive properties of IL10 have been linked to an inhibition of tumor development and progression, which is supported by inflammatory processes. However, as high IL10 serum levels have been found repeatedly to be associated with a worse treatment outcome, the probability that IL10 has cancer inhibiting properties in aNHL is low.

Tumor progression, invasion, metastasis and angiogenesis are supported by a persistent inflammatory tumor microenvironment. Deregulation of certain cytokines, released by tumor cells or cells in the microenvironment, can lead to a sustained inflammatory response. Even though IL10 inhibits the production of proinflammatory cytokines like TNF-α, high levels of IL10 have been shown to be associated with an adverse prognosis. Therefore, one could speculate that the normal negative feed-back loop, leading to inhibition of TNF-α by IL10 is impaired. Instead of inhibiting TNF-α production, IL10 contributes to tumor progression by acting as an autocrine growth factor. Only recently, IL10 has been reported to activate JAK2 in certain DLBCL cell lines, leading to STAT3 activation and upregulation of c-myc expression, an important survival factor for DLBCL (Gupta et al., 2012).

However, it also has to be taken into account that increased IL10 serum levels in aNHL patients could solely reflect an active immune response against more aggressive disease and the attempt to stop chronic inflammation processes not controlled by the host.

To validate the obtained results, optimally a patient cohort that can be divided into a CHOP and an R-CHOP treatment arm should be used. Due to ethical reasons, patients are no longer treated only with CHOP nowadays, as R-CHOP has been shown to result in a better treatment outcome. The DSHNHL recruited patients for a follow up clinical trial of RICOVER-60, the CHOP-R-ESC trial. These patients all received R-CHOP. Serum of 258 patients was available. IL10 serum levels of these samples have been measured via ELISA and the data are currently evaluated in the IMISE in Leipzig.

In addition to this, *in vitro* analyses revealed a negative effect of IL10 on Rituximab-mediated antibody dependent cellular cytotoxicity (ADCC) but not complement dependent cytotoxicity (CDC) (Figure 3-29).

The B cell lymphoma cell lines Ramos and Karpas422 were treated for 12h with recombinant human IL10 before adding of NK cells together with Rituximab in different concentrations. This means that the effect of IL10 on the target cells rather than the effect on NK cells was investigated. Natural cytotoxicity of NK cells as well as NK cell-mediated ADCC are regulated by HLA/KIR interactions (Borgerding et al., 2010). An absence or blocking of the inhibitory signal mediated by HLA/KIR interactions has been found to cause an enhanced Rituximab-mediated ADCC.

IL10 expression as well as treatment with recombinant IL10 has been reported to induce a reduction of HLA class I expression in different tumour entities (Kundu and Fulton, 1997; Kurte et al., 2004; Petersson et al., 1998). The same was found for EBV-induced *IL10* expression in B cells (Zeidler et al., 1997). The reduction of HLA class I expression increased the sensitivity of target cells to natural cytotoxicity of NK cells and according to the results of Borgerding et al. should lead to an increased Rituximab-mediated ADCC. This was not the case in our experimental set up. HLA class I expression has been assessed as a general control prior to the ADCC assay in the examined cell lines. IL10 treatment did not lead to conspicuous changes in overall surface expression of HLA class I.

Therefore, the hypothesis that IL10 treatment leads to increased expression of a nonclassical HLA class Ib molecule, HLA-G seems more likely. The IL10-induced upregulation of HLA-G by tumor cells has been found to inhibit lysis mediated by natural cytotoxicity of NK cells (Urosevic and Dummer, 2003). Therefore, it could also be associated with a decreased Rituximab-mediated ADCC. Flow cytometric analysis of HLA-G expression with and without IL10 treatment would be a useful tool to test this hypothesis.

However, an effect of IL10 on NK cells cannot be excluded, as these have been co-incubated for 4h during the ADCC assay. Opposing effects of IL10 on NK cells have been reported. IL10 has been shown to inhibit production of IFN-ɣ and TNF by NK cells in vitro (Moore et al., 2001). Nevertheless, NK cell-mediated cytotoxicity against Daudi cells has been enhanced by IL10, albeit to a lesser extent compared to IL2 (Mocellin et al., 2004). The NK cells used here had been cultivated with IL2 over

night before the ADCC assay was performed. Therefore, the addition of IL10 to NK cells does not further enhance cytotoxic activity but rather inhibits it. Additional assays, with different conditions for overnight culture of NK cells, prior to the ADCC might be useful to analyse this.

Taken together, it could be shown that elevated serum levels are an adverse prognostic factor for aNHL treatment outcome. This was still observed in patients treated with Rituximab. Furthermore, it was observed that IL10 treatment of B cells is associated with a decrease in Rituximab-mediated ADCC. Therefore, Rituximab treatment does not overcome adverse prognostic features of elevated IL10 levels and in addition an important Rituximab-mediated anti-cancer response seems to be decreased by elevated IL10 levels.

Survival analyses have been conducted to assess associations between *IL10* gene variations and treatment outcome.

In a previous study, aNHL patients carrying the IL10-7400DelDel genetic variation have been found to be characterized by a worse treatment outcome compared to carriers of the other two genotypes of IL10-7400In/Del (Kube et al., 2008). However, this negative predictive effect of IL10-7400DelDel could not be validated in the extended NHL-B cohort (Figure 3-2).

Moreover, the IL10-7400DelDel gene variation was associated with a better treatment outcome in patients from the RICOVER-60 trial (Figure 3-4). This effect was not restricted to patients treated with Rituximab. Patients from the CHOP cohort, who have been treated similar to patients within the NHL-B trial also showed an insignificant trend towards better treatment outcome for carriers of IL10-7400DelDel. However, it has to be taken into account that these two cohorts differ to some extent in terms of age, IPI risk score, extranodal involvement, general OS as well as period of patient accrual (1993-2000 for NHL-B and 2000-2005 for RICOVER-60). General treatment conditions within the clinics improved during these years.

In the RICOVER-60 cohort several *IL10* gene variations showed significant associations with OS and EFS. Based on haplotype analyses (Figure 3-1) the IL10-11.668G/A gene variation was considered to be the gene variation causing this effect.

The IL10-11.668AA genotype showed significant associations with a better treatment outcome in the RICOVER-60 as well as the R-CHOP cohort. The same trend was observed for the CHOP cohort (Figure 3-3).

The relative risk for shorter OS and EFS periods, estimated in multivariate analyses adjusted to IPI factors was lowest in the R-CHOP cohort compared to the other two cohorts (Table 3-6). The confidence intervals of the R-CHOP cohort and the RICOVER-60 do not include the value 1. However, the trend for IL10-11.668AA observed within the CHOP cohort was the same as for the other two cohorts and it has to be taken into account that the confidence intervals of the R-CHOP and the CHOP cohort overlap to some extent. This means that the “true relative risk” could be the same for both cohorts.

Notably, no association of better or worse treatment outcome with IL10-11.668G/A was observed for the NHL-B cohorts. However, as mentioned above, the RICOVER-60 cohorts and the NHL-B cohorts differ with respect to clinical and histological characteristics as well as the period of patient accrual.

However, before a final conclusion about the prognostic relevance the IL10-11.668G/A can be drawn, this effect has to be validated in another patient cohort. DNA was available for 258 patients of the above mentioned CHOP-R-ESC trial. Genotyping for *IL10* gene variations has already been conducted and the data are currently evaluated in the IMISE in Leipzig.

Interestingly, the IL10-11.668G/A gene variation is located within CNS-12, which has been shown to possess enhancer activity by ChIP analyses using the H3K4me1 antibody (Figure 3-17). Even though it still has to be validated that IL10-11.668G/A is of prognostic relevance for treatment outcome, this finding raises the possibility that this gene variation could be involved in *IL10* gene regulation. Based on the results of the survival analyses, this would indicate that IL10-11.668AA somehow causes low *IL10* expression.

IL10-11.668A is in Linkage Disequilibrium (LD) with the A-G/A-A haplotypes (compare to figure 1-3 and figure 3-1), formed by IL10-3538A/T, IL10-2812G/A and IL10-2726C/A, which is postulated to be associated with low IL10 production in whole blood cultures stimulated with LPS (Gibson et al., 2001). However, IL10-11.668A is also observed together with the GCC haplotype (IL10-1087G, -824C, -597C) as well as the IL10-7400Del,

which have both been described to be associated with higher IL10 production capacities (Crawley et al., 1999; Rieth et al., 2004).

This issue has been assessed within this thesis using LCLs (chapter 3.2). No association of an *IL10* gene variation could be identified with high or low IL10 production capacities using this system, even though high number of LCLs was analysed. Therefore, it is likely that differences in IL10 production capacities of LCLs could be influenced by other factors associated with EBV infection, the "age" of each cell line or an interaction of these factors with *IL10* gene variations. The level of one EBV associated protein, LMP1 was assessed as it was shown to induce *IL10* expression in Burkitt's lymphoma cell lines (Vockerodt et al., 2001). No association of LMP1 expression with IL10 production was found. Maybe other EBV gene products, like EBV-encoded small proteins, expressed in LCLs, have a higher influence (Samanta et al., 2008). Moreover, it has been observed that LCLs, comprised of polyclonal cell populations directly after EBV immortalization, become monoclonal over time (data not shown). This could further influence *IL10* expression levels. However, no conspicuous differences have been observed between old LCLs and newly established LCLs.

Even though LCLs possess different IL10 production capacities, they were found to be limited for their utilization as model for the analysis of the influence of *IL10* gene variations on IL10 production. No answer can be given to the question on how IL10-11.668G/A influences IL10 production capacity. However, the fact that IL10-11.668G/A is located within an important regulatory region in B cells underlines the importance of further elucidation of its function for *IL10* gene regulation. This could be conducted for example by luciferase assays comparing the effect of the A- to the G-allele on a basic promoter fragment. In addition PBMCs derived from voluntary blood donors might be a better model for the elucidation of the influence of this gene variation on IL10 production. Two different stimuli, LPS and cAMP could be used for this purpose.

IL10 gene variations are thought to be predictive for treatment outcome due to the fact that they influence IL10 production. Therefore, one might ask why searching for these gene variations should be conducted, instead of using IL10 serum levels. Both approaches, *IL10* gene variations and IL10 serum levels as prognostic factors for aNHL outcome, possess important advantages and disadvantages. IL10, as well as

other cytokines, is very unstable in serum (van der Linden et al., 1998). Therefore, the logistic effort is much higher. Serum has to be kept cool or better frozen. This is especially challenging if samples have to be delivered to external institutions for diagnosis. Compared to this, DNA in blood samples is stable and the results of genotyping assays are more reliable and reproducible.

Clinical trials for testing new therapeutic regiments conducted in the future should be designed in a way that DNA samples and pre-treatment serum samples should be collected from all patients. Thereby, the number of patients included into genotyping analyses would be enlarged and the validity of respective survival analyses would be higher. Validation cohorts should be included into the study design for the validity of both, the clinical trial itself and the prognostic relevance of gene variations. Furthermore, it would be interesting to analyse IL10 serum levels and *IL10* gene variations of patients who achieved complete remission and those who relapsed to answer the question if these two factors have an impact on the likelihood of an relapse.

In conclusion the here reported results provide evidence that deregulation of IL10, leading to elevated IL10 levels, is an important factor for the clinical course of aNHL. High serum levels of IL10 have been shown to be an adverse prognostic factor. Furthermore, an inherited far distal *IL10* gene variations, IL10-11.668G/A could be associated with treatment outcome of aNHL.

4.2 Distal enhancer activity is involved in *IL10* gene regulation in B cells

In this work several B cell lines with inducible or constitutive *IL10* expression have been used as model systems for the analysis of mechanisms contributing to *IL10* gene regulation in B cells, a goal that received only minor attention in the past. Using specific pathway inhibitors the PKC, PI3K and the ERK signalling pathways were demonstrated to be involved in *IL10* gene regulation in the L428 cell line.

ChIP experiments revealed certain histone modifications to be associated with *IL10* expression. These histone modifications could be localized to specific regions of the *IL10* gene locus. Some of these regions are common to all analysed cell lines while others are more unique. The most important finding of the ChIP experiments was that far distal regions around CNS-12 are characterized by mono-methylation of lysine 4 at Histone 3 (H3K4me1), an enhancer-specific histone modification in B cells with

active *IL10* expression. Moreover, a long ncRNA has been shown to be transcribed from the *IL10* gene locus in all analysed B cell lines.

Tri-methylation of lysine 4 at Histone 3 (H3K4me3) has been detected at the proximal promoter regions as well as at the coding regions of *IL10* in all three B cell lines with active *IL10* transcription but not in unstimulated L428 by ChIP (Figure 3-17 and 3-18, middle). Acetylation of H3 (acH3) has been observed basically at the same regions as H3K4me3 (Figure 3-17 and 3-18, top). These findings are in line with previously reported data. H3K4me3 has been found to be associated with RNA polymerase II (RNA-Pol II) binding (Guenther et al., 2007). H3K4me3 and RNA-Pol II binding are generally detected at promoters and immediately downstream of TSS. Most studies found H3K4me3 together with acH3 to be associated with actively transcribed genes (Koch et al., 2007; Santos-Rosa et al., 2002; Schneider et al., 2004). The fact that this modification could not be detected at regions further upstream indicates that no other TSS or active promoters are located within the examined regions. Regarding the *IL10* gene locus this modification was firstly described here, therefore no comparison to other cell types can be made.

In cells with active *IL10* expression acH3 could be detected at the proximal promoter and the *IL10* coding regions. Almost no acH3 was found in unstimulated L428 cells. At the CNS+6, which corresponds to CNS+6.45 in mice, acH3 could only be detected in the BJAB cell line. This indicates that mechanisms of *IL10* gene regulation even differ between B cell lines.

Interestingly, a slight increase in acH3 was also observed at more distal parts of the *IL10* gene locus, around CNS-12, indicating that these regions could also be of importance for *IL10* gene regulation.

In contrast to H3K4me3, acH3 at the *IL10* gene locus was assessed in the past in macrophages and T cells. In macrophages acH3 has been observed at the TSS of *IL10* and at the HSS at -4.5kb, even without the IL10-inducing stimulus IC/LPS (Saraiva et al., 2005). However, the level of acH3 changes after stimulation with IC/LPS within the proximal *IL10* promoter and the time course of acH3 resembles that of IL10 mRNA induction (Zhang et al., 2006). This means acH3 is increased when *IL10* expression is up-regulated in macrophages. In T cells the infection with a GATA3 containing retrovirus leads to induction of *IL10* expression accompanied by

acH3 at three examined regions of the *IL10* locus, including CNS+6.4 (Shoemaker et al., 2006). Therefore, our data obtained in the three B cell lines, L428, BJAB and MC116 are only partially in line with the data obtained in macrophages and Th cells. Similarities are found in terms of inducibility of acH3 at the proximal promoter and the *IL10* coding regions. No acH3 could be seen at the postulated macrophage specific HSS-4.5 (Saraiva et al., 2005).

In addition to acH3 and H3K4me3, H3K4me1 has been assessed at the *IL10* locus (Figures 3-17 and 3-18, bottom). This modification has been associated with enhancer activity (Heintzman et al., 2007). H3K4me1 has been observed at the proximal promoter as well as in the coding regions of *IL10*. In BJAB and MC116 the proximal promoter regions show higher enhancer activity than regions within the coding region. In L428 this enhancer activity was inducible at the proximal promoter but in the coding region it was already detectable in unstimulated cells. Therefore, these regions seem to have an intrinsic enhancer activity, which may reflects a certain competence rather than activity in unstimulated L428, indicating that an enhancer element could be located in Intron 2. Taken together, this implies that these proximal promoter regions act as enhancers during active transcription of *IL10* in all three B cell lines.

The most interesting observations were made in more distal parts of the *IL10* gene locus around CNS-12. In all three cell lines H3K4me1 could be observed at CNS-12, whereby this was most pronounced in L428 stimulated with PMA. Even though H3K4me1 was detected in unstimulated cells, the levels of H3K4me1 increased considerably after PMA stimulation. In BJAB and in MC116 low levels of H3K4me1 could be detected at CNS-12. These findings provide evidence that this region could be of high importance for *IL10* gene regulation in B cells.

H3K4me1 could also be detected at the second important CNS, CNS+6, containing a putative AP1 binding site. In L428 it could be detected without prior stimulation and considerably high levels of H3K4me1 could be observed in BJAB at CNS+6.

In BJAB, H3K4me1 was also found to be localized HSS-4.5, a putative NF-κB binding site. This indicates that this region is not only relevant for *IL10* gene regulation in macrophages but also in some B cells. Notably, NF-κB cannot be a relevant transcription factor for *IL10* expression in L428. In L428 NF-κB is constitutively active and no *IL10* is expressed without additional stimulation with

PMA. These results underline once more that even in different B cell lines or B cell lymphomas different molecular mechanisms seem to contribute to *IL10* gene regulation.

As H3K4 methylation of the *IL10* gene locus in immune cells has been observed for the first time here, no comparison to other cell types can be made. The only publication that addressed was a review about histone modifications in T cells (Lee et al., 2009b). The authors mentioned that methylation of H3K4 at several CNS is higher in Th2 cells than in Th1 cells as so far unpublished results. But whether they assessed mono- and/or tri-methylation was not described (Lee et al., 2009b).

H3K4me1 was found to be distributed in a cell type specific manner and was associated with differences in gene expression (Heintzman et al., 2009; Koch et al., 2007). In a recent work on different T cell subsets the authors came to a similar conclusion and stated that it is likely that transcriptional enhancers are primary mediators of cell-type specific patterns of gene expression (Tian et al., 2011). This underlines the importance of assessing enhancer regions for elucidating mechanisms of gene regulation in different cell types. Future studies should assess these modifications also in macrophages and T cells to elucidate cell type specific modification patterns.

As mentioned above (chapter 4.1) the gene variation IL10-11668G/A is located within CNS-12. Therefore, the finding that this is an enhancer region in transformed B cell lines could also be of clinical relevance. It would be interesting to know whether CNS-12 also has enhancer activity in B cells derived from primary lymphoma material.

Luciferase assays would allow a validation of enhancer activity of these regions in B cells. Plasmids containing a functional basic *IL10* promoter could be used to address this question. Furthermore, transcription factor binding at the *IL10* gene locus could be assessed by ChIP. Computer algorithm-based prediction of transcription factor binding sites, as well as the knowledge provided here about the pathways involved in IL10 induction in L428 could be used to find suitable candidate transcription factors. AP1 binding at CNS+6 in B cell lines or NF-κB binding at HSS4.5 in BJAB could be good candidates.

4.3 A long ncRNA is transcribed from the *IL10* gene locus

Encouraged by the study of Jones and Flavell (Jones and Flavell, 2005), who detected transcription of ncRNA from certain CNS and HSS, the transcription of ncRNA from the *IL10* gene locus was assessed in this thesis. In their study most of the sequences transcribing ncRNA have been shown to possess enhancer activity by luciferase assays. The actual length of the ncRNA was not described and the publication indicated that several small ncRNAs were transcribed from CNS. Until now nothing is known about the function of the ncRNA.

Only approximately 2% of the human genome consist of protein-coding genes even though at least 90% are actively transcribed (Gibb et al., 2011). Increasing evidence exists that these 90% of human DNA are transcribed into molecules that are ncRNAs. This ncRNA can be grouped into small and long ncRNAs. The group of the small ncRNAs includes for example the better characterized miRNAs. Little is known so far about long ncRNAs, which range between 200nt to 100kb in length, even though an increasing attention to this subject is reflected by an increasing amount of publications (Gibb et al., 2011). Transcription of the ncRNA from the *IL10* gene locus in the B cell lines used here was detected from all analysed regions. Therefore, it is likely that the ncRNA is one long transcript of at least 23kb.

Even though some long ncRNAs have been described to mediate gene repression, for example during imprinting processes (Saxena and Carninci, 2011), the ncRNA detected here was associated with activation of gene expression from the *IL10* gene locus. In line with this, most genome wide studies suggest that transcription of long ncRNA is positively correlated with activity of neighboring genes (Orom and Shiekhattar, 2011). These long ncRNAs could mediate their effects though different mechanisms. They could solely be a byproduct of transcription, helping to open the DNA to activate nearby genes. This has been shown to be a stepwise process during which ncRNA is transcribed, leading to an open chromatin configuration as well as translocation of RNA-Pol II (Hirota et al., 2008). In contrast to this, it was found that knock-down of certain long ncRNAs abolished their enhancer activity and therefore the ncRNA itself was important (Orom et al., 2010). One hypothesis how this enhancer function is achieved, is that ncRNA mediates the formation of chromatin loops between enhancer and promoter region, allowing transcriptional activators to be recruited to respective regions. Alternatively, ncRNA could be endowed with

enzymatic activity to mediate modifications of chromatin or the DNA (Orom and Shiekhattar, 2011). Several other mechanisms have been proposed.

As an oligo-dT primer has been used for reverse transcription in some assays in the L428 cell line during this work, it can be concluded that the ncRNA is polyadenylated. This means it is transcribed by RNA-Pol II. This already excludes some kinds of long ncRNAs described in the literature, like enhancer RNAs, which are non-polyadenylated RNAs transcribed from enhancers (Kim et al., 2010). Notably, no H3K4me3 could be detected within the examined distal regions by ChIP. As this is usually found to be associated with RNA-Pol II binding, it is likely that the transcription start of the ncRNA lies even further upstream than -16.400bp or within the *IL10* coding region, for example in introns.

In order to further characterize the ncRNA transcribed from the *IL10* gene locus, to allow conclusions regarding its function, several tools are available. So far, it is known that the ncRNA is transcribed from several regions within a 23kb range of the *IL10* gene locus. Regions further upstream or downstream still need to be included into this analysis. Northern Blot analysis could help to estimate its exact length and if different splice variants could be involved. Furthermore, it would be useful to analyse the 3’ and 5’-end of the ncRNA by RACE-PCR. This would also allow the characterization of different splice products, if these exist.

Even though a final statement about the long ncRNA described herein cannot be made, it should be pointed out that deregulation of several long ncRNAs have been found to be associated with cancer (Gibb et al., 2011). Moreover, long ncRNAs have been shown to be transcribed in a developmental and tissue specific manner. Therefore, the elucidation of its function for *IL10* gene expression in B cells or B cell lymphoma and also other immune cells is an important goal for the future.

5 Conclusion

The identification of biological factors which influence treatment outcome of aNHL is an essential tool for the improvement of individual treatment strategies.

The finding that high serum levels of IL10 are associated with worse treatment outcome of aNHL indicates that deregulation of IL10, leading to elevated IL10 serum levels, is involved in the progression of this disease. Furthermore, it was shown for the first time in a large cohort of 523 aNHL patients, that the observed adverse prognostic features of elevated IL10 serum levels are not overcome by Rituximab treatment. Therefore, Rituximab-mediated downregulation of IL10 does not seem to be a dominant factor for the treatment outcome of aNHL. In addition to this, IL10 treatment of B cells seems to reduce Rituximab-mediated ADCC, an important Rituximab-mediated anti-cancer response. Furthermore, this study provides evidence that a far distal *IL10* gene variation, IL10-11.668G/A, which is located within CNS-12, could be associated with treatment outcome of aNHL patients. It remains to be elucidated if and how the IL10-11.668G/A gene variation influences differences in interindividual IL10 production. To validate the results obtained here for patients from the RICOVER-60 trial, *IL10* gene variations and serum levels have been determined in 258 patients from a follow-up trial, the CHOP-R-ESC, and are currently evaluated.

ChIP experiments in different B cell lines revealed for the first time that regions around CNS-12 and regions further upstream are characterized by the enhancer-specific histone modification, H3K4me1. This indicates that far distal regions of the *IL10* gene locus could be involved in regulation of *IL10* expression in transformed B cells. These findings underline the importance to include far distal *IL10* gene variations into survival analyses, to identify gene variations with prognostic significance. Moreover, it was shown that active *IL10* expression is accompanied by transcription of a very long ncRNA from the *IL10* gene locus. Further characterization of the ncRNA in different B cell lines combined with analyses of enhancer activity by luciferase assays or transcription factor binding by ChIP could help to elucidate the exact role of the distal regions for *IL10* gene regulation.

Taken together, this study suggests an important role for IL10 in the progression of aNHL. Furthermore it provides evidence that far distal conserved regions as well as a long ncRNA could be involved in mechanisms of *IL10* gene regulation.

Bibliography

(1997). A clinical evaluation of the International Lymphoma Study Group classification of non-Hodgkin's lymphoma. The Non-Hodgkin's Lymphoma Classification Project. Blood *89*, 3909-3918.

Alas, S., and Bonavida, B. (2001). Rituximab inactivates signal transducer and activation of transcription 3 (STAT3) activity in B-non-Hodgkin's lymphoma through inhibition of the interleukin 10 autocrine/paracrine loop and results in down-regulation of Bcl-2 and sensitization to cytotoxic drugs. Cancer Res *61*, 5137-5144.

Alas, S., Emmanouilides, C., and Bonavida, B. (2001). Inhibition of interleukin 10 by rituximab results in down-regulation of bcl-2 and sensitization of B-cell non-Hodgkin's lymphoma to apoptosis. Clin Cancer Res *7*, 709-723.

Alexander, D.D., Mink, P.J., Adami, H.O., Chang, E.T., Cole, P., Mandel, J.S., and Trichopoulos, D. (2007). The non-Hodgkin lymphomas: a review of the epidemiologic literature. Int J Cancer *120 Suppl 12*, 1-39.

Alizadeh, A.A., Eisen, M.B., Davis, R.E., Ma, C., Lossos, I.S., Rosenwald, A., Boldrick, J.C., Sabet, H., Tran, T., Yu, X.*, et al.* (2000). Distinct types of diffuse large B-cell lymphoma identified by gene expression profiling. Nature *403*, 503-511.

Armitage, J.O., Vose, J.M., and Weisenburger, D.D. (2004). Towards understanding the peripheral T-cell lymphomas. Ann Oncol *15*, 1447-1449.

Bellan, C., Lazzi, S., De Falco, G., Nyongo, A., Giordano, A., and Leoncini, L. (2003). Burkitt's lymphoma: new insights into molecular pathogenesis. Journal of clinical pathology *56*, 188-192.

Benjamin, D., Knobloch, T.J., and Dayton, M.A. (1992). Human B-cell interleukin-10: B-cell lines derived from patients with acquired immunodeficiency syndrome and Burkitt's lymphoma constitutively secrete large quantities of interleukin-10. Blood *80*, 1289-1298.

Benkhart, E.M., Siedlar, M., Wedel, A., Werner, T., and Ziegler-Heitbrock, H.W. (2000). Role of Stat3 in lipopolysaccharide-induced IL-10 gene expression. J Immunol *165*, 1612-1617.

Berglund, M., Thunberg, U., Roos, G., Rosenquist, R., and Enblad, G. (2005). The interleukin-10 gene promoter polymorphism (-1082) does not correlate with clinical outcome in diffuse large B-cell lymphoma. Blood *105*, 4894-4895; author reply 4895.

Blay, J.Y., Burdin, N., Rousset, F., Lenoir, G., Biron, P., Philip, T., Banchereau, J., and Favrot, M.C. (1993). Serum interleukin-10 in non-Hodgkin's lymphoma: a prognostic factor. Blood *82*, 2169-2174.

Bohlen, H., Kessler, M., Sextro, M., Diehl, V., and Tesch, H. (2000). Poor clinical outcome of patients with Hodgkin's disease and elevated interleukin-10 serum levels. Clinical significance of interleukin-10 serum levels for Hodgkin's disease. Ann Hematol *79*, 110-113.

Bonavida, B. (2006). What signals are generated by anti-CD20 antibody therapy? Curr Hematol Malig Rep *1*, 205-213.

Boonstra, A., Rajsbaum, R., Holman, M., Marques, R., Asselin-Paturel, C., Pereira, J.P., Bates, E.E., Akira, S., Vieira, P., Liu, Y.J.*, et al.* (2006). Macrophages and

myeloid dendritic cells, but not plasmacytoid dendritic cells, produce IL-10 in response to MyD88- and TRIF-dependent TLR signals, and TLR-independent signals. J Immunol *177*, 7551-7558.

Borgerding, A., Hasenkamp, J., Engelke, M., Burkhart, N., Trumper, L., Wienands, J., and Glass, B. (2010). B-lymphoma cells escape rituximab-triggered elimination by NK cells through increased HLA class I expression. Experimental hematology *38*, 213-221.

Bradford, M.M. (1976). A rapid and sensitive method for the quantitation of microgram quantities of protein utilizing the principle of protein-dye binding. Analytical biochemistry *72*, 248-254.

Breen, E.C., Boscardin, W.J., Detels, R., Jacobson, L.P., Smith, M.W., O'Brien, S.J., Chmiel, J.S., Rinaldo, C.R., Lai, S., and Martinez-Maza, O. (2003). Non-Hodgkin's B cell lymphoma in persons with acquired immunodeficiency syndrome is associated with increased serum levels of IL10, or the IL10 promoter -592 C/C genotype. Clin Immunol *109*, 119-129.

Burdin, N., Peronne, C., Banchereau, J., and Rousset, F. (1993). Epstein-Barr virus transformation induces B lymphocytes to produce human interleukin 10. The Journal of experimental medicine *177*, 295-304.

Cervenak, L., Morbidelli, L., Donati, D., Donnini, S., Kambayashi, T., Wilson, J.L., Axelson, H., Castanos-Velez, E., Ljunggren, H.G., Malefyt, R.D.*, et al.* (2000). Abolished angiogenicity and tumorigenicity of Burkitt lymphoma by interleukin-10. Blood *96*, 2568-2573.

Chang, H.D., Helbig, C., Tykocinski, L., Kreher, S., Koeck, J., Niesner, U., and Radbruch, A. (2007). Expression of IL-10 in Th memory lymphocytes is conditional on IL-12 or IL-4, unless the IL-10 gene is imprinted by GATA-3. European journal of immunology *37*, 807-817.

Ci, W., Polo, J.M., and Melnick, A. (2008). B-cell lymphoma 6 and the molecular pathogenesis of diffuse large B-cell lymphoma. Current opinion in hematology *15*, 381-390.

Coiffier, B., Lepage, E., Briere, J., Herbrecht, R., Tilly, H., Bouabdallah, R., Morel, P., Van Den Neste, E., Salles, G., Gaulard, P.*, et al.* (2002). CHOP chemotherapy plus rituximab compared with CHOP alone in elderly patients with diffuse large-B-cell lymphoma. N Engl J Med *346*, 235-242.

Cortes, J., and Kurzrock, R. (1997). Interleukin-10 in non-Hodgkin's lymphoma. Leuk Lymphoma *26*, 251-259.

Cortes, J.E., Talpaz, M., Cabanillas, F., Seymour, J.F., and Kurzrock, R. (1995). Serum levels of interleukin-10 in patients with diffuse large cell lymphoma: lack of correlation with prognosis. Blood *85*, 2516-2520.

Crawley, E., Kay, R., Sillibourne, J., Patel, P., Hutchinson, I., and Woo, P. (1999). Polymorphic haplotypes of the interleukin-10 5' flanking region determine variable interleukin-10 transcription and are associated with particular phenotypes of juvenile rheumatoid arthritis. Arthritis Rheum *42*, 1101-1108.

Cunningham, L.M., Chapman, C., Dunstan, R., Bell, M.C., and Joske, D.J. (2003). Polymorphisms in the interleukin 10 gene promoter are associated with susceptibility to aggressive non-Hodgkin's lymphoma. Leuk Lymphoma *44*, 251-255.

Demidem, A., Lam, T., Alas, S., Hariharan, K., Hanna, N., and Bonavida, B. (1997). Chimeric anti-CD20 (IDEC-C2B8) monoclonal antibody sensitizes a B cell lymphoma cell line to cell killing by cytotoxic drugs. Cancer biotherapy & radiopharmaceuticals *12*, 177-186.

Dillon, S., Agrawal, A., Van Dyke, T., Landreth, G., McCauley, L., Koh, A., Maliszewski, C., Akira, S., and Pulendran, B. (2004). A Toll-like receptor 2 ligand stimulates Th2 responses in vivo, via induction of extracellular signal-regulated kinase mitogen-activated protein kinase and c-Fos in dendritic cells. J Immunol *172*, 4733-4743.

Domingo-Domenech, E., Benavente, Y., Gonzalez-Barca, E., Montalban, C., Guma, J., Bosch, R., Wang, S.S., Lan, Q., Whitby, D., Fernandez de Sevilla, A.*, et al.* (2007). Impact of interleukin-10 polymorphisms (-1082 and -3575) on the survival of patients with lymphoid neoplasms. Haematologica *92*, 1475-1481.

Donnelly, R.P., Dickensheets, H., and Finbloom, D.S. (1999). The interleukin-10 signal transduction pathway and regulation of gene expression in mononuclear phagocytes. J Interferon Cytokine Res *19*, 563-573.

Dranoff, G. (2004). Cytokines in cancer pathogenesis and cancer therapy. Nat Rev Cancer *4*, 11-22.

Dyer, M.J., Fischer, P., Nacheva, E., Labastide, W., and Karpas, A. (1990). A new human B-cell non-Hodgkin's lymphoma cell line (Karpas 422) exhibiting both t (14;18) and t(4;11) chromosomal translocations. Blood *75*, 709-714.

Epstein, A.L., Herman, M.M., Kim, H., Dorfman, R.F., and Kaplan, H.S. (1976). Biology of the human malignant lymphomas. III. Intracranial heterotransplantation in the nude, athymic mouse. Cancer *37*, 2158-2176.

Epstein, A.L., Levy, R., Kim, H., Henle, W., Henle, G., and Kaplan, H.S. (1978). Biology of the human malignant lymphomas. IV. Functional characterization of ten diffuse histiocytic lymphoma cell lines. Cancer *42*, 2379-2391.

Eskdale, J., Gallagher, G., Verweij, C.L., Keijsers, V., Westendorp, R.G., and Huizinga, T.W. (1998). Interleukin 10 secretion in relation to human IL-10 locus haplotypes. Proc Natl Acad Sci U S A *95*, 9465-9470.

Eskdale, J., Kube, D., Tesch, H., and Gallagher, G. (1997). Mapping of the human IL10 gene and further characterization of the 5' flanking sequence. Immunogenetics *46*, 120-128.

Felsenfeld, G., and Groudine, M. (2003). Controlling the double helix. Nature *421*, 448-453.

Ferlay, J., Parkin, D.M., and Steliarova-Foucher, E. (2010). Estimates of cancer incidence and mortality in Europe in 2008. Eur J Cancer *46*, 765-781.

Fiorentino, D.F., Zlotnik, A., Mosmann, T.R., Howard, M., and O'Garra, A. (1991). IL-10 inhibits cytokine production by activated macrophages. J Immunol *147*, 3815-3822.

Friedberg, J.W., and Fisher, R.I. (2008). Diffuse large B-cell lymphoma. Hematol Oncol Clin North Am *22*, 941-952, ix.

Gibb, E.A., Brown, C.J., and Lam, W.L. (2011). The functional role of long non-coding RNA in human carcinomas. Molecular cancer *10*, 38.

Gibson, A.W., Edberg, J.C., Wu, J., Westendorp, R.G., Huizinga, T.W., and Kimberly, R.P. (2001). Novel single nucleotide polymorphisms in the distal IL-10 promoter affect IL-10 production and enhance the risk of systemic lupus erythematosus. J Immunol *166*, 3915-3922.

Gisselbrecht, C., Gaulard, P., Lepage, E., Coiffier, B., Briere, J., Haioun, C., Cazals-Hatem, D., Bosly, A., Xerri, L., Tilly, H.*, et al.* (1998). Prognostic significance of T-cell phenotype in aggressive non-Hodgkin's lymphomas. Groupe d'Etudes des Lymphomes de l'Adulte (GELA). Blood *92*, 76-82.

Glennie, M.J., French, R.R., Cragg, M.S., and Taylor, R.P. (2007). Mechanisms of killing by anti-CD20 monoclonal antibodies. Molecular immunology *44*, 3823-3837.

Goto, N., Tsurumi, H., Takemura, M., Hara, T., Sawada, M., Kasahara, S., Kanemura, N., Yamada, T., Shimizu, M., Takahashi, T.*, et al.* (2006). Serum-soluble tumor necrosis factor receptor 2 (sTNF-R2) level determines clinical outcome in patients with aggressive non-Hodgkin's lymphoma. Eur J Haematol *77*, 217-225.

Grulich, A.E., and Vajdic, C.M. (2005). The epidemiology of non-Hodgkin lymphoma. Pathology *37*, 409-419.

Guenther, M.G., Levine, S.S., Boyer, L.A., Jaenisch, R., and Young, R.A. (2007). A chromatin landmark and transcription initiation at most promoters in human cells. Cell *130*, 77-88.

Gupta, M., Han, J.J., Stenson, M., Maurer, M., Wellik, L., Hu, G., Ziesmer, S., Dogan, A., and Witzig, T.E. (2012). Elevated serum IL-10 levels in diffuse large B-cell lymphoma: a mechanism of aberrant Janus kinase 2 activation. Blood.

Habermann, T.M., Wang, S.S., Maurer, M.J., Morton, L.M., Lynch, C.F., Ansell, S.M., Hartge, P., Severson, R.K., Rothman, N., Davis, S.*, et al.* (2008). Host immune gene polymorphisms in combination with clinical and demographic factors predict late survival in diffuse large B-cell lymphoma patients in the pre-rituximab era. Blood *112*, 2694-2702.

Hackstein, H., Hecker, M., Kruse, S., Bohnert, A., Ober, C., Deichmann, K.A., and Bein, G. (2001). A novel polymorphism in the 5' promoter region of the human interleukin-4 receptor alpha-chain gene is associated with decreased soluble interleukin-4 receptor protein levels. Immunogenetics *53*, 264-269.

Hammer, M., Mages, J., Dietrich, H., Schmitz, F., Striebel, F., Murray, P.J., Wagner, H., and Lang, R. (2005). Control of dual-specificity phosphatase-1 expression in activated macrophages by IL-10. European journal of immunology *35*, 2991-3001.

Heintzman, N.D., Hon, G.C., Hawkins, R.D., Kheradpour, P., Stark, A., Harp, L.F., Ye, Z., Lee, L.K., Stuart, R.K., Ching, C.W.*, et al.* (2009). Histone modifications at human enhancers reflect global cell-type-specific gene expression. Nature *459*, 108-112.

Heintzman, N.D., Stuart, R.K., Hon, G., Fu, Y., Ching, C.W., Hawkins, R.D., Barrera, L.O., Van Calcar, S., Qu, C., Ching, K.A.*, et al.* (2007). Distinct and predictive chromatin signatures of transcriptional promoters and enhancers in the human genome. Nature genetics *39*, 311-318.

Hirota, K., Miyoshi, T., Kugou, K., Hoffman, C.S., Shibata, T., and Ohta, K. (2008). Stepwise chromatin remodelling by a cascade of transcription initiation of non-coding RNAs. Nature *456*, 130-134.

Hummel, M., Bentink, S., Berger, H., Klapper, W., Wessendorf, S., Barth, T.F., Bernd, H.W., Cogliatti, S.B., Dierlamm, J., Feller, A.C.*, et al.* (2006). A biologic definition of Burkitt's lymphoma from transcriptional and genomic profiling. N Engl J Med *354*, 2419-2430.

Im, S.H., Hueber, A., Monticelli, S., Kang, K.H., and Rao, A. (2004). Chromatin-level regulation of the IL10 gene in T cells. J Biol Chem *279*, 46818-46825.

Jazirehi, A.R., Vega, M.I., Chatterjee, D., Goodglick, L., and Bonavida, B. (2004). Inhibition of the Raf-MEK1/2-ERK1/2 signaling pathway, Bcl-xL down-regulation, and chemosensitization of non-Hodgkin's lymphoma B cells by Rituximab. Cancer Res *64*, 7117-7126.

Jemal, A., Bray, F., Center, M.M., Ferlay, J., Ward, E., and Forman, D. (2011). Global cancer statistics. CA: a cancer journal for clinicians *61*, 69-90.

Jones, E.A., and Flavell, R.A. (2005). Distal enhancer elements transcribe intergenic RNA in the IL-10 family gene cluster. J Immunol *175*, 7437-7446.

Kaye, K.M., Izumi, K.M., and Kieff, E. (1993). Epstein-Barr virus latent membrane protein 1 is essential for B-lymphocyte growth transformation. Proc Natl Acad Sci U S A *90*, 9150-9154.

Keen, L.J. (2002). The extent and analysis of cytokine and cytokine receptor gene polymorphism. Transplant immunology *10*, 143-146.

Kieser, A., Kilger, E., Gires, O., Ueffing, M., Kolch, W., and Hammerschmidt, W. (1997). Epstein-Barr virus latent membrane protein-1 triggers AP-1 activity via the c-Jun N-terminal kinase cascade. The EMBO journal *16*, 6478-6485.

Kilger, E., Kieser, A., Baumann, M., and Hammerschmidt, W. (1998). Epstein-Barr virus-mediated B-cell proliferation is dependent upon latent membrane protein 1, which simulates an activated CD40 receptor. The EMBO journal *17*, 1700-1709.

Kim, T.K., Hemberg, M., Gray, J.M., Costa, A.M., Bear, D.M., Wu, J., Harmin, D.A., Laptewicz, M., Barbara-Haley, K., Kuersten, S.*, et al.* (2010). Widespread transcription at neuronal activity-regulated enhancers. Nature *465*, 182-187.

Klein, G., Giovanella, B., Westman, A., Stehlin, J.S., and Mumford, D. (1975). An EBV-genome-negative cell line established from an American Burkitt lymphoma; receptor characteristics. EBV infectibility and permanent conversion into EBV-positive sublines by in vitro infection. Intervirology *5*, 319-334.

Koch, C.M., Andrews, R.M., Flicek, P., Dillon, S.C., Karaoz, U., Clelland, G.K., Wilcox, S., Beare, D.M., Fowler, J.C., Couttet, P.*, et al.* (2007). The landscape of histone modifications across 1% of the human genome in five human cell lines. Genome research *17*, 691-707.

Kube, D., Hua, T.D., Kloss, M., Kulle, B., Brockmoller, J., Wojnowski, L., Loffler, M., Pfreundschuh, M., and Trumper, L. (2007). The interleukin-10 gene promoter polymorphism -1087AG does not correlate with clinical outcome in non-Hodgkin's lymphoma. Genes Immun *8*, 164-167.

Kube, D., Hua, T.D., von Bonin, F., Schoof, N., Zeynalova, S., Kloss, M., Gocht, D., Potthoff, B., Tzvetkov, M., Brockmoller, J.*, et al.* (2008). Effect of interleukin-10 gene polymorphisms on clinical outcome of patients with aggressive non-Hodgkin's lymphoma: an exploratory study. Clin Cancer Res *14*, 3777-3784.

Kube, D., Laser, H., von Knethen, A., and Tesch, H. (1999). The AT-rich region between -54 to -66 is important for the promoter activity of interleukin-10 in Epstein-Barr virus positive Burkitt's lymphoma cells. Genes Immun *1*, 105-114.

Kube, D., Platzer, C., von Knethen, A., Straub, H., Bohlen, H., Hafner, M., and Tesch, H. (1995). Isolation of the human interleukin 10 promoter. Characterization of the promoter activity in Burkitt's lymphoma cell lines. Cytokine *7*, 1-7.

Kundu, N., and Fulton, A.M. (1997). Interleukin-10 inhibits tumor metastasis, downregulates MHC class I, and enhances NK lysis. Cellular immunology *180*, 55-61.

Kuppers, R. (2005). Mechanisms of B-cell lymphoma pathogenesis. Nat Rev Cancer *5*, 251-262.

Kurte, M., Lopez, M., Aguirre, A., Escobar, A., Aguillon, J.C., Charo, J., Larsen, C.G., Kiessling, R., and Salazar-Onfray, F. (2004). A synthetic peptide homologous to functional domain of human IL-10 down-regulates expression of MHC class I and Transporter associated with Antigen Processing 1/2 in human melanoma cells. J Immunol *173*, 1731-1737.

Lech-Maranda, E., Baseggio, L., Bienvenu, J., Charlot, C., Berger, F., Rigal, D., Warzocha, K., Coiffier, B., and Salles, G. (2004). Interleukin-10 gene promoter polymorphisms influence the clinical outcome of diffuse large B-cell lymphoma. Blood *103*, 3529-3534.

Lech-Maranda, E., Bienvenu, J., Broussais-Guillaumot, F., Warzocha, K., Michallet, A.S., Robak, T., Coiffier, B., and Salles, G. (2010). Plasma TNF-alpha and IL-10 level-based prognostic model predicts outcome of patients with diffuse large B-Cell lymphoma in different risk groups defined by the International Prognostic Index. Archivum immunologiae et therapiae experimentalis *58*, 131-141.

Lech-Maranda, E., Bienvenu, J., Michallet, A.S., Houot, R., Robak, T., Coiffier, B., and Salles, G. (2006). Elevated IL-10 plasma levels correlate with poor prognosis in diffuse large B-cell lymphoma. Eur Cytokine Netw *17*, 60-66.

Lee, C.G., Kang, K.H., So, J.S., Kwon, H.K., Son, J.S., Song, M.K., Sahoo, A., Yi, H.J., Hwang, K.C., Matsuyama, T.*, et al.* (2009a). A distal cis-regulatory element, CNS-9, controls NFAT1 and IRF4-mediated IL-10 gene activation in T helper cells. Molecular immunology *46*, 613-621.

Lee, C.G., Sahoo, A., and Im, S.H. (2009b). Epigenetic regulation of cytokine gene expression in T lymphocytes. Yonsei medical journal *50*, 322-330.

Lee, J.J., Kim, D.H., Lee, N.Y., Sohn, S.K., Kim, J.G., Kim, H.J., Do, Y.R., and Park, Y.H. (2007). Interleukin-10 gene polymorphism influences the prognosis of T-cell non-Hodgkin lymphomas. Br J Haematol *137*, 329-336.

Levy, Y., and Brouet, J.C. (1994). Interleukin-10 prevents spontaneous death of germinal center B cells by induction of the bcl-2 protein. J Clin Invest *93*, 424-428.

Li, B., Carey, M., and Workman, J.L. (2007). The role of chromatin during transcription. Cell *128*, 707-719.

Lin, W.W., and Karin, M. (2007). A cytokine-mediated link between innate immunity, inflammation, and cancer. J Clin Invest *117*, 1175-1183.

Ljunggren, H.G., and Karre, K. (1990). In search of the 'missing self': MHC molecules and NK cell recognition. Immunology today *11*, 237-244.

Lok, M.S., Koshiba, H., Han, T., Abe, S., Minowada, J., and Sandberg, A.A. (1979). Establishment and characterization of human B-lymphocytic lymphoma cell lines (BALM-3, -4 and -5); intraclonal variation in the B-cell differentiation stage. Int J Cancer *24*, 572-578.

Lu, Z.Y., Zhang, X.G., Rodriguez, C., Wijdenes, J., Gu, Z.J., Morel-Fournier, B., Harousseau, J.L., Bataille, R., Rossi, J.F., and Klein, B. (1995). Interleukin-10 is a proliferation factor but not a differentiation factor for human myeloma cells. Blood *85*, 2521-2527.

Lucas, M., Zhang, X., Prasanna, V., and Mosser, D.M. (2005). ERK activation following macrophage FcgammaR ligation leads to chromatin modifications at the IL-10 locus. J Immunol *175*, 469-477.

Macpherson, I., and Stoker, M. (1962). Polyoma transformation of hamster cell clones--an investigation of genetic factors affecting cell competence. Virology *16*, 147-151.

Magrath, I.T., Freeman, C.B., Pizzo, P., Gadek, J., Jaffe, E., Santaella, M., Hammer, C., Frank, M., Reaman, G., and Novikovs, L. (1980). Characterization of lymphoma-derived cell lines: comparison of cell lines positive and negative for Epstein-Barr virus nuclear antigen. II. Surface markers. Journal of the National Cancer Institute *64*, 477-483.

Mahadevan, D., and Fisher, R.I. (2011). Novel therapeutics for aggressive non-Hodgkin's lymphoma. J Clin Oncol *29*, 1876-1884.

Masood, R., Zhang, Y., Bond, M.W., Scadden, D.T., Moudgil, T., Law, R.E., Kaplan, M.H., Jung, B., Espina, B.M., Lunardi-Iskandar, Y.*, et al.* (1995). Interleukin-10 is an autocrine growth factor for acquired immunodeficiency syndrome-related B-cell lymphoma. Blood *85*, 3423-3430.

Melnyk, A., Rodriguez, A., Pugh, W.C., and Cabannillas, F. (1997). Evaluation of the Revised European-American Lymphoma classification confirms the clinical relevance of immunophenotype in 560 cases of aggressive non-Hodgkin's lymphoma. Blood *89*, 4514-4520.

Menezes, J., Leibold, W., Klein, G., and Clements, G. (1975). Establishment and characterization of an Epstein-Barr virus (EBC)-negative lymphoblastoid B cell line (BJA-B) from an exceptional, EBV-genome-negative African Burkitt's lymphoma. Biomedicine / [publiee pour l'AAICIG] *22*, 276-284.

Mocellin, S., Marincola, F.M., and Young, H.A. (2005). Interleukin-10 and the immune response against cancer: a counterpoint. J Leukoc Biol *78*, 1043-1051.

Mocellin, S., Panelli, M., Wang, E., Rossi, C.R., Pilati, P., Nitti, D., Lise, M., and Marincola, F.M. (2004). IL-10 stimulatory effects on human NK cells explored by gene profile analysis. Genes Immun *5*, 621-630.

Moore, K.W., de Waal Malefyt, R., Coffman, R.L., and O'Garra, A. (2001). Interleukin-10 and the interleukin-10 receptor. Annu Rev Immunol *19*, 683-765.

Mormann, M., Rieth, H., Hua, T.D., Assohou, C., Roupelieva, M., Hu, S.L., Kremsner, P.G., Luty, A.J., and Kube, D. (2004). Mosaics of gene variations in the Interleukin-10 gene promoter affect interleukin-10 production depending on the stimulation used. Genes Immun *5*, 246-255.

Murawski, N., and Pfreundschuh, M. (2010). New drugs for aggressive B-cell and T-cell lymphomas. Lancet Oncol *11*, 1074-1085.

Nickelsen, M., Ziepert, M., Zeynalova, S., Glass, B., Metzner, B., Leithaeuser, M., Mueller-Hermelink, H.K., Pfreundschuh, M., and Schmitz, N. (2009). High-dose CHOP plus etoposide (MegaCHOEP) in T-cell lymphoma: a comparative analysis of patients treated within trials of the German High-Grade Non-Hodgkin Lymphoma Study Group (DSHNHL). Ann Oncol *20*, 1977-1984.

Nieters, A., Beckmann, L., Deeg, E., and Becker, N. (2006). Gene polymorphisms in Toll-like receptors, interleukin-10, and interleukin-10 receptor alpha and lymphoma risk. Genes Immun *7*, 615-624.

Nilsson, K., and Ponten, J. (1975). Classification and biological nature of established human hematopoietic cell lines. Int J Cancer *15*, 321-341.

O'Leary, H.M., and Savage, K.J. (2008). Novel therapies in peripheral T-cell lymphomas. Curr Hematol Malig Rep *3*, 213-220.

Orom, U.A., Derrien, T., Beringer, M., Gumireddy, K., Gardini, A., Bussotti, G., Lai, F., Zytnicki, M., Notredame, C., Huang, Q.*, et al.* (2010). Long noncoding RNAs with enhancer-like function in human cells. Cell *143*, 46-58.

Orom, U.A., and Shiekhattar, R. (2011). Long non-coding RNAs and enhancers. Current opinion in genetics & development *21*, 194-198.

Ozdemir, F., Aydin, F., Yilmaz, M., Kavgaci, H., Bektas, O., Yavuz, M.N., and Yavuz, A.A. (2004). The effects of IL-2, IL-6 and IL-10 levels on prognosis in patients with aggressive Non-Hodgkin's Lymphoma (NHL). Journal of experimental & clinical cancer research : CR *23*, 485-488.

Peterson, C.L., and Laniel, M.A. (2004). Histones and histone modifications. Current biology : CB *14*, R546-551.

Petersson, M., Charo, J., Salazar-Onfray, F., Noffz, G., Mohaupt, M., Qin, Z., Klein, G., Blankenstein, T., and Kiessling, R. (1998). Constitutive IL-10 production accounts for the high NK sensitivity, low MHC class I expression, and poor transporter associated with antigen processing (TAP)-1/2 function in the prototype NK target YAC-1. J Immunol *161*, 2099-2105.

Pfreundschuh, M., Schubert, J., Ziepert, M., Schmits, R., Mohren, M., Lengfelder, E., Reiser, M., Nickenig, C., Clemens, M., Peter, N.*, et al.* (2008). Six versus eight cycles of bi-weekly CHOP-14 with or without rituximab in elderly patients with aggressive CD20+ B-cell lymphomas: a randomised controlled trial (RICOVER-60). Lancet Oncol *9*, 105-116.

Pfreundschuh, M., Trumper, L., Kloess, M., Schmits, R., Feller, A.C., Rube, C., Rudolph, C., Reiser, M., Hossfeld, D.K., Eimermacher, H.*, et al.* (2004a). Two-weekly or 3-weekly CHOP chemotherapy with or without etoposide for the treatment of elderly patients with aggressive lymphomas: results of the NHL-B2 trial of the DSHNHL. Blood *104*, 634-641.

Pfreundschuh, M., Trumper, L., Kloess, M., Schmits, R., Feller, A.C., Rudolph, C., Reiser, M., Hossfeld, D.K., Metzner, B., Hasenclever, D.*, et al.* (2004b). Two-weekly or 3-weekly CHOP chemotherapy with or without etoposide for the treatment of young patients with good-prognosis (normal LDH) aggressive lymphomas: results of the NHL-B1 trial of the DSHNHL. Blood *104*, 626-633.

Pfreundschuh, M., Trumper, L., Osterborg, A., Pettengell, R., Trneny, M., Imrie, K., Ma, D., Gill, D., Walewski, J., Zinzani, P.L.*, et al.* (2006). CHOP-like chemotherapy plus rituximab versus CHOP-like chemotherapy alone in young patients with good-prognosis diffuse large-B-cell lymphoma: a randomised controlled trial by the MabThera International Trial (MInT) Group. Lancet Oncol *7*, 379-391.

Reff, M.E., Carner, K., Chambers, K.S., Chinn, P.C., Leonard, J.E., Raab, R., Newman, R.A., Hanna, N., and Anderson, D.R. (1994). Depletion of B cells in vivo by a chimeric mouse human monoclonal antibody to CD20. Blood *83*, 435-445.

Reimer, P., Rudiger, T., Geissinger, E., Weissinger, F., Nerl, C., Schmitz, N., Engert, A., Einsele, H., Muller-Hermelink, H.K., and Wilhelm, M. (2009). Autologous stem-cell transplantation as first-line therapy in peripheral T-cell lymphomas: results of a prospective multicenter study. J Clin Oncol *27*, 106-113.

Reuss, E., Fimmers, R., Kruger, A., Becker, C., Rittner, C., and Hohler, T. (2002). Differential regulation of interleukin-10 production by genetic and environmental factors--a twin study. Genes Immun *3*, 407-413.

Rieth, H., Mormann, M., Luty, A.J., Assohou-Luty, C.A., Roupelieva, M., Kremsner, P.G., and Kube, D. (2004). A three base pair gene variation within the distal 5'-flanking region of the interleukin-10 (IL-10) gene is related to the in vitro IL-10 production capacity of lipopolysaccharide-stimulated peripheral blood mononuclear cells. Eur Cytokine Netw *15*, 153-158.

Rothman, N., Skibola, C.F., Wang, S.S., Morgan, G., Lan, Q., Smith, M.T., Spinelli, J.J., Willett, E., De Sanjose, S., Cocco, P.*, et al.* (2006). Genetic variation in TNF and IL10 and risk of non-Hodgkin lymphoma: a report from the InterLymph Consortium. Lancet Oncol *7*, 27-38.

Rousset, F., Garcia, E., Defrance, T., Peronne, C., Vezzio, N., Hsu, D.H., Kastelein, R., Moore, K.W., and Banchereau, J. (1992). Interleukin 10 is a potent growth and differentiation factor for activated human B lymphocytes. Proc Natl Acad Sci U S A *89*, 1890-1893.

Samanta, M., Iwakiri, D., and Takada, K. (2008). Epstein-Barr virus-encoded small RNA induces IL-10 through RIG-I-mediated IRF-3 signaling. Oncogene *27*, 4150-4160.

Santos-Rosa, H., Schneider, R., Bannister, A.J., Sherriff, J., Bernstein, B.E., Emre, N.C., Schreiber, S.L., Mellor, J., and Kouzarides, T. (2002). Active genes are tri-methylated at K4 of histone H3. Nature *419*, 407-411.

Saraiva, M., Christensen, J.R., Tsytsykova, A.V., Goldfeld, A.E., Ley, S.C., Kioussis, D., and O'Garra, A. (2005). Identification of a macrophage-specific chromatin signature in the IL-10 locus. J Immunol *175*, 1041-1046.

Saraiva, M., Christensen, J.R., Veldhoen, M., Murphy, T.L., Murphy, K.M., and O'Garra, A. (2009). Interleukin-10 production by Th1 cells requires interleukin-12-induced STAT4 transcription factor and ERK MAP kinase activation by high antigen dose. Immunity *31*, 209-219.

Saxena, A., and Carninci, P. (2011). Long non-coding RNA modifies chromatin: epigenetic silencing by long non-coding RNAs. BioEssays : news and reviews in molecular, cellular and developmental biology *33*, 830-839.

Schaadt, M., Fonatsch, C., Kirchner, H., and Diehl, V. (1979). Establishment of a malignant, Epstein-Barr-virus (EBV)-negative cell-line from the pleura effusion of a patient with Hodgkin's disease. Blut *38*, 185-190.

Schmitz, N., Trumper, L., Ziepert, M., Nickelsen, M., Ho, A.D., Metzner, B., Peter, N., Loeffler, M., Rosenwald, A., and Pfreundschuh, M. (2010). Treatment and prognosis of mature T-cell and NK-cell lymphoma: an analysis of patients with T-cell lymphoma treated in studies of the German High-Grade Non-Hodgkin Lymphoma Study Group. Blood *116*, 3418-3425.

Schneider, R., Bannister, A.J., Myers, F.A., Thorne, A.W., Crane-Robinson, C., and Kouzarides, T. (2004). Histone H3 lysine 4 methylation patterns in higher eukaryotic genes. Nature cell biology *6*, 73-77.

Shan, D., Ledbetter, J.A., and Press, O.W. (2000). Signaling events involved in anti-CD20-induced apoptosis of malignant human B cells. Cancer immunology, immunotherapy : CII *48*, 673-683.

Shoemaker, J., Saraiva, M., and O'Garra, A. (2006). GATA-3 directly remodels the IL-10 locus independently of IL-4 in CD4+ T cells. J Immunol *176*, 3470-3479.

Skibola, C.F., Curry, J.D., and Nieters, A. (2007). Genetic susceptibility to lymphoma. Haematologica *92*, 960-969.

Stasi, R., Zinzani, P.L., Galieni, P., Lauta, V.M., Damasio, E., Dispensa, E., Dammacco, F., Papa, G., and Tura, S. (1994). Prognostic value of serum IL-10 and soluble IL-2 receptor levels in aggressive non-Hodgkin's lymphoma. Br J Haematol *88*, 770-777.

Suzuki, E., Umezawa, K., and Bonavida, B. (2007). Rituximab inhibits the constitutively activated PI3K-Akt pathway in B-NHL cell lines: involvement in chemosensitization to drug-induced apoptosis. Oncogene *26*, 6184-6193.

Tian, Y., Jia, Z., Wang, J., Huang, Z., Tang, J., Zheng, Y., Tang, Y., Wang, Q., Tian, Z., Yang, D.*, et al.* (2011). Global mapping of H3K4me1 and H3K4me3 reveals the chromatin state-based cell type-specific gene regulation in human Treg cells. PloS one *6*, e27770.

Turner, D.M., Williams, D.M., Sankaran, D., Lazarus, M., Sinnott, P.J., and Hutchinson, I.V. (1997). An investigation of polymorphism in the interleukin-10 gene promoter. European journal of immunogenetics : official journal of the British Society for Histocompatibility and Immunogenetics *24*, 1-8.

Turner, J.J., Morton, L.M., Linet, M.S., Clarke, C.A., Kadin, M.E., Vajdic, C.M., Monnereau, A., Maynadie, M., Chiu, B.C., Marcos-Gragera, R.*, et al.* (2010). InterLymph hierarchical classification of lymphoid neoplasms for epidemiologic research based on the WHO classification (2008): update and future directions. Blood *116*, e90-98.

Tweeddale, M., Jamal, N., Nguyen, A., Wang, X.H., Minden, M.D., and Messner, H.A. (1989). Production of growth factors by malignant lymphoma cell lines. Blood *74*, 572-578.

Urosevic, M., and Dummer, R. (2003). HLA-G and IL-10 expression in human cancer--different stories with the same message. Seminars in cancer biology *13*, 337-342.

van der Linden, M.W., Huizinga, T.W., Stoeken, D.J., Sturk, A., and Westendorp, R.G. (1998). Determination of tumour necrosis factor-alpha and interleukin-10 production in a whole blood stimulation system: assessment of laboratory error and individual variation. Journal of immunological methods *218*, 63-71.

Vega, M.I., Huerta-Yepaz, S., Garban, H., Jazirehi, A., Emmanouilides, C., and Bonavida, B. (2004). Rituximab inhibits p38 MAPK activity in 2F7 B NHL and decreases IL-10 transcription: pivotal role of p38 MAPK in drug resistance. Oncogene *23*, 3530-3540.

Vilches, C., and Parham, P. (2002). KIR: diverse, rapidly evolving receptors of innate and adaptive immunity. Annu Rev Immunol *20*, 217-251.

Vockerodt, M., Haier, B., Buttgereit, P., Tesch, H., and Kube, D. (2001). The Epstein-Barr virus latent membrane protein 1 induces interleukin-10 in Burkitt's lymphoma cells but not in Hodgkin's cells involving the p38/SAPK2 pathway. Virology *280*, 183-198.

Voorzanger, N., Touitou, R., Garcia, E., Delecluse, H.J., Rousset, F., Joab, I., Favrot, M.C., and Blay, J.Y. (1996). Interleukin (IL)-10 and IL-6 are produced in vivo by non-Hodgkin's lymphoma cells and act as cooperative growth factors. Cancer Res *56*, 5499-5505.

Wang, S.S., Cerhan, J.R., Hartge, P., Davis, S., Cozen, W., Severson, R.K., Chatterjee, N., Yeager, M., Chanock, S.J., and Rothman, N. (2006). Common genetic variants in proinflammatory and other immunoregulatory genes and risk for non-Hodgkin lymphoma. Cancer Res *66*, 9771-9780.

Westendorp, R.G., Langermans, J.A., Huizinga, T.W., Elouali, A.H., Verweij, C.L., Boomsma, D.I., and Vandenbroucke, J.P. (1997). Genetic influence on cytokine production and fatal meningococcal disease. Lancet *349*, 170-173.

Yi, A.K., Yoon, J.G., Yeo, S.J., Hong, S.C., English, B.K., and Krieg, A.M. (2002). Role of mitogen-activated protein kinases in CpG DNA-mediated IL-10 and IL-12 production: central role of extracellular signal-regulated kinase in the negative feedback loop of the CpG DNA-mediated Th1 response. J Immunol *168*, 4711-4720.

Zeidler, R., Eissner, G., Meissner, P., Uebel, S., Tampe, R., Lazis, S., and Hammerschmidt, W. (1997). Downregulation of TAP1 in B lymphocytes by cellular and Epstein-Barr virus-encoded interleukin-10. Blood *90*, 2390-2397.

Zhang, X., Edwards, J.P., and Mosser, D.M. (2006). Dynamic and transient remodeling of the macrophage IL-10 promoter during transcription. J Immunol *177*, 1282-1288.

Ziegler-Heitbrock, L., Lotzerich, M., Schaefer, A., Werner, T., Frankenberger, M., and Benkhart, E. (2003). IFN-alpha induces the human IL-10 gene by recruiting both IFN regulatory factor 1 and Stat3. J Immunol *171*, 285-290.

Appendix

Table A-1A Histological characteristics of NHL patients from NHL-B trial analysed for *IL10* gene variations

Histology	NHL-B1/B2 patients included (n=942)	NHL-B1/B2 patients complete (n=1399)	NHL-B1 patients included (n=477)	NHL-B1 patients complete (n=710)	NHL-B2 patients included (n=465)	NHL-B2 patients complete (n=689)
B cell	843 (89.5%)	1256 (89.9%)	409 (85.7%)	609 (85.8%)	434 (93.3%)	647 (93.9%)
Lymphoblastic	1 (0.1%)	2 (0.1%)	0 (0%)	0 (0%)	1 (0.2%)	2 (0.3%)
Diffuse large	594 (63.1%)	913 (65.3%)	275 (57.7%)	424 (59.7%)	319 (68.6%)	489 (71.0%)
Centroblastic	454 (48.2%)	687 (49.1%)	214 (44.9%)	326 (45.9%)	240 (51.6%)	361 (52.4%)
Immunoblastic	72 (7.6%)	114 (8.1%)	23 (4.8%)	35 (4.9%)	49 (10.5%)	79 (11.5%)
Anaplastic	20 (2.1%)	28 (2.0%)	13 (2.7%)	17 (2.4%)	7 (1.5%)	11 (1.6%)
T-cell rich	13 (1.4%)	24 (1.7%)	7 (1.5%)	16 (2.3%)	6 (1.3%)	8 (1.2%)
NOS	35 (3.7%)	60 (4.3%)	18 (3.8%)	30 (4.2%)	17 (3.7%)	30 (4.4%)
Mediastinal B cell	17 (1.8%)	25 (1.8%)	16 (3.4%)	21 (3.0%)	1 (0.2%)	4 (0.6%)
Follicular	81 (8.6%)	105 (7.5%)	47 (9.9%)	63 (8.9%)	34 (7.3%)	42 (6.1%)
Mantle cell lymphoma	9 (1.0%)	16 (1.1%)	7 (1.5%)	10 (1.4%)	2 (0.4%)	6 (0.9%)
Burkitt lymphoma	30 (3.2%)	35 (2.5%)	10 (2.1%)	10 (1.4%)	20 (4.3%)	25 (3.6%)
Aggressive marginal zone	9 (1.0%)	14 (1.0%)	5 (1.0%)	10 (1.4%)	4 (0.9%)	4 (0.6%)
Unspecified for technical reasons*	53 (5.6%)	74 (5.3%)	26 (5.5%)	38 (5.4%)	27 (5.8%)	36 (5.2%)
NOS	49 (5.2%)	72 (5.1%)	23 (4.8%)	33 (4.6%)	26 (5.6%)	39 (5.7%)
T cell	97 (10.3%)	139 (9.9%)	67 (14.0%)	98 (13.8%)	30 (6.5%)	41 (6.0%)
Anaplastic large cell	65 (6.9%)	91 (6.5%)	50 (10.5%)	67 (9.4%)	15 (3.2%)	24 (3.5%)
Lymphoblastic	2 (0.2%)	3 (0.2%)	2 (0.4%)	3 (0.4%)	0 (0%	0 (0%
Peripheral T, unspecified	23 (2.4%)	31 (2.2%)	11 (2.3%)	18 (2.5%)	12 (2.6%)	13 (1.9%)
Angioimmunoblastic	2 (0.2%)	3 (0.2%)	0 (0%)	1 (0.1%)	2 (0.4%)	2 (0.3%)
Extranodal NK/T, nasal type	1 (0.1%)	6 (0.4%)	1 (0.2%)	5 (0.7%)	0 (0%)	1 (0.1%)
Unspecified for technical reasons*	1 (0.1%)	1 (0.1%)	0 (0%)	0 (0%)	1 (0.2%)	1 (0.1%)
Lymphoblastic, NOS	2 (0.2%)	4 (0.3%)	1 (0.2%)	3 (0.4%)	1 (0.2%)	1 (0.1%)

Table A-1B Histological characteristics of NHL patient from RICOVER-60 trial analysed for *IL10* gene variations

Histology	RICOVER-60 patients included (n=604)	RICOVER-60 patients complete (n=1222)	CHOP patients included (n=301)	CHOP patients complete (n=612)	R-CHOP patients included (n=303)	R-CHOP patients complete (n=610)
B cell	591 (97.8%)	1160 (94.9%)	296 (98.3%)	582 (95.1%)	295 (97.4%)	569 (93.3%)
lymphoblastic	1 (0.2%)	1 (0.1%)	0 (0.0%)	0 (0.0%)	1 (0.3%)	1 (0.2%)
DLBCL	499 (82.6%)	949 (77.7%)	253 (84.1%)	475 (77.6%)	246 (81.2%)	474 (77.7%)
centroblastic	286 (47.4%)	516 (42.2%)	150 (49.8%)	263 (43%)	136 (44.9%)	253 (41.5%)
immunoblastic	35 (5.8%)	63 (5.2%)	18 (6.0%)	36 (5.9%)	17 (5.6%)	27 (4.4%)
plasmoblastic (DLBCL)	2 (0.3%)	7 (0.6%)	0 (0.0%)	0 (0.0%)	2 (0.7%)	7 (1.1%)
anaplastic large cell	11 (1.8%)	19 (1.6%)	4 (1.3%)	6 (1.0%)	7 (2.3%)	13 (2.1%)
T cell-rich	9 (1.5%)	18 (1.5%)	7 (2.3%)	13 (2.1%)	2 (0.7%)	5 (0.8%)
DLBC, NOS	149 (24.7%)	313 (25.6%)	68 (22.6%)	147 (24%)	81 (26.7%)	166 (27.2%)
primary mediastinal B cell lymphoma	7 (1.2%)	13 (1.1%)	6 (2.0%)	10 (1.6%)	1 (0.3%)	3 (0.5%)
Follicular grade III	57 (9.4%)	116 (9.5%)	29 (9.6%)	65 (10.6%)	28 (9.2%)	51 (8.4%)
Follicular grade III + DLBCL	32 (5.3%)	55 (4.5%)	16 (5.3%)	32 (5.2%)	16 (5.3%)	23 (3.8%)
Burkitt's lymphoma	6 (1.0%)	17 (1.4%)	3 (1.0%)	8 (1.3%)	3 (1.0%)	9 (1.5%)
Burkitt-like	4 (0.7%)	8 (0.7%)	2 (0.7%)	5 (0.8%)	2 (0.7%)	3 (0.5%)
Mantle cell blastic	3 (0.5%)	17 (1.4%)	1 (0.3%)	6 (1.0%)	2 (0.7%)	11 (1.8%)
aggresive marginal	4 (0.7%)	13 (1.1%)	2 (0.7%)	5 (0.8%)	2 (0.7%)	8 (1.3%)
Unclassified (technically insufficient)	11 (1.8%)	22 (1.8%)	5 (1.7%)	9 (1.5%)	6 (2.0%)	13 (2.1%)
Other lymphoma or no lymphoma	6 (1.0%)	27 (2.2%)	2 (0.7%)	15 (2.5%)	4 (1.3%)	12 (2.0%)
T cell	1 (0.2%)	2 (0.2%)	0 (0.0%)	1 (0.2%)	1 (0.3%)	1 (0.2%)
Angioimmunoblastic T cell lymphoma	1 (0.2%)	1 (0.1%)	0 (0.0%)	0 (0.0%)	1 (0.3%)	1 (0.2%)
extranodal NK/T cell, nasal type	0 (0.0%)	1 (0.1%)	0 (0.0%)	1 (0.2%)	0 (0.0%)	0 (0.0%)

Table A-2 Clinical and histological characteristics of the T-NHL patients analysed for *IL10* gene variations in cytokine receptors

Values in table are expressed as total number of patients and respective percentage are in parenthesis (%), unless otherwise indicated. * IPI= International Prognostic Index LDH >N, age >60 years, ECOG >1, stage III/IV, and number of extranodal sites ≥2.Anaplastic large cell lymphoma (ALCL), Anaplastic lymphoma kinase (ALK), Peripheral T cell lymphoma, not otherwise specified (PTCL, NOS), Angioimmunoblastic T cell lymphoma (AILT), Natural Killer cell (NK), T cell lymphoma not otherwise specified (T cell, NOS) for other than technical reasons.(taken from the Manuscript "Circulating levels of TNF-receptor II are prognostic for patients with peripheral T cell Non-Hodgkin lymphoma" by Heemann et al.)

Patients characteristics	**T-NHL patients included (n=117)**	**T-NHL patients complete (n= 197)**
Sex male	69 (59%)	120 (61%)
female	48 (41%)	77 (39%)
Age Median (Min.;Max.)	58 (18;78)	61 (18;78)
Serum LDH > N	22 (18.8%)	45 (22.8%)
Age Older than 60 y	50 (42.7%)	99 (50.3%)
Performance status ECOG > 1	13 (11.1%)	31 (15.7%)
Ann Arbor stage III,IV	47 (40.2%)	85 (43.2%)
IPI*		
low (IPI=0,1)	72 (61.5%)	111 (56.4%)
intermediate low (IPI=2)	23 (19.7%)	39 (19.8%)
intermediate high (IPI=3)	12 (10.3%)	25 (12.7%)
high (IPI=4,5)	10 (8.6%)	22 (11.2%)
No of extranodal sites >1	23 (19.7%)	36 (18.3%)
Bulky tumor (>7,5 cm)	30 (25.7%)	51 (25.9%)
B symptoms	45 (38.5%)	75 (38.1%)
extranodal involvement	51 (43.6%)	88 (44.7%)
study		
NHL-B1/B2	95	138
RICOVER-60	22	59
Histology		
ALCL/ALK+	28 (23.93)	37 (18.78)
ALCL/ALK-	34 (29.06)	68 (34.52)
PTCL	28 (23.93)	44 (22.34)
AILT	9 (7.69)	16 (8.12)
T/NK	3 (2.56)	8 (4.06)
Lymphoblastic	2 (1.71)	4 (2.03)
Intestinal T/NK	0 (0)	1 (0.51)
Hepatosplenic $\gamma\delta$	1 (0.85)	1 (0.51)
ALCL/ALK unknown	7 (5.98)	11 (5.58)
T cell NOS	3 (2.56)	5 (2.54)
T cell,subtype technically not possible	2 (1.71)	2 (1.02)

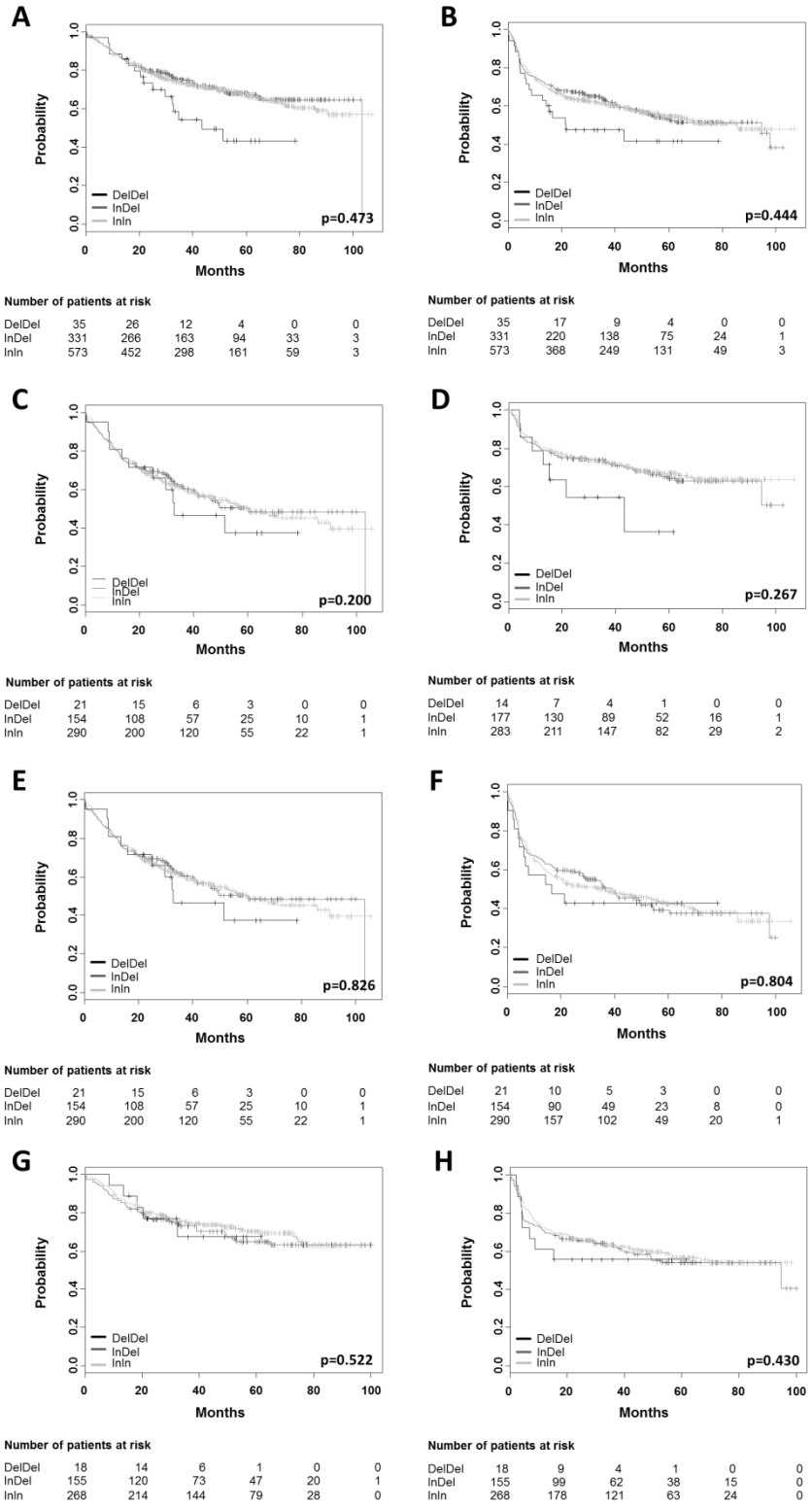

Figure A-1 No significant association of IL10-7400DelDel with shorter survival rates

Shown are the survival curves (Kaplan-Meier plots) for OS (**A,C,E,G**) and EFS (**B,D,F,H**) of aNHL patients from the NHL-B cohorts in comparison with all the genotypes of IL10-7400In/Del. **A.** OS of patients from NHL-B. **B.** EFS of patients from NHL-B. **C.** OS of patients from NHL-B1. **D.** EFS of patients from NHL-B1. **E.** OS of patients from NHL-B2. **F.** EFS of patients from NHL-B2. **G.** OS of patients from NHL-B_CCR-excluded. **H.** EFS of patients from NHL-B_CCR-excluded. *P* refers to the log-rank test. Patients at risk represents the number of patients which still can develop an event (OS or EFS) at defined time points.

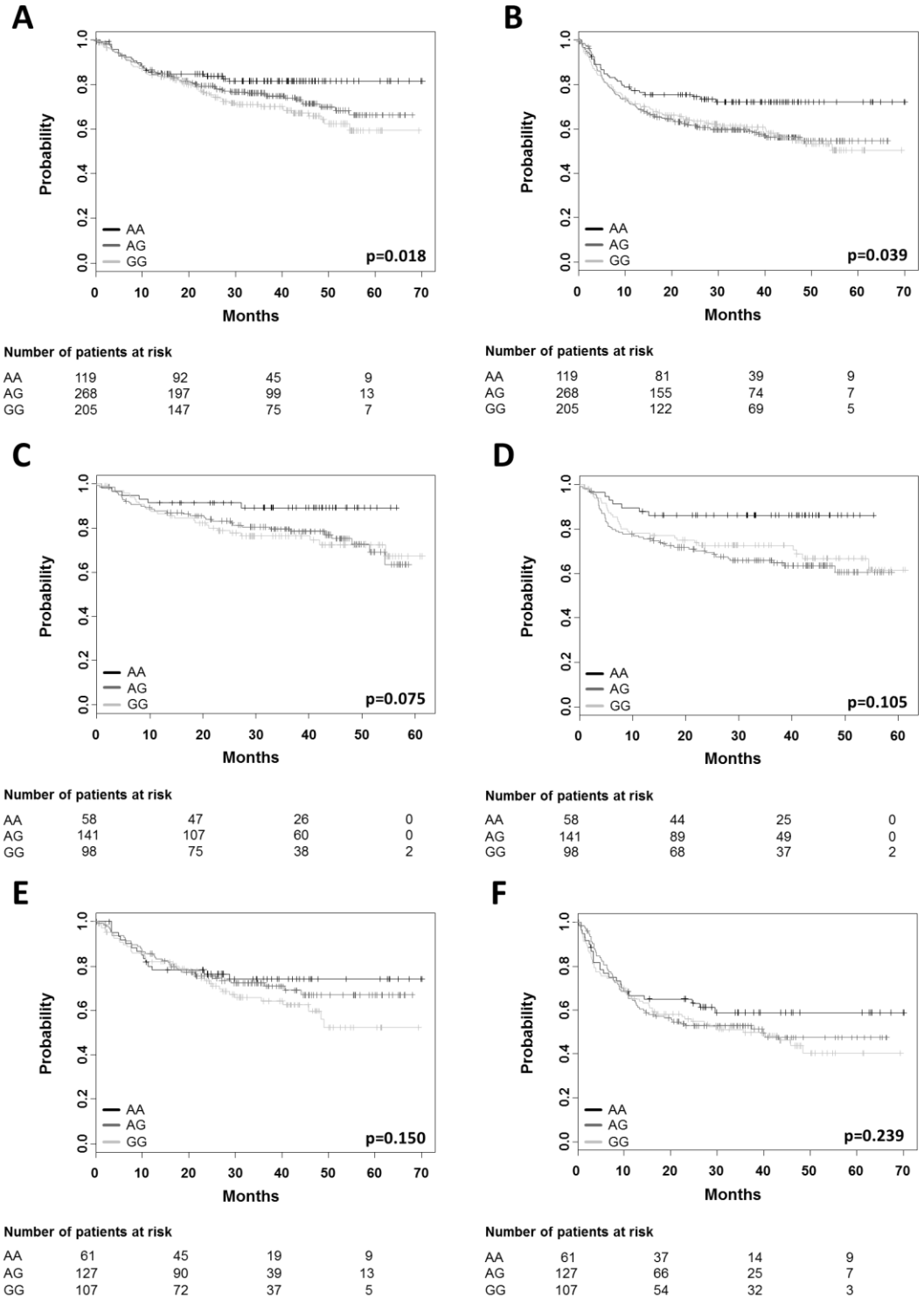

Figure A-2 The IL10-11.668AA genotype is associated with longer survival rates for OS and EFS in patients from the RICOVER-60 cohort

Shown are the survival curves (Kaplan-Meier plots) for OS (**A,C,E**) and EFS (**B,D,F**) of aNHL patients from the RICOVER-60 cohorts in comparison with all three genotypes of IL10-11.668G/A. **A.** OS of patients from RICOVER-60. **B.** EFS of patients from RICOVER-60.**C.** OS of patients from R-CHOP arm of RICOVER-60. **D.** EFS of patients from R-CHOP arm of RICOVER-60. **E.** OS of patients from CHOP arm of RICOVER-60. **F.** EFS of patients from CHOP arm of RICOVER-60. *P* refers to the log-rank test. Patients at risk represents the number of patients which still can develop an event (OS or EFS) at defined time points. Significant values have been observed for OS and EFS rates for patients from RICOVER-60 cohort (A,B).

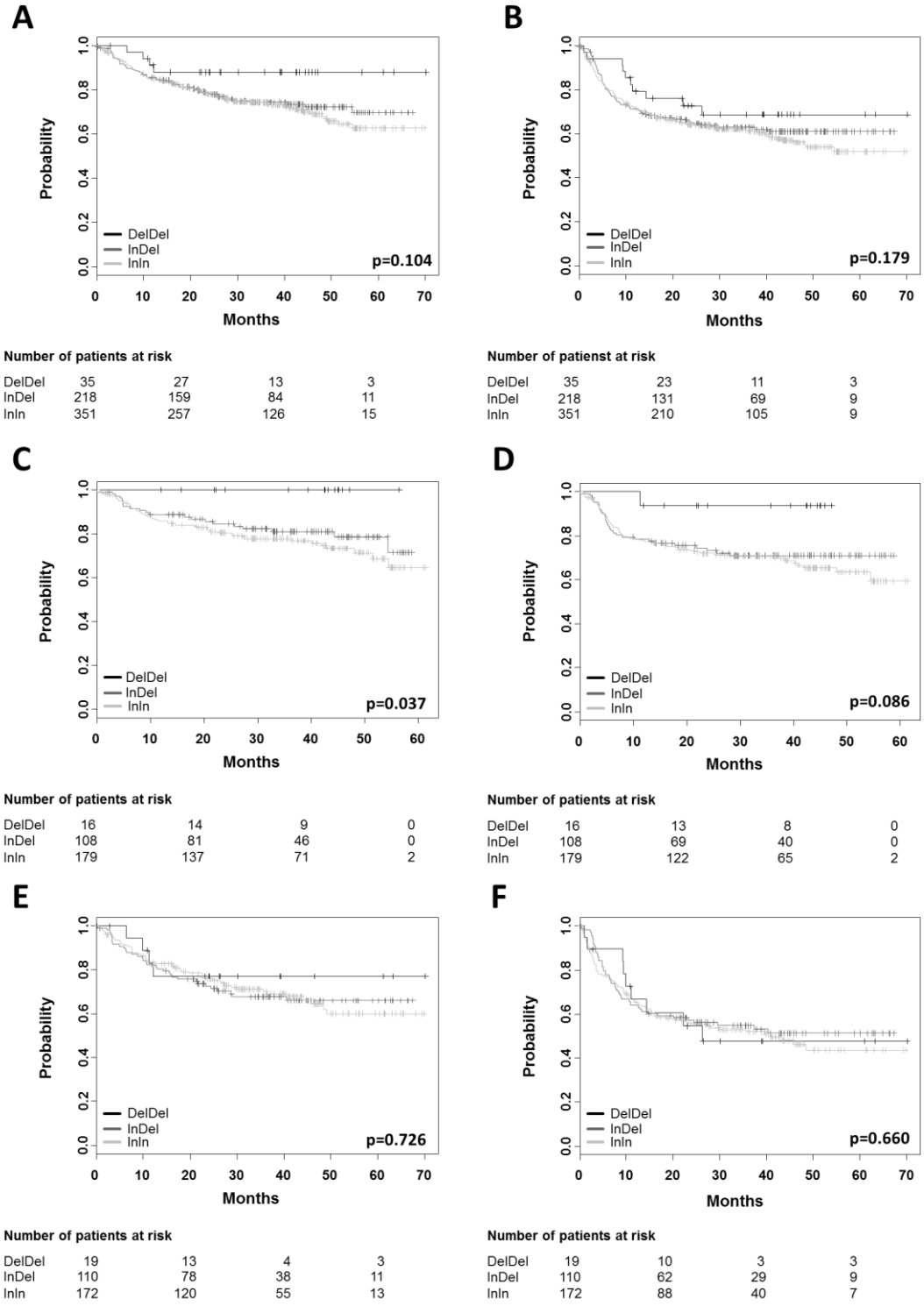

Figure A-3 The IL10-7400DelDel genotype is associated with longer survival rates for OS and EFS in patients from the R-CHOP cohort.

Shown are the survival curves (Kaplan-Meier plots) for OS (**A,C,E**) and EFS (**B,D,F**) of aNHL patients from the RICOVER-60 cohorts in comparison with all three genotypes of IL10-7400In/Del. **A.** OS of patients from RICOVER-60. **B.** EFS of patients from RICOVER-60. **C.** OS of patients from R-CHOP arm of RICOVER-60. **D.** EFS of patients from R-CHOP arm of RICOVER-60. **E.** OS of patients from CHOP arm of RICOVER-60. **F.** EFS of patients from CHOP arm of RICOVER-60. *P* refers to the log-rank test. Patients at risk represents the number of patients which still can develop an event (OS or EFS) at defined time points. A Significant association has been observed for OS rates for patients from the R-CHOP arm (C).

Table A-3 No associations between *IL10* genotypes and *IL10* high or *IL10* low expressing LCLs.

LCLs have been grouped according to the median *IL10* gene expression (0.000762 NSM IL10/NSM β2m) into IL10 high and low expressing cells. Number and percentage of LCLs within each group, carrying different *IL10* genotypes are shown for each analysed *IL10* gene variation in a two-way summary table. Associations between respective gene variations with low or high *IL10* gene expression were examined using Pearson X^2 test. In case of n total ≠111 respective genotyping analysis was not successful.

			IL10 low		IL10 high		total	
SNP Name	**rs-number**	**Genotype**	**number of LCLs**	**% of LCLs**	**number of LCLs**	**% of LCLs**	**number of LCLs**	**Pearson X^2**
IL10-12806C/T	rs17015865	TT	6	66.7	3	33.3	9	0.494
		CT	17	44.7	21	55.3	38	
		CC	32	50.0	32	50.0	64	
		total	55		56		111	
IL10-11777A/G	rs4072227	GG	0	0	0	0,0	0	0.616
		AG	7	43,8	9	56,3	16	
		AA	48	50,5	47	49,5	95	
		total	55		56		111	
IL10-11668G/A	rs4072226	AA	19	50,0	19	50.0	38	0.572
		AG	20	44,4	25	55,6	45	
		GG	16	57,1	12	42,9	28	
		total	55		56		111	
IL10-7400In/Del	7400In/Del	DelDel	4	57,1	3	42,9	7	0.856
		InDel	19	50,0	19	50,0	38	
		InIn	30	46,9	34	53,1	64	
		total	53		56		109	
IL10-6752A/T	rs6676671	TT	21	51,2	20	48,8	41	0.811
		AT	21	46,7	24	53,3	45	
		AA	9	42,9	12	57,1	21	
		total	51		56		107	
IL10-6208G/C	rs10494879	CC	13	48,1	14	51,9	27	0.978-
		CG	21	47,7	23	52,3	44	
		GG	19	50,0	19	50,0	38	
		total	53		56		109	
IL10-3538T/A	rs1800890	AA	11	47,8	12	52,2	23	0.801
		AT	21	46,7	24	53,3	45	
		TT	23	53,5	20	46,5	43	
		total	55		56		111	
IL10-2812G/A	rs6703630	AA	7	58,3	5	41,7	12	0.610
		AG	20	52,6	18	47,4	38	
		GG	27	45,0	33	55,0	60	
		total	54		56		110	
IL10-2726C/A	rs6693899	AA	7	46,7	8	53,3	15	0.696
		AC	26	54,2	22	45,8	48	
		CC	22	45,8	26	54,2	48	
		total	55		56		111	
IL10-1087A/G	rs1800896	GG	17	51,5	16	48,5	33	0.876
		AG	14	45,2	17	54,8	31	
		AA	21	47,7	23	52,3	44	
		total	52		56		108	
IL10-824C/T	rs1800871	TT	2	33,3	4	66,7	6	0.227
		CT	35	55,6	28	44,4	63	
		CC	16	40,0	24	60,0	40	
		total	53		56		109	
IL10-597C/A	rs1800872	AA	2	33,3	4	66,7	6	0.227
		AC	35	55,6	28	44,4	63	
		CC	16	40,0	24	60,0	40	
		total	53		56		109	
IL10+4259A/G	rs3024498	GG	20	58,8	14	41,2	34	0.263
		AG	7	58,3	5	41,7	12	
		AA	27	42,9	36	57,1	63	
		total	54		55		109	
IL10+5876C/T	rs3024505	TT	0	0,0	2	100,0	2	0.083
		CT	13	38,2	21	61,8	34	
		CC	41	56,2	32	43,8	73	
		total	54		55		109	

Table A-4 No associations between *IL10* genotypes and IL10 high or IL10 low secreting LCLs.

LCLs have been grouped according to the median IL10 secretion level measured via ELISA (737pg IL10/ml) into IL10 high and low secreting cells. Number and percentage of LCLs within each group, carrying different *IL10* genotypes are shown for each analysed *IL10* gene variation. Associations between respective gene variations with low or high IL10 secretion were examined using Pearson X^2 test. In case of n≠108 respective genotyping analysis was not successful.

			IL10 low		IL10 high		total	
SNP Name	rs-number	Genotype	number of LCLs	% of LCLs	number of LCLs	% of LCLs	number of LCLs	Pearson X^2
IL10-12806C/T	rs17015865	TT	5	62,5	3	37,5	8	0.518
		CT	20	54,1	17	45,9	37	
		CC	28	45,2	34	54,8	62	
		total	53		54		107	
IL10-11777A/G	rs4072227	GG	0	0	0	0	0	0.968
		AG	8	50,0	8	50,0	16	
		AA	45	49,5	46	50,5	91	
		total	53		54		107	
IL10-11668G/A	rs4072226	AA	14	53,8	12	46,2	26	0.400
		AG	24	54,5	20	45,5	44	
		GG	15	40,5	22	59,5	37	
		total	53		54		107	
IL10-7400In/Del	7400In/Del	DelDel	4	57,1	3	42,9	7	0.464
		InDel	20	55,6	16	44,4	36	
		InIn	27	43,5	35	56,5	62	
		total	51		54		105	
IL10-6752A/T	rs6676671	TT	9	45,0	11	55,0	20	0.335
		AT	25	56,8	19	43,2	44	
		AA	16	41,0	23	59,0	39	
		total	50		53		103	
IL10-6208G/C	rs10494879	CC	13	50,0	13	50,0	26	0.570
		CG	23	53,5	20	46,5	43	
		GG	15	41,7	21	58,3	36	
		total	51		54		105	
IL10-3538T/A	rs1800890	AA	10	45,5	12	54,5	22	0.450
		AT	25	56,8	19	43,2	44	
		TT	18	43,9	23	56,1	41	
		total	53		54		107	
IL10-2812G/A	rs6703630	AA	8	66,7	4	33,3	12	0.237
		AG	20	55,6	16	44,4	36	
		GG	25	43,1	33	56,9	58	
		total	53		53		106	
IL10-2726C/A	rs6693899	AA	5	35,7	9	64,3	14	0.078
		AC	29	61,7	18	38,3	47	
		CC	19	41,3	27	58,7	46	
		total	53		54		107	
IL10-1087A/G	rs1800896	GG	17	53,1	15	46,9	32	0.202
		AG	24	54,5	20	45,5	44	
		AA	10	34,5	19	65,5	29	
		total	51		54		105	
IL10-824C/T	rs1800871	TT	2	33,3	4	66,7	6	0.379
		CT	16	42,1	22	57,9	38	
		CC	33	54,1	28	45,9	61	
		total	51		54		105	
IL10-597C/A	rs1800872	AA	2	33,3	4	66,7	6	0.379
		AC	16	42,1	22	57,9	38	
		CC	33	54,1	28	45,9	61	
		total	51		54		105	
IL10+4259A/G	rs3024498	GG	8	66,7	4	33,3	12	0.420
		AG	16	50,0	16	50,0	32	
		AA	28	45,9	33	54,1	61	
		total	52		53		105	
IL10+5876C/T	rs3024505	TT	1	50,0	1	50,0	2	0.614
		CT	14	42,4	19	57,6	33	
		CC	37	52,9	33	47,1	70	
		total	52		53		105	

Danksagung

Prof. Dr. Dieter Kube möchte ich für die kompetente Betreuung dieser Arbeit während der letzten drei Jahre danken. Diese bestand aus einer steten Diskussionsbereitschaft sowie vielen guten Ratschlägen und Ideen, nicht nur während der Anfangszeit dieser Arbeit.

Bei Prof. Dr. Lorenz Trümper möchte ich mich für die Möglichkeit bedanken, diese Arbeit in seiner Abteilung durchzuführen.

Prof. Dr. Heike Bickeböller und Prof. Dr. Steven Johnsen möchte ich dafür danken, dass sie als meines Thesis Committee diese Arbeit begleitet haben. Die Diskussionen während der Thesis Committee Meetings und manchmal auch darüber hinaus, spiegelten ein ehrliches Interesse an meiner Arbeit wider und waren mir eine große Hilfe und Motivation.

At this point I would like to thank Prof. Dr. Steven Johnsen for his support with the ChIP protocol, for the opportunity to use the Biorupter and his ideas concerning my project. I would also like to thank his working group for hosting me during the sonication of my samples. I am especially grateful for the improved crosslinking protocol from Dr. Magali Hennion, which significantly improved my ChIP results.

Mein ganz besonderer Dank gilt Frederike von Bonin, dem wandelnden Lexikon wenn es um PCR Optimierung, Telefonnummern oder die Berechnung von Konzentrationen geht, wenn das Brett vorm Kopf mal wieder zu groß geworden ist.
Zudem danke ich ihr für die unzähligen PCRs, die sie für dieses Projekt durchgeführt hat und ihre Reise nach Homburg um dort IL10 Serum Level von besonders vielen Patienten zu messen. Ohne ihre Arbeit würde ein essentieller Teil dieser Arbeit fehlen.

Außerdem danke ich Angela Lenz für ihre tatkräftige Unterstützung in den ersten beiden Jahren dieser Arbeit. Susanne Hengst danke ich für ihre Unterstützung bei der Durchführung der Proliferationsassays und die Versorgung vieler, vieler Zelllinien.

Dr. Nils Schoof und Julia Stächele danke ich für ihre Arbeiten im Bereich SNPery, die nicht nur für mein Projekt wichtige Vorarbeiten waren. Zudem danke ich Euch dafür, dass ihr mich in der ersten Zeit als Doktorandin eingearbeitet habt.

Ganz besonders dankbar bin ich Markus Kreuz vom IMISE in Leipzig, der nicht nur sämtliche statistische Überlebenszeitanalysen für uns gerechnet hat, sondern sich auch immer die Zeit genommen hat mir alles möglichst genau zu erklären. Zudem danke ich ihm für die Unterstützung beim Schreiben unseres Manuskriptes sowie seine Last-Minute Analysen, die ein wichtiger Teil dieser Arbeit geworden sind.

Ich möchte allen Mitgliedern des GRK 1034 danken. Im Besonderen danke ich Dr. Mladen Tzvetkov für seine Phase Analysen und Kristin Bokelmann für ihre Hilfe bei verschiedenen Methoden, die leider ihren Weg in diese Arbeit nicht gefunden haben.

Hans-Joachim Helms von der Abteilung für Medizinische Statistik möchte ich für seine Hilfe bei den Analysen zu den LCLs danken.

Für ihre spontane Begeisterung sowie die daraus resultierende Unterstützung bzw. die Durchführung der ADCC Assays möchte ich Dr. Justin Hasenkamp und Kristina Kiecke danken.

Ich danke allen Mädels aus der AG Kube und der AG Binder. Die letzten drei Monate zu Hause haben mir deutlich gezeigt, wie sehr ich Euch in meinem Alltag vermissen werde! Zum Glück können aus Kolleginnen auch Freundinnen werden! An dieser Stelle möchte ich mich ganz besonders bei allen fleißigen Korrekturleserinnen bedanken, Elisabeth Hand, Alexandra Schrader. Kerstin Menck, Eva Rietkötter und Dr. Sonja Eberth.
Neele Walther, Antje Ulrich und Elisabeth Hand möchte ich sagen, dass mir das Büro nachmittags ohne Euch echt zu leer war. Neele danke ich besonders für den besten Kaffee in ganz Göttingen und die Spaziergänge, denen hoffentlich in den nächsten Semesterferien und auch danach viele folgen werden.

Meinen Freundinnen Eva und Claudia, Ina und Constanze möchte ich an dieser Stelle sagen wie froh ich bin, dass es so etwas wie eine O-Phase gibt. Aus den letzten 11 Jahren seid ihr nicht wegzudenken! Und aus den Jahren, die noch folgen auch nicht!

Meinen Eltern möchte ich dafür danken, dass sie mich bei jeder Entscheidung unterstützt haben und mich jeden Umweg haben gehen lassen. Ohne sie wäre ich nicht dort angekommen wo ich bin.

Martin und Momme möchte ich einfach nur sagen wie glücklich ich bin, dass es Euch gibt! Ihr zeigt mir jeden Tag was wichtig ist.